DATE ISSUED SEP 26 1989

ORNL MASTER COPY

OAK RIDGE NATIONAL LABORATORY LIBRARIES

3 4456 0599555 8

ornl

ORNL/ANS/INT-5/V14

[redacted]

OAK RIDGE NATIONAL LABORATORY

MARTIN MARIETTA

Monthly Progress Report for May 1989

Advanced Neutron Source

CAUTION

This document has not been given final patent clearance and is for internal use only. If this document is to be given public release, it must be cleared through the site Technical Information Office which will see that the proper patent and technical information reviews are completed in accordance with Energy Systems Policy.

OPERATED BY
MARTIN MARIETTA ENERGY SYSTEMS, INC.
FOR THE UNITED STATES
DEPARTMENT OF ENERGY

ORNL/ANS/INT-5/V14

MONTHLY PROGRESS REPORT FOR MAY 1989

Compilers:

J. A. Johnson
M. R. McBee
D. L. Selby

Contributing Authors:

R. G. Alsmiller, Jr
D. J. Alexander
Y. Y. Azmy
R. M. Beckers
R. C. Birtcher
N. C. J. Chen
G. L. Copeland
F. C. Difilippo
J. R. Dixon
R. F. Domagala
C. D. Fletcher
R. R. Fullwood
W. R. Gambill
M. L. Gildner
R. C. Gwaltney
C. L. Hahs
R. M. Harrington
J. B. Hayter
D. L. Henderson
L. M. Jordan
R. A. Lillie
C. R. Luttrell
T. J. McManamy
M. Mueller
T. Nishigori
R. E. Pawel
F. J. Peretz
R. T. Primm, III
J. W. Richardson
A. E. Ruggles
J. M. Ryskamp
J. L. Snelgrove
W. F. Swinson
R. P. Taleyarkhan
H. R. Thresh
L. M. Wang
C. D. West
T. C. Wiencek
G. T. Yahr

June 1989

Prepared by the
OAK RIDGE NATIONAL LABORATORY
Oak Ridge, Tennessee 37831
operated by
MARTIN MARIETTA ENERGY SYSTEMS, INC.
for the
U.S. DEPARTMENT OF ENERGY
under Contract No. DE-AC05-84OR21400

MARTIN MARIETTA

Internal Correspondence

MARTIN MARIETTA ENERGY SYSTEMS, INC.

June 27, 1989

Distribution

Monthly Progress Report for May 1989

The attached monthly reports are unedited, unreviewed, timely reports of work done. In some cases, the work is incomplete or preliminary. In others, problems are identified that will, presumably, be resolved in later reports. I ask you, therefore, to be cautious in using this information; it has not been given patent clearance and is intended as a means of internal communication. If you have any questions or reactions to any of the results reported, you could contact the author directly.

Some items described in our monthly reports may be patentable, which is why I have been asked to remind you of the "warning" paragraph on the cover of this report, and of the subcontract terms relating to such material.

Your Monthly Progress Report contributions should be submitted to James A. Johnson, FEDC Bldg, MS-8218. However, if you are using the U.S. mail services, please note that our mailing address is Advanced Neutron Source Project, Oak Ridge National Laboratory, FEDC, MS-8218, P. O. Box 2009, Oak Ridge, TN 37831-8218. Your reports are due to James by the 10th of the month, and reports received after that date may or may not be included in the Monthly Progress Report.

Colin D. West, Director, ANS Project, FEDC (4-0558)

:MRM

Attachments

PROJECT HIGHLIGHTS FOR MAY 1989

BUSINESS

The non-technical activities for the month of May were dominated by briefings to various organizations. The French Director of the Institut Laue-Langevin (ILL) visited ORNL, received a briefing on the ANS project and provided the project with an overview of the future plans for the ILL. A presentation was given to the ORNL Site Planning Committee as part of the review of the preferred ANS site. Senate staff visited the laboratory and attended a presentation on ANS that was given as part of an overview of major activities at ORNL. A briefing on the ANS was given to ORNL security to broaden the interface between project planning and the laboratory's security requirements.

TECHNICAL

WBS 1.1.1 - Reactor Core Development

a) Work continued on the optimization and sensitivity of PS2 type core designs (see Attachment 1).

b) Estimates of Cf-252 and Es-254 production within the ANS current design concept have now been made (see Attachment 2).

c) The idea of a Zircalloy core pressure boundary tube (CPBT), a concept originated by INEL, is being reconsidered. With the anticipated lower heat loads of the new cores, cooling a Zircalloy vessel may now be feasible, and the softer spectrum of the present cores makes the improvement in peak flux encountered by using Zircalloy significant (see Attachment 3). Note that the flux improvements shown are for cores with different reactivities. If fuel were removed to reduce k-effective back to that required for a 14 day cycle, the total peak flux improvement may be as much as 10%. The appendices in this attachment were too lengthy to include in the monthly but can be obtained from Trent Primm if needed.

d) A summary of recent work on relationships among various critical heat fluxes has been prepared (see Attachment 4).

WBS 1.1.2 - Fuel Development and Evaluation

a) The capsule of ANS fuels is awaiting irradiation in the first normal HFIR cycle (see Attachment 5). Delays in the restart of HFIR will result in further delays in this R&D task activity.

WBS 1.1.3 - Corrosion Loop

a) Data from CTEST No. 11 imply that the coolant temperature may be an important factor in estimating oxide because of its effect on formation of the protective iron-rich layer (see Attachment 6).

WBS 1.1.5 - Control Concepts

a) Work continued on the use of control rod movement, burnable poison placement, and radial fuel grading to shape the power distribution within the ANS core (see Attachment 7).

WBS 1.1.7 - Structural Analysis

a) Last month it was reported that "the addition of combs will probably make the PS2 core plates stable under the anticipated flow rates". This conclusion did not account for the use of intermittent weld attachments. It is anticipated that this will reduce the critical velocity by as much as 20%. With this reduction, the present combination of flow velocity and plate geometry does not provide enough margin to assure plate stability (see Attachment 8).

WBS 1.1.8 - Cold Source Development

a) A 2D neutronics analysis of a combined liquid nitrogen-15 and LD2 cold source geometry has been initiated (see Attachment 9).

WBS 1.1.9 - Instrument Development

a) A survey of current detector capabilities and limitations has been made and some initial results are available (see Attachment 10).

b) A comparison of beam tube designs at Saclay and ILL has been performed that analyzes the efficiency gains achieved by the Saclay design (see Attachment 10).

c) Information from the nuclear and fundamental physics community has now been obtained that will allow more detailed conceptual layout studies of a second-floor beam room (see Attachment 10).

WBS 1.1.11 - Neutron Transport and Shielding

a) A transport model of the PS2 reference core has now been developed (see Attachment 11). As noted in that attachment, the results reported are very preliminary and more detailed information will be supplied in future monthlies.

WBS 1.2.3 - Safety Activities

a) Portions of the RELAP loop model have been assembled by INEL and are under review (see Attachment 13 and Attachment 2).

b) Preliminary discussions have been held with SNL staff concerning fuel-coolant interactions for the ANS fuel (see Attachment 13).

WBS 1.2.5 - Quality Assurance Activities

a) An audit was initiated of the HANS-1 capsule for fuels irradiation experimentation at HFIR (see Attachment 14).

WBS 1.3 - Reactor Systems

a) Design of the removable CPBT and the hardware for handling spent fuel, targets, etc. have been identified as the key design decisions for the reactor systems task (see Attachment 15).

WBS 1.4 - Experiment Systems

a) Allocation of experiment space in all areas of the facility has been identified as the key decision task for experiment systems (see Attachment 15).

WBS 1.5 and WBS 1.6 - Balance of Plant

a) Two principle design decisions have been identified for this task: (1) develop sizing, layout and equipment for the normal and emergency primary coolant systems and (2) define the components and operating parameters for the containment concept (see Attachment 15).

LIST OF ATTACHMENTS

1 More on Optimization and Sensitivity of PS-2 Type Core Designs, by C. D. West

2 INEL Monthly Progress Report, by J. M. Ryskamp, et al.

3 Reactor Physics Studies, by R. T. Primm, III

4 Heat Removal Monthly Progress Report, by W. R. Gambill

5 Fuel Development and Evaluation, by G. L. Copeland; Management/Experiment Design, by J. L. Snelgrove; Fuel Development and Fabrication, by R. F. Domagala, T. C. Wiencek, and H. R. Thresh; Structural Changes in Irradiated U_3Si and U_3Si_2 Determined by Neutron Scattering, by R. C. Birtcher, M. Mueller, and J. W. Richardson; and Ion Irradiation Simulation of Fuel Burnup, by R. C. Birtcher and L. M. Wang

6 ANS Corrosion Test Loop Monthly Progress Report, by R. E. Pawel, et al.

7 Limitations of "Only Radial Grading" to Improve the Thermal Hydraulic Performance of the Core, by F. C. Difilippo

8 Structural Stability of Involute Fuel Plates, by R. C. Gwaltney, C. R. Luttrell, W. F. Swinson, and G. T. Yahr; and ANS Materials Characterization, by D. J. Alexander

9 Design Calculations for the ANS Cold Source, by D. L. Henderson, R. A. Lillie, and R. G. Alsmiller, Jr.

10 Neutron Sciences Monthly Progress Report, by J. B. Hayter

11 Preliminary Considerations on Some Transport Characteristics of the Final Preconceptual Design Core, by T. Nishigori

12 Heating Rate Calculations for the ANS, by Y. Y. Azmy

13 ANS Project Safety Activities Monthly Progress Report, by R. M. Harrington; RELAP5 Code Development and Validation, by A. E. Ruggles; RELAP5 Model Development and Review, by N. C. J. Chen; Assumptions Used in Developing the RELAP5 Model of the ANS Heat Exchanger Loop, by C. D. Fletcher; ANS Severe Accident Analysis Report, by R. P. Taleyarkhan; and Probabilistic Risk Assessment for ANS, by R. R. Fullwood

14 Quality Assurance Activities Monthly Progress Report, by M. L. Gildner and L. M. Jordan

15 Design Activities on the ANS Monthly Progress Report, by F. J. Peretz; Component Cooling Calculations, by J. R. Dixon; and Experiment Systems, by R. M. Beckers, C. L. Hahs, and T. J. McManamy

Mickie R. McBee

Mickie R. McBee

ATTACHMENT 1

MORE ON OPTIMIZATION AND SENSITIVITY OF PS-2 TYPE CORE DESIGNS

C. D. West

The monthly report for April described how the correlations between fuel element length, permissible power density, and rendement could be used to optimize the core height to maximize power capability, thermal neutron flux and margin to incipient boiling, or to minimize the power needed for a given flux.

In this note, the minimum power density needed to provide a given peak thermal neutron flux is calculated. The results, along with those from last month's report, are used to refine some sensitivity plots previously calculated. The symbols and equations used are those defined in the April monthly report.

Although the incipient boiling limit is one bound on the power that can be accommodated by a given core, there may be other considerations. For example, we might wish to minimize heat flux, perhaps to reduce oxide growth. For cores with similar peaking factors, plate thickness and gap,peak heat flux will be minimized by minimizing the power density. For a given neutron flux, what core length minimizes the power density and what power level must it be operated at?

$$\bar{\rho} = \frac{\phi}{A H_L (\bar{E}_0 - \bar{E}_1 H_L)}$$

The minimum occurs when the denominator is maximized, i.e. when $H_L = E_0/2E_1 = 1232$ mm. However, this is a non-physical case because the incipient boiling power density falls to zero when $H_L = \rho_0/\rho_1 = 1026$ mm. Therefore, the minimum power density core will be the one for which H_L is as large as possible within the allowable (incipient boiling) power density correlation.

Now,

$$\bar{\rho}(\phi, H_L) = \frac{\phi}{A H_L (\bar{E}_0 - \bar{E}_1 H_L)}$$

and $\bar{\rho}(H_L)$ for the minimum power density core $= \bar{\rho}_{max}(H_L) = \rho_o - \rho_1 H_L$. Therefore,

$$\bar{\rho}_{min}(\phi) = \frac{\phi}{A H_L (E_o - E_1 H_L)}$$

where

$$H_L = \frac{\rho_o - \bar{\rho}_{min}(\phi)}{\rho_1}$$

so

$$\bar{\rho}_{min}(\phi) = \frac{\phi}{\frac{A}{\rho_1}\left(\rho_o - \bar{\rho}_{min}(\phi)\right)\left(E_o - \frac{E_1}{\rho_1}\left(\rho_o - \bar{\rho}_{min}(\phi)\right)\right)}$$

This cubic equation in $\bar{\rho}_{min}$ can be solved analytically. However it is easier (much easier) to use TK Solver. The results are shown in Table 1.

Table 1. Specifications of PS-2 type cores designed to minimize power density

Relative flux $MW.m^{-2}$	Power density MW/L	Volume L	Power MW	Heated length mm
1.0 x 1069.22*	5.47	67.4	368	449
0.9 x 1069.22	3.93	91.8	361	611
0.8 x 1069.22	3.25	102.5	334	683
0.7 x 1069.22	2.71	110.0	301	740
0.6 x 1069.22	2.25	118.5	266	789
0.5 x 1069.22	1.82	125.2	228	834

*The maximum achievable value - see April monthly report.

Note that all of these cores (apart from the nominal one) are much longer than the ones used to derive the PS-2 correlations, and the inlet pressure would need to be raised - which might affect the incipient boiling correlations. Nevertheless, in case we wish to consider minimizing the power density (for example, to reduce oxide growth) these figures may be a useful guide.

Figures 1 and 2 show the power and power density relationships assuming (which is approximately true) that an optimized core operating at 100% of the incipient boiling limit, instead of only at 90% as is the case for the present reference core, would give a maximum unperturbed flux $\sim 10^{20}\ m^{-2}.s^{-1}$.

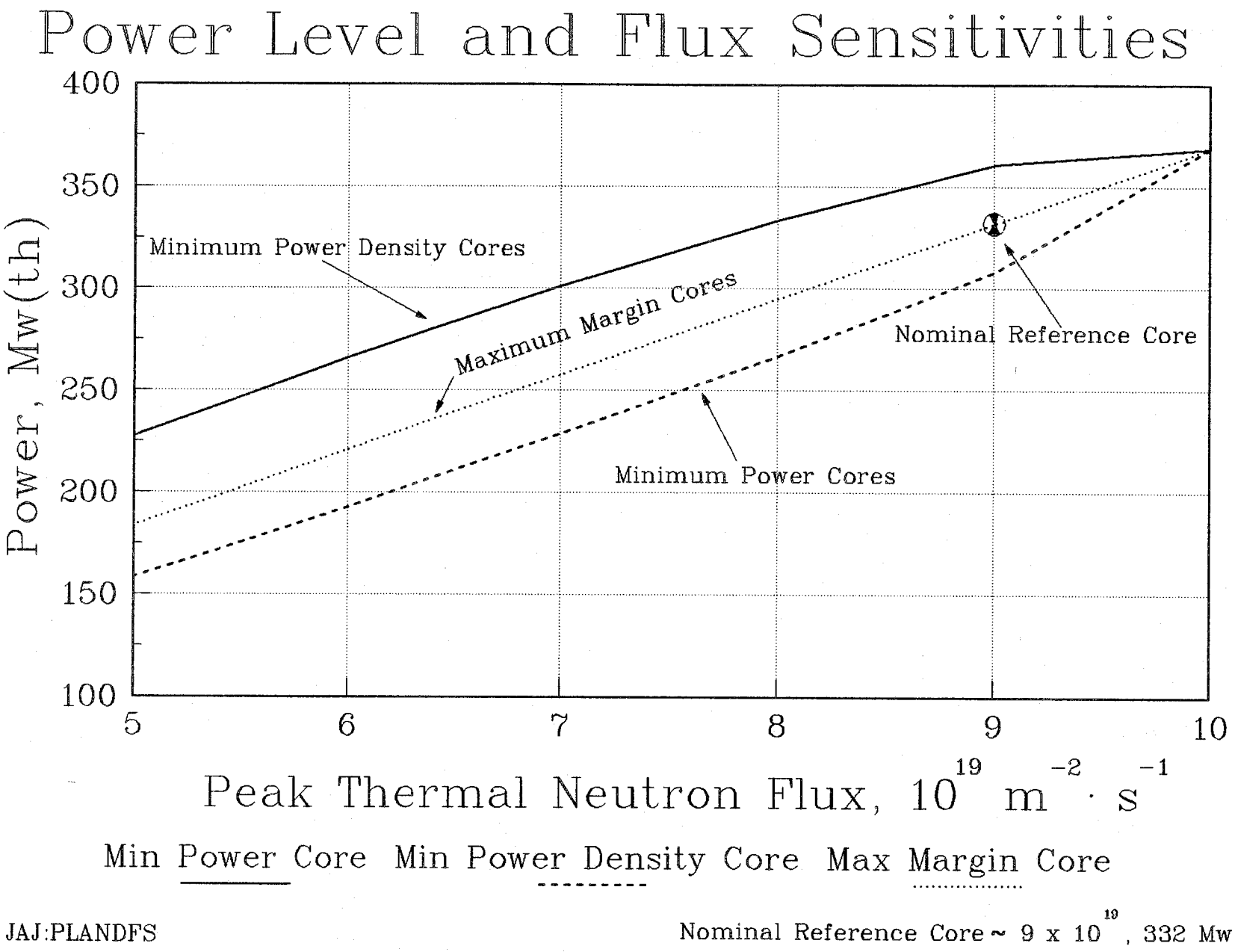
Power Level and Flux Sensitivities
400
350
300
250
200
150
100
Power, Mw(th)
Minimum Power Density Cores
Maximum Margin Cores
Nominal Reference Core
Minimum Power Cores
5
6
7
8
9
10
Peak Thermal Neutron Flux, 10^{19} $m^{-2} \cdot s^{-1}$
Min Power Core
Min Power Density Core
Max Margin Core
JAJ:PLANDFS
Nominal Reference Core ~ 9 x 10^{19}, 332 Mw

Figure 1

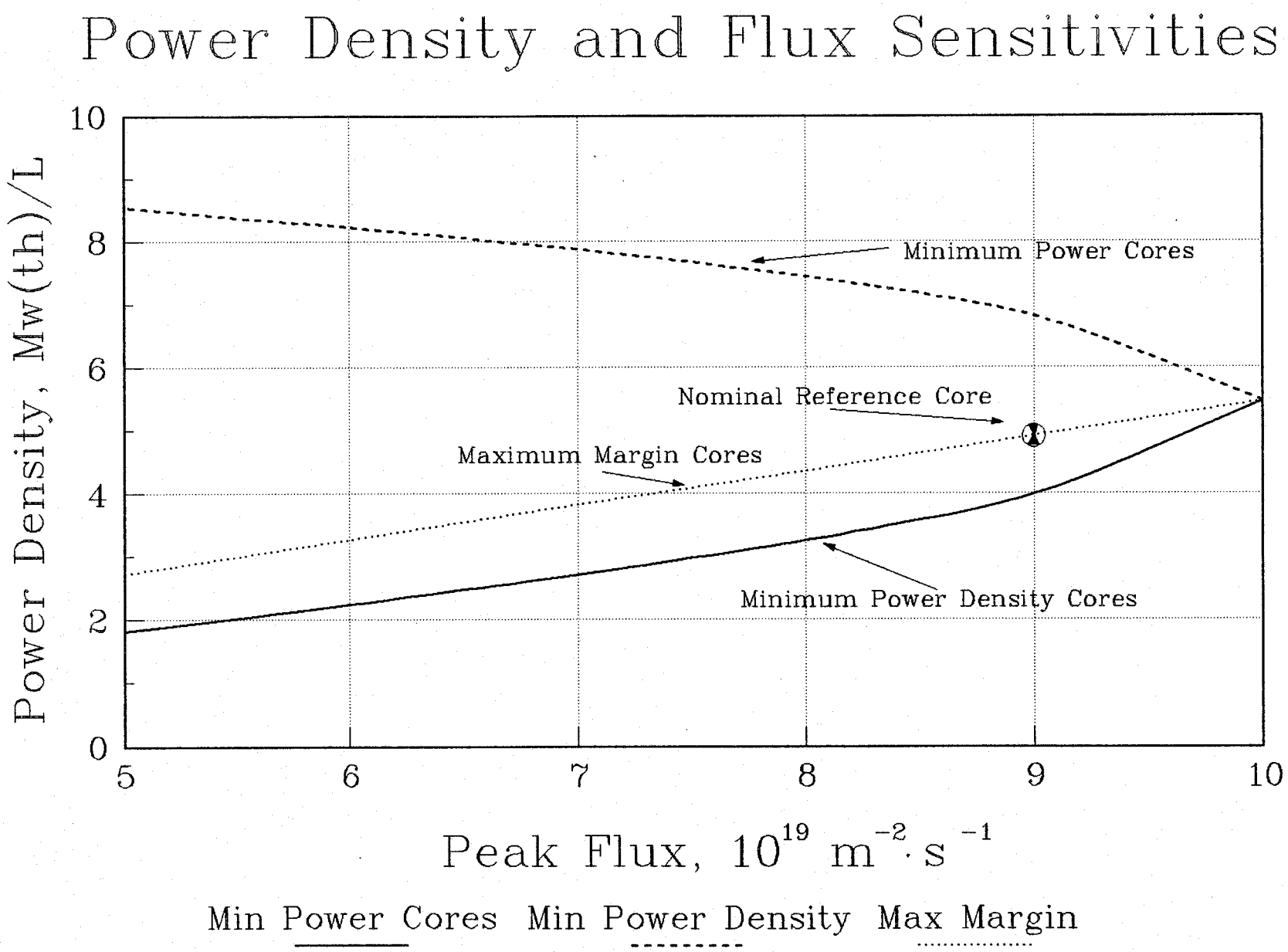

JAJ:PDANDFS

Figure 2

ATTACHMENT 2

ADVANCED NEUTRON SOURCE
IDAHO NATIONAL ENGINEERING LABORATORY
MONTHLY REPORT FOR MAY 1989

J. M. Ryskamp, C. D. Fletcher, and E. S. Marwil
FTS 583-9533 or (208) 526-9533

Target Irradiation Analyses

R. T. Primm of ORNL supplied infinite dilute four-group cross sections for several transplutonium nuclides. His cross sections for Cf-252, Cf-253, and Es-253 were added to the PDQ-7 model input. This will allow a more accurate estimate of Cf-252 and Es-254 production. All target isotope cross sections were generated for fresh targets. Exposure-dependent cross sections may be needed for accurate production calculations. However, the beginning-of-target-cycle cross sections are adequate for assessing the impact of target location on various production rates.

The PDQ-7 model of the reference core was run a few times through the 14-day cycle to flatten the core power by grading the U-235 distribution radially and axially. The core contained 18.24 kg U-235 and 15 g B-10. The B-10 was distributed in the aluminum end caps of the top fuel element and in the upper end caps of the bottom fuel element. The hafnium control rods in the central hole were withdrawn downward with fuel exposure to maintain a core multiplication factor close to unity. With the reactor operating at 350 MWf, the peak thermal neutron flux in the reflector is $7.84 \times 10^{19}\ m^{-2}s^{-1}$.

An area (regions 1 and 2) of high fast neutron flux for engineering materials irradiation is located adjacent to the inside of the upper fuel element. An area (regions 3, 4, and 5) of high epithermal flux for production of transplutonium isotopes is located between the outside of the lower fuel element and the core pressure boundary tube (CPBT). An area (regions 6, 7, and 8) of high thermal neutron flux for other isotope production is located outside the CPBT in the large heavy water reflector. Table 1 presents the neutron fluxes in these regions. Region 1 is at the axial midpoint of region 2, and region 3 is at the axial midpoint of region 4. This indicates the extent of axial flux variation in these regions. Table 1 shows that a wide variety of flux spectra are available with high flux magnitudes.

Selection of the target positions has been examined. Materials irradiation and transplutonium targets should be as close to the fuel as possible to be in the hardest spectra available. For example, region 4 is adjacent to the lower fuel element, and region 5 is similar to region 4 but further out radially, just inside the CPBT. Figure 1 illustrates the Cf-252 and Es-254 production versus time in the reactor for these two positions, each with 30 identical curium targets. Region 4 produces a bit more Cf-252 and a lot more Es-254. The Es-254 obtains a lower saturation value in region 5. Thus the target positions are important depending on the desired isotopes that need to be produced. However, safety concerns such as flow blockage of the upper fuel element caused by a loose target may limit the transplutonium targets to region 5.

TABLE 1. EXPOSURE-DEPENDENT FOUR-GROUP NEUTRON FLUXES IN VARIOUS TARGET IRRADIATION POSITIONS IN THE ADVANCED NEUTRON SOURCE AT 350 MW.

Target Region	Region Volume (liters)	Cycle Time (days)	Neutron Flux (10^{19} m^{-2} s^{-1})			
			Group 1	Group 2	Group 3	Group 4
1	0.97	0	1.641	4.606	5.111	0.880
		7	1.563	4.398	5.195	1.090
		14	1.436	3.970	4.939	1.659
2	7.62	0	1.427	3.969	4.537	0.915
		7	1.450	3.970	4.745	1.250
		14	1.348	3.635	4.598	1.926
3	1.25	0	1.066	2.883	2.759	1.764
		7	1.049	2.911	3.008	1.955
		14	1.177	3.440	3.897	2.492
4	9.86	0	0.924	2.558	2.672	1.733
		7	0.924	2.615	2.933	1.979
		14	1.066	3.123	3.756	2.637
5	11.68	0	0.223	1.132	2.021	3.819
		7	0.218	1.145	2.154	4.266
		14	0.242	1.324	2.615	4.298
6	11.48	0	0.090	0.437	1.282	6.377
		7	0.090	0.440	1.335	6.906
		14	0.078	0.408	1.335	7.365
7	56.20	0	0.000	0.005	0.052	3.801
		7	0.000	0.005	0.052	3.975
		14	0.000	0.004	0.051	4.156
8	171.59	0	0.000	0.000	0.000	0.832
		7	0.000	0.000	0.000	0.871
		14	0.000	0.000	0.000	0.919

Group Energy Boundaries

Group 1	0.821 MeV < E < 17 MeV	
Group 2	5531 eV < E < 0.821 MeV	
Group 3	0.683 eV < E < 5531 eV	
Group 4	0.0 eV < E < 0.683 eV	

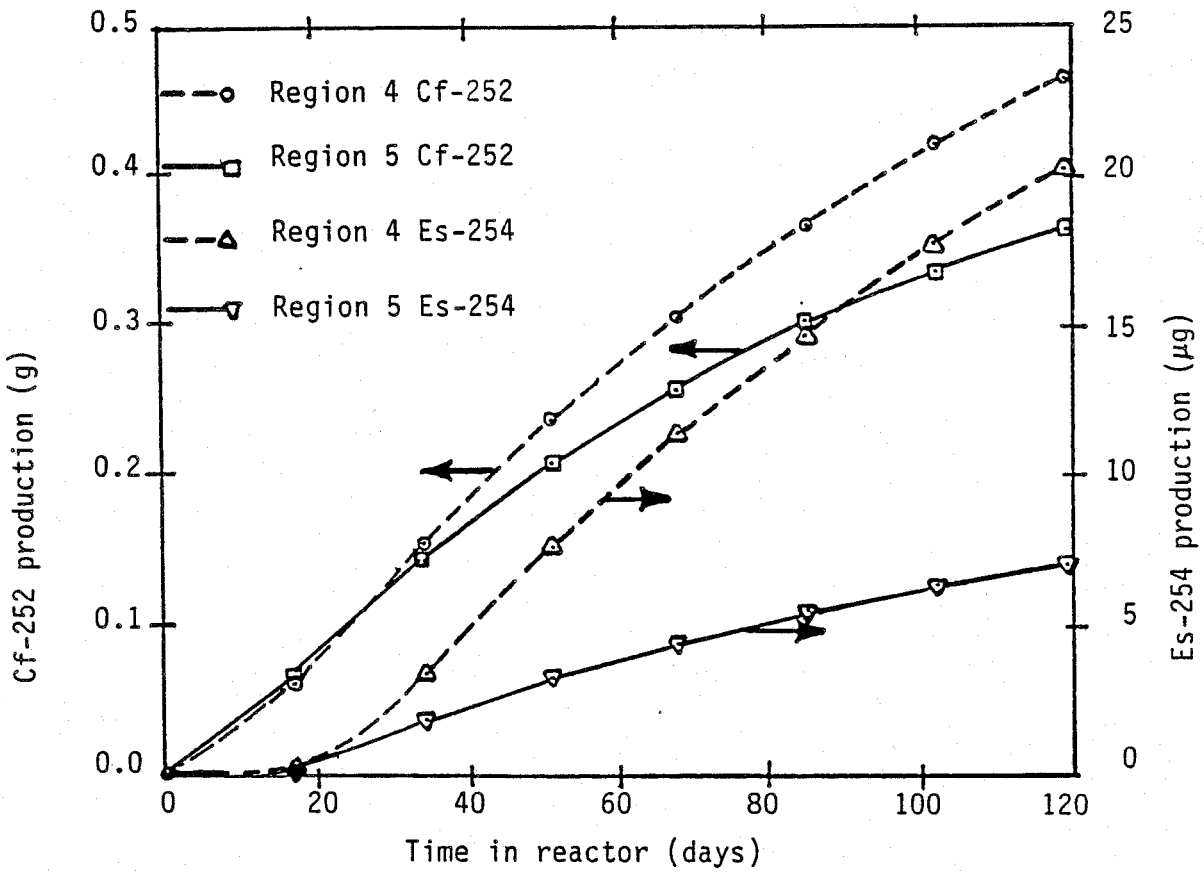

Fig. 1. Cf-252 and Es-254 production as a function of target time depends on the target's location in the Advanced Neutron Source. Targets closer to the lower fuel element produce more Cf-252 and Es-254.

The axial variation of fluxes and isotope production in the transplutonium targets is given in Table 2. Control rod withdrawal from the central hole significantly shifts the axial profile over the 14-day cycle. The highest Cf-252 and Es-254 production per unit target volume occurs in the top of the targets (near the core midplane) and decreases slowly toward the bottom of the targets. The production density is roughly proportional to the epithermal (group 3) and thermal (group 4) fluxes. More neutrons yield higher production as expected.

The yearly production estimates are in the right range of the ANS production requirements of 1.5 g Cf-252/year and 40 μg Es-254/year. For example, from Figure 1 region 4, if 30 fresh curium targets are placed in the reactor three times each year and irradiated for seven 14-day full power plus 3-day shutdown cycles (7 x 17 = 119 days), the ANS will produce about 1.4 g Cf-252/year and 61 μg Es-254/year. Selecting the optimum target time in the reactor is complicated because other nuclides produced in the targets can be recycled into new targets. Therefore, the initial target composition changes over several years, which increases the annual production capability.

The actual target loading (g actinides) and number of targets that can be placed in the core influence production capability and depend on the neutron and gamma heating and the ability to cool the targets. Currently, about 0.55 MW at 0 days and 0.36 MW at 14 days are produced from fission in 30 targets. This may be a significant heat removal problem and limit the production capability.

The production estimates are adequate to influence the decision on where to locate the targets. However, exposure-dependent cross sections that also account for the effect of smearing the targets into the r-z ring in the PDQ-7 model must be used for more accurate production estimates. The targets have very low actinide concentrations, so the self-shielding effects are not expected to be large. In addition, there is very little target-to-target self-shielding because the targets are dispersed around the fuel element. This is quite different from the High Isotope Flux Reactor where the transplutonium targets are located close together in the central hole.

Cycle Depletion Models

Modifications were made to the fuel depletion model to provide the capability to analyze targets in the reactor over several fuel cycles. A time step from 14 to 17 days at a very low power level (35 kW) was added to represent a 3 day refueling time. This accounts for the decay of Cf-253 (17.8 day half-life), Es-253 (20.5 day half-life) and other nuclides during refueling when the targets are left in the reactor. Therefore, the Cf-252 and Es-253 concentrations decrease during refueling of each cycle, but this detail is not shown in Figure 1.

Every 17 days new fuel elements are loaded, yet the targets remain in the reactor. The presence of the targets has very little effect on neutron fluxes over the cycle. Therefore, we can generate exposure-dependent fluxes for the first 17-day cycle. These same fluxes can be used for every 17-day cycle. Thus the second cycle PDQ reads in fluxes at each time step computed at each time step of the first cycle. Fresh fuel concentrations are read in for the start of the second

TABLE 2. AXIAL VARIATION OF FLUXES AND ISOTOPE PRODUCTION IN TRANSPLUTONIUM TARGETS.

Target Region	Region Volume (liters)	Cycle Time (days)	Neutron Flux (10^{19} m^{-2} s^{-1}) Group 1	Group 2	Group 3	Group 4	Cf-252 (g)	Es-254 (μg)
Top	1.748	0	0.837	2.637	3.390	1.782		
		7	0.906	2.844	3.845	2.291		
		14	0.990	3.153	4.502	3.047		
		119					0.0977	4.122
Mid-Top	2.560	0	1.061	2.909	3.024	1.895		
		7	1.072	3.015	3.368	2.168		
		14	1.173	3.458	4.185	2.711		
		119					0.1333	5.718
Middle Region 3	1.249	0	1.066	2.883	2.759	1.764		
		7	1.049	2.911	3.008	1.955		
		14	1.177	3.440	3.897	2.492		
		119					0.0606	2.756
Mid-Bottom	2.560	0	0.949	2.538	2.383	1.601		
		7	0.923	2.525	2.551	1.747		
		14	1.108	3.156	3.456	2.338		
		119					0.1111	5.227
Bottom	1.748	0	0.670	1.761	1.802	1.618		
		7	0.637	1.719	1.893	1.748		
		14	0.845	2.328	2.719	2.659		
		119					0.0616	2.509

Average and/or total values for the transplutonium targets (region 4) are given in Table 1 and Figure 1.

cycle, but the target concentrations from the end of the first cycle are read in. Fuel and target depletion throughout the second cycle are performed with first cycle fluxes read in at each time step. Thus at the end of the second cycle, the fuel has the same composition as at the end of the first cycle, but the targets have gone through two cycles (34 days). This process is repeated for several cycles and is called "redepletion" in PDQ-7. Thus, we pay a lot to compute the eigenvalue and fluxes in the first cycle, but nothing to compute them in subsequent cycles. Table 3 illustrates this cost difference. Most of the cost of the subsequent cycles is associated with nuclide depletion.

TABLE 3. COST TO RUN THE PDQ-7 MODEL OF THE ANS ON THE INEL CRAY-XMP WITH DIFFERENT DEPLETION OPTIONS.

Depletion Method	Point	Point	Block	Block
17-day Cycle	First	Subsequent	First	Subsequent
Cost ($/cycle)	125	86	40	5

The PDQ-7 model is 4-group, two-dimensional with 99 x 140 mesh points (r-z), diffusion theory, and with six time steps for the 17-day cycle.

Table 3 also shows the cost difference between depletion at each mesh point and depletion for each block or region. Block depletion is significantly cheaper than pointwise depletion. Comparisons between methods show that the differences in fluxes and concentrations are very small. This results partly from having so many fuel regions (160) to provide an accurate depletion model. The Cf-252 and Es-254 concentrations differ by less than 0.4% after two cycles between the two methods. Thus a very inexpensive model has been developed to accurately compute target concentrations over several cycles.

Block depletion can also save considerable computer expense for power flattening or setting control rod positions throughout the cycle. For example, full cycle depletions could be performed with block depletion several times iterating on a set of control rod positions. Then a final cycle with pointwise depletion could be run to confirm the flux and power distributions. This would greatly reduce computer cost.

VENTURE-PC Conversion and MCNP Installation

Assisted Trent Primm in using the VENTURE code on the Livermore CRAY 2. Several minor changes in the input data file were required to obtain a successful run.

In a separate consultation, there was a problem in running a depletion calculation with the Burner module. The file RZFLUX was apparently deleted from the internal table in VENTURE. This occurred in all VENTURE-PC versions (Livermore CRAY 2, INEL CRAY X-MP and PC) and has been referred to the University of Cincinnati for resolution.

The Los Alamos CRAY Unicos version of the MCNP code is being installed on the INEL CRAY X-MP. This will be available for use by about the middle of June.

RELAP5 System Modeling

The RELAP5 model of the ANS heat exchanger loop was completed and checked out. Main circulating pump rated conditions were adjusted to match the hot and cold leg distribution header conditions (pressures, temperatures, and flow rates) provided by the core region model. The single checked-out heat exchanger loop model was then reproduced twice to provide the three independent heat exchanger loop models. The models of the core and three coolant loops were then joined and satisfactorily executed together as a system model at full-power steady conditions.

The shutdown cooler loop model has been developed and is currently being checked out. This model will be sized to provide a rated flow through the core assuming no heat exchanger loop flow. The two independent shutdown cooler loops have been combined into one in the model. No shutdown cooler loop flow is anticipated during normal operation because of the back pressure created by the head of the main circulating pumps. Once checked out, the shutdown cooler loop model will be added to the ANS system model described above.

The pressurizing pump system model is currently under development. Primary system pressure is presently being artificially controlled in the system model. Once implemented, this model will control the primary coolant system pressure through modulation of the letdown valves. Development of this model will be facilitated by experience gained with RELAP5 modeling of a similar pressurizing pump system in High Flux Isotope Reactor.

A technical exchange meeting was attended at Oak Ridge on May 25. The RELAP5 model was informally presented and discussed, and points of contact were established with the ANS designers. More recent data were obtained on the heat exchanger loop layout and on the expected water pool temperature. This data will be incorporated into the RELAP5 model at this time.

Reactor Physics Studies

R. T. Primm, III

Intermediate Reference Core for Advanced Neutron Source (ANS) Studies

At a meeting held on April 3, 1989, R. G. Alsmiller, Jr. requested that an intermediate reference design be selected so that preliminary investigations by various members of the Advanced Neutron Source Design Team would not have to await the completion of the fuel grading procedure. This memorandum documents the completion of that task.

A calculation designated D9 by Difilippo was selected to be the intermediate reference design. The geometric configuration of the core is that selected by ANS Project Management on February 1, 1989. The fuel thickness was graded radially but not axially. Boron (13.4 grams) was placed in the endcaps of the fuel elements. The hafnium control rods were withdrawn upward (scram down). Appendices are as follows:

A - Flux and flux ratios (beginning-of-life)

B - Flux and flux ratios (end-of-life)

C - Fuel distribution (beginning-of-life)

D - Fuel distribution (end-of-life)

E - Power density ratio (all time steps)

F - Fission source data (samples only, full tables too long)

G - Listing of power factor data set.

The U-235 loading for the intermediate core is 14.9 kg. The control rod position and Boron-10 concentration as a function of cycle time are shown in Table 1.

Table 1

Control Rod Positions for Various Cycle Times

Time in Cycle (days)	Control Rod Position[a] (mm)	Core Boron-10 Inventory (g)	K-effective
0	257	13.43	1.006
3.5	257	5.95	1.003
7.0	257	1.84	1.008
10.5	87	0.39	1.020
14.0	–[b]	0.06	1.005

[a]Distance measured from top of fueled region of the core to lower Hf loaded edge of control rod.
[b]Control rod not present in model.

Additionally, two computer files have been generated. These are fission source distributions at all time steps and peak point-to-core-average power densities for each zone for all time steps. The power density file - POWER.DAT - is listed in Appendix G and stored on Primm's file space on the STC10 VAX (user ID-RTP). The fission source files are stored in a catalogued dataset on the IBM-3033 named X.RTP24062.INTERMED.FISSOR.

Guidance on ANS Neutronics Priorities

As requested by Selby, an extensive list of neutronics issues was reviewed and assigned priorities. A memorandum containing the concensus viewpoint of Alsmiller, Primm, and Difilippo was forwarded to Selby.

Four-Group Cross Sections for Actinides Having Mass Numbers Greater Than 242

A letter was sent to J. M. Ryskamp describing the production of a four-group library containing data for the higher actinides. The four-group data were collapsed from an 84-group library which itself is derived from a preliminary ENDF/B-V dataset. The data were transmitted electronically to the Lawrence Livermore Cray and copied by INEL personnel.

Neutronic Effects on the Final Preconceptual Core Design of a Zircalloy Pressure Vessel

The model of the final preconceputal core design was modified to include a 10 mm zirconium vessel rather than the 13 mm aluminum vessel. The remainder of the model was unchanged from that described in the ANS progress report for January 1989. The results are shown in Table 2.

Table 2

Calculated Neutronnics Parameters for Final Preconceptual Core Design[a]

	Pressure Vessel Material		
	Al-6061[b]	Zirconium[c]	None
K-effective (Beginning-Of-Life)	1.287	1.3215	1.3667
Estimated Peak Thermal Flux in Reflector (10^{19}n/m^2/s)	8.005	8.419	8.725

[a]Core model documented in Primm contribution to ANS monthly report for January 1989

[b]Thickness = 13 mm.

[c]Thickness = 10 mm, Zircalloy -4 contains 96.91 wt % Zr, 1.59 wt % Sn, 0.5 wt % Fe, pure Zr metal assumed in calculation.

As noted in the footnote to that table, zircalloy contains trace quantities of alloying agents. Cross section data for tin are not available in the current library, but can be included in future libraries. The values in Table 2 can be regarded as estimates of the maximum flux and reactivity available with a zircalloy vessel. The zircalloy vessel calculations were performed on the LLL Cray using the PC version of VENTURE stored by E. Marwil, INEL.

Selby also requested a calculation with the pressure vessel removed. The results of this calculation are also reported in Table 2.

Miscellaneous

A draft Technical Memorandum titled "Advanced Neutron Source Final Preconceptual Reference Core Design" was reviewed and comments returned to C. D. West. Two figures showing the areas of the reflector in which the thermal flux exceeds either 80% of the peak (Fig. 1) or 90% of the peak (Fig. 2) were prepared. The data plotted are for the Intermediate Reference Core described earlier in this report. Note that the "arm" present on Fig. 1 is an artifact of the mesh size utilized in the calculation. The flux regions shown in each figure represent >X% of the peak thermal flux at that point in time (beginning- or end-of-life).

Fig. 1

CORE GEOMETRY AND USABLE FLUX VOLUME

(>80% of peak thermal flux)

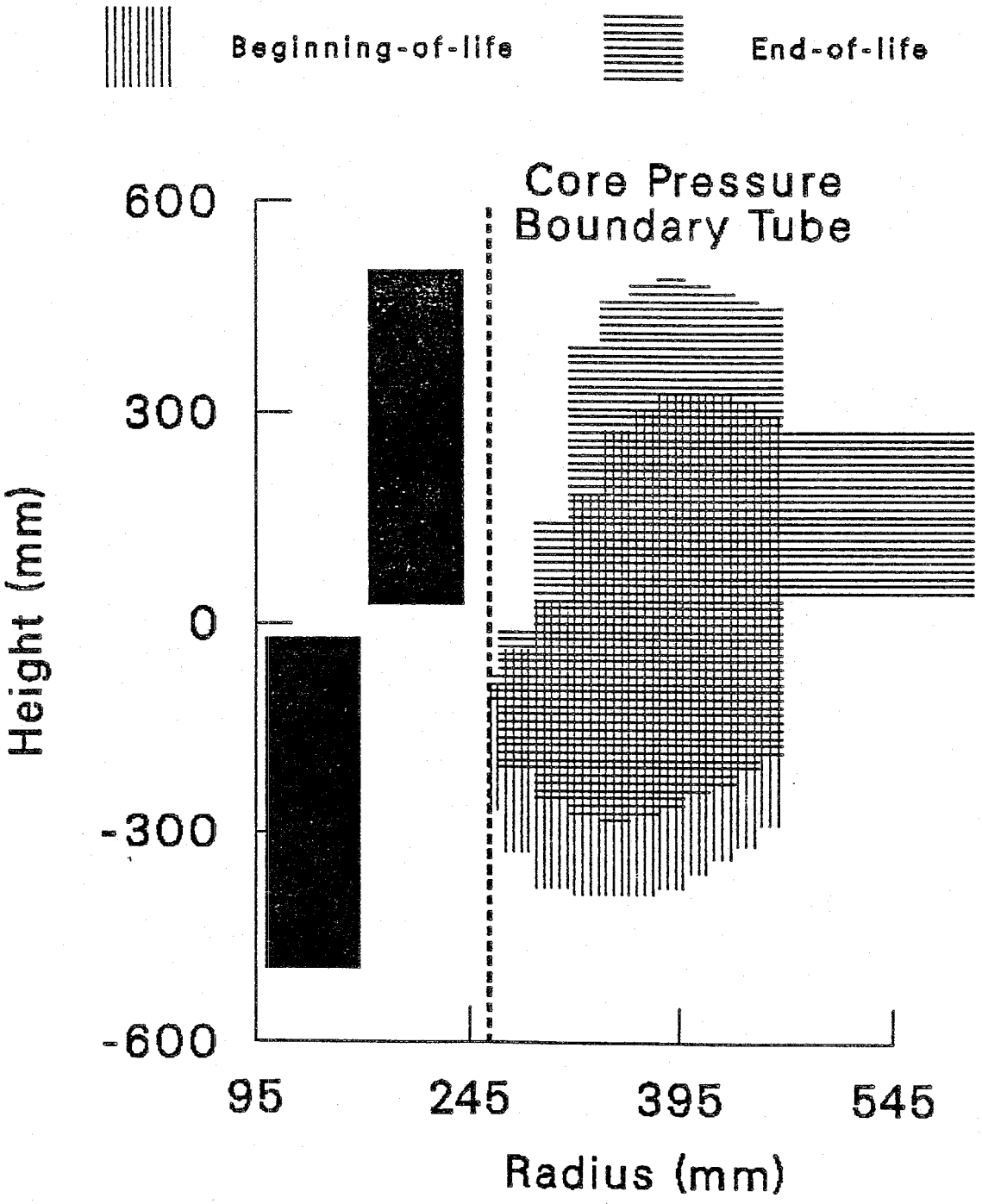

Fig. 2

CORE GEOMETRY AND USABLE FLUX VOLUME

(>90% of peak thermal flux)

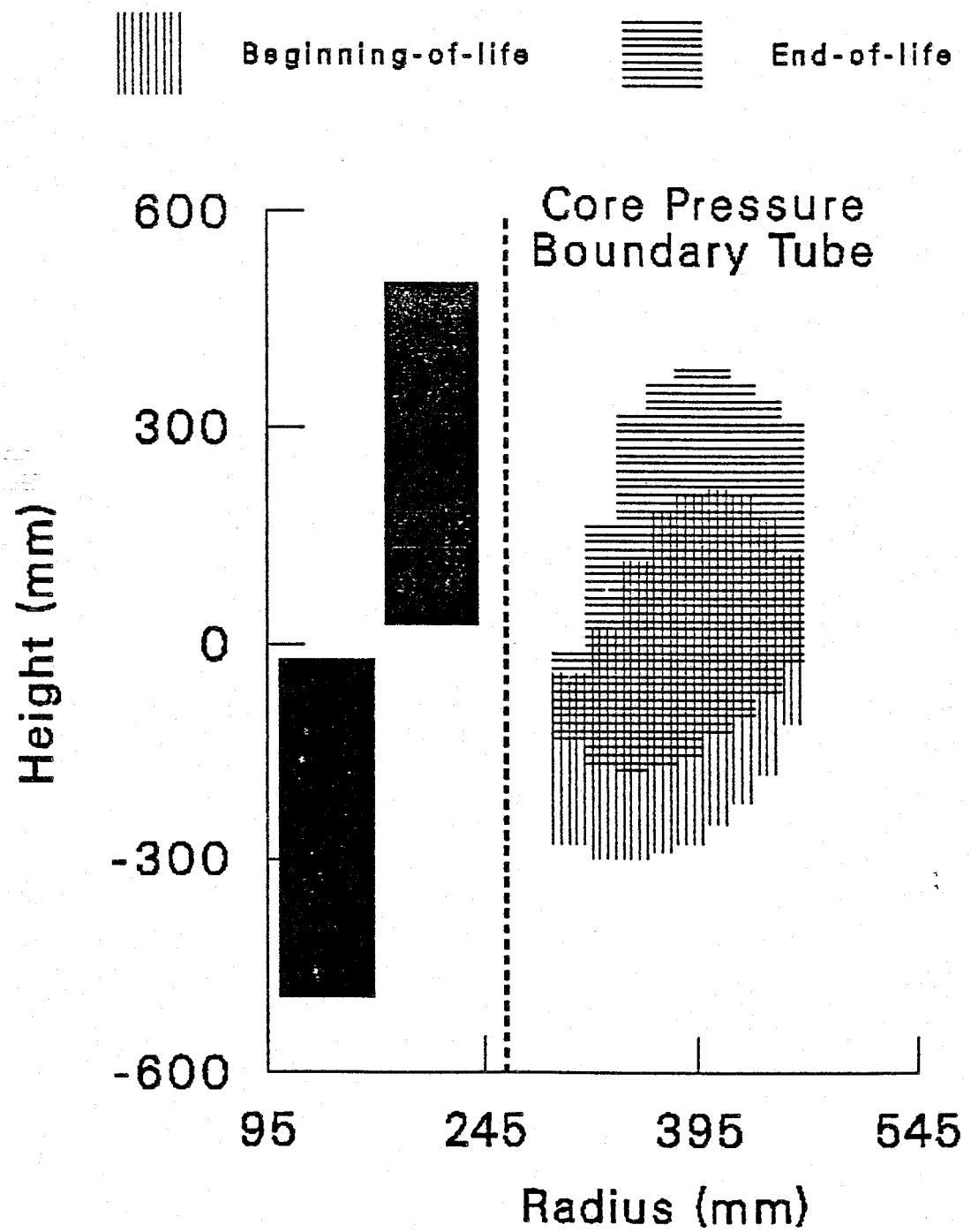

ANS Project – Heat Removal. Monthly Report for May 1989.

W. R. Gambill

1. A letter describing recent work on relationships among various critical heat fluxes was distributed; the text is included here as Attachment A.

2. A comparison was made between two methods of calculating the minimum nonboiling heat transfer coefficient h_{nb}. The older, conservative approach used h_{mean} from the Rohsenow-Clark correlation and $h_{min} = 0.826\ h_{mean}$ (TM-2421, November 1968). The newer method, used now for ANSR design, obtains h_{mean} from the more comprehensive Petukhov correlation and h_{min} from 0.94 h_{mean}. For the following conditions:

H_2O coolant	$L_h/d_e = 120$
$V = 27.43$ m/s	$\mu_b/\mu_w = 2.0$
$d_e = 2.49$ mm	$P = 4.0$ MPa

the result is shown in the graph included here as Attachment B, in which $(h_{nb})_{min}$ is plotted vs. bulk temperature t_b from 50°-150° C. The large increases in the heat transfer coefficient, tabulated below:

t_b (°C)	–	50	100	150
$(h_{new}/h_{old})_{nb,min}$	–	1.546	1.342	1.205

translate to significant increases in the critical heat flux ϕ_c, as calculated with the superposition correlations, as long as the forced-convection contribution to ϕ_c is large.

3. An "intermediate reference core" with radial fuel grading only was described in a letter of May 9 from F. C. Difilippo and R. T. Primm, III. The maximum values of the hot-spot factor (2.615) and of the hot-streak factor (2.052) occurred at BOC at the outer perimeter of the lower fuel element. It was noted that these neutronics-only ratios at BOC are very large compared with either the HFIR or with the assumptions made for the PS-2 Committee studies (values of 1.7 and 1.3, respectively) and indicate that the fuel must be graded axially as well as radially.

4. A letter summarizing some observations concerning a recent approach to correlating clad oxide data with bulk coolant temperature was distributed and is included here as Attachment C. Both the "hot patch" test-section approach mentioned in item e of the subject letter and the earlier proposal to conduct limited oxide tests under saturated pool-boiling conditions are in the early stages of implementation. In the former tests, a large change in local ϕ will occur with a significant change in t_i but only a quite

small change in t_b; in the latter, a large ϕ change will be accompanied by a quite small change in t_i and by none in t_b (ϕ = heat flux, t_i = interface temperature, and t_b = bulk temperature).

5. Several maximum temperature gradients in the new reference core at 333 MWt were calculated to be (rounded but by no more than 0.5 %):

Location	°C/mm
Of the D_2O, avg. from inlet to hot-streak exit	0.15
Across the cladding	87
Across the fuel	130
Across the oxide film	6900
Across the D_2O thermal boundary layer	23,000

The basis was the same set of T/H groundrules used in the calculations leading to the reference core selection.

Attachment A

Further consideration of critical flux phenomena in differing geometries with both natural-circulation and forced-convection flows has led to the development of several relationships among various critical heat fluxes in which $(\phi_c)_{SPB}$ [the ϕ_c for saturated pool boiling] is the common element. The cases addressed in the following summary and examples include:

$(\phi_c)_{NC,ODC}$ – natural circulation with an open downcomer,
$(\phi_c)_{NC,BDC}$ – natural circulation with a blocked downcomer,
$(\phi_c)_{BB}$ – countercurrent flow with a blocked base,
$(\phi_c)_{FC,sat}$ – forced convection of a saturated liquid, and
$(\phi_c)_{FC,sub}$ – forced convection of a subcooled liquid,

as well as two or three transition criteria. I described my experimental and analytical results for the blocked-base case in a 1965 paper titled "Overheating and Burnout of Blocked Vertical Channels Cooled Internally by Water" and in a section of a 1966 "Nuclear Safety" article. The notation is that used in my March and April 1989 monthly reports.

a. The ratio of the BDC and BB critical heat fluxes can be expressed as:

$$\frac{(\phi_c)_{BDC}}{(\phi_c)_{BB}} = \frac{L_h \delta_c^{1/2}}{100} \left(\frac{\Delta\rho}{\sigma}\right)_{sat}^{3/4} \left[1 + (\rho_v/\rho_\ell)^{1/4}\right]_{sat}^2 , \tag{1}$$

in which L_h is the heated length. For the HFIR and ANSR cores cooled by H_2O at P = 0.15 - 0.18 MPa and subcooled above and below the cores by 55°-83°C, the results are:

Core	L_h/D_e	$(\phi_c)_{BDC}/(\phi_c)_{BB}$
HFIR	200	2.0
ANSR	187	1.9

The ratio exceeds unity because the heated channels can pulse flow up and down in the BDC case but only upward in the BB case.

b. $(\phi_c)_{BB}$ can be related to $(\phi_c)_{SPB}$ in a general way:

$$(\phi_c)_{BB} = \frac{10(\phi_c)_{SPB}(\delta_c^{3/2}/L_h)(\Delta\rho/\sigma)^{1/4}}{[1 + (\rho_v/\rho_\ell)^{1/4}]^2} . \tag{2}$$

Equation (2) is valid for $\delta_c < (\delta_c)_{tr}$, a transition coolant gap above which flooding (holdup of incoming liquid by outflowing vapor) will not occur and will be replaced by pool boiling (SPB) as the cause of burnout.

c. The transition value of δ_c or of equivalent diameter $D_e (D_e = 2\delta_c)$ just noted is given by:

$$\frac{(D_e)_{tr}^{3/2}}{L_h} = 0.280 \left(\frac{\sigma}{\Delta\rho}\right)^{1/4} \left[1 + (\rho_v/\rho_\ell)^{1/4}\right]^2 . \tag{3}$$

For H_2O at P = 0.17 - 3.45 MPa, Eq. (3) can be reduced, within a maximum deviation of ± 9%, to:

$$(D_e)_{tr} = 0.2623 L_h^{2/3}, \tag{4}$$

in which the units of D_e and L_h are each (mm/25.4).

Restated, the nominal ϕ_c in the BB case is $(\phi_c)_{SPB}$ when $D_e > (D_e)_{tr}$ and $\phi_c = (\phi_c)_{BB}$ from Eq. (2) when $D_e \leq (D_e)_{tr}$. If the two ϕ_c mechanisms (flooding and SPB) coexist over a range of ϕ or L/D, $(D_e)_{tr}$ and $(\delta_c)_{tr}$ will also occupy an interval, rather than being characterized by a single value at a fixed length. I think the transition criterion proposed here is probably valid within a factor of two.

Applying the preceding:

L_h, mm(in.)	$(\delta_c)_{tr}$, mm(in.)	$(L_h/D_e)_{tr}$
25.4(1)	3.33(0.131)	7.6
254(10)	15.47(0.609)	8.2
474(18.66)[a]	23.42(0.922)	10.1
508(20)[b]	24.54(0.966)	10.4
1524(60)	51.05(2.01)	14.9
2540(100)	71.76(2.83)	17.7
25,400(1000)	333.0(13.11)	38.1

[a]ANSR.

[b]HFIR.

d. $(\phi_c)_{NC,ODC}$ is given by:

$$(\phi_c)_{ODC} = 0.383(\phi_c)_{SPB}\left(\frac{\Delta\rho\delta_c^2}{\sigma}\right), \tag{5}$$

and $(\phi_c)_{NC,BDC}$ by:

$$(\phi_c)_{BDC} = 0.077(\phi_c)_{SPB}\left(\frac{\Delta\rho\delta_c^2}{\sigma}\right). \tag{6}$$

e. For forced convection, my superposition correlation is:

$$(\phi_c)_{FC,sub} = (\phi_c)_{SPB}\, F_{sub} + h_{nb}(\Delta t_{sub} + \Delta t_{sat})_c, \tag{7}$$

in which F_{sub} is the pool subcooling factor, h_{nb} the nonboiling heat transfer coefficient, Δt_{sub} the coolant subcooling, and Δt_{sat} the wall superheat. As stated by A. E. Bergles (1977), this "is still the most widely verified correlation for forced-convection subcooled boiling." For vapor quality $x = \Delta t_{sub} = 0$,

$$(\phi_c)_{FC,sat} = (\phi_c)_{SPB} + h_{nb}(\Delta t_{sat})_c. \tag{8}$$

f. As noted in the March monthly report, $(\phi_c)_{NC}$ cannot increase with δ_c^2 indefinitely, as indicated by Eq. (5). Using the mean dimensional correlation from the March report:

$$\frac{(\phi_c)_{NC,ODC}}{(\phi_c)_{SPB}} = (\pi/50)(\delta_c)^2_{mm}, \tag{9}$$

$(\phi_c)_{NC}$ equals $(\phi_c)_{SPB}$ when $\delta_c = 4$ mm, which is clearly not only too narrow a gap for the transition, but also a gap independent of L_h. Assuming, with reason, that $(\delta_c)_{tr}$ for $(\phi_c)_{BB} \rightarrow (\phi_c)_{SPB}$ also applies to $(\phi_c)_{NC} \rightarrow (\phi_c)_{SPB}$ [in the pool case, at least], the $(\delta_c)_{tr}$ taken as the average value for the HFIR and ANSR cases is 24 mm (6 × larger and dependent on L_h). The trend is illustrated in Fig. 1, in which curve a corresponds to the ordinate $\alpha\ \delta_c^2$ and curve b to the suggested transition. The tested data follow curve a for $\delta_c = 0.58$ - 1.42 mm, and probably would at smaller δ_c values also, but at larger δ_c ($\gtrsim$ 2 mm?) would be expected to inflect and follow curve b to an asymptote at an ordinate of one and a δ_c (or D_e) given by Eq. (3). Although I consider the material in this section as plausible, it should be viewed as somewhat more speculative at this time than the relationships given in sections a through e.

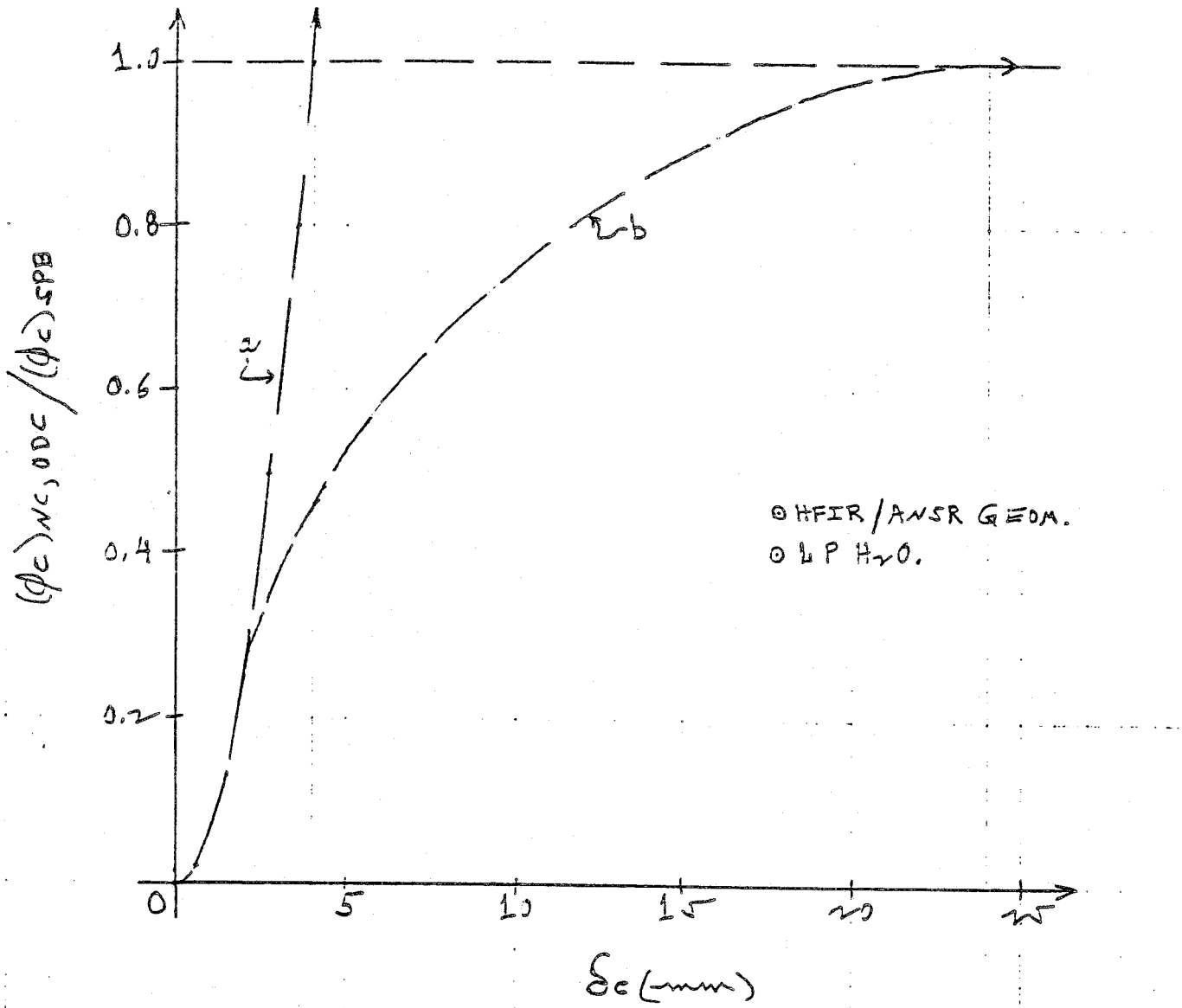

Fig. 1.
Variation of $(\phi_c)_{NC}$ with coolant gap.
(Illustrative only)

GRAPH PAPER GRAPHIC CONTROLS CORPORATION Buffalo, New York
Printed in U.S.A. SQUARE 10 X 10 TO THE INCH AS 0807 GD

WRG
5/16/89

ATTACHMENT B.

MIN. h_{nb} vs. t_b.

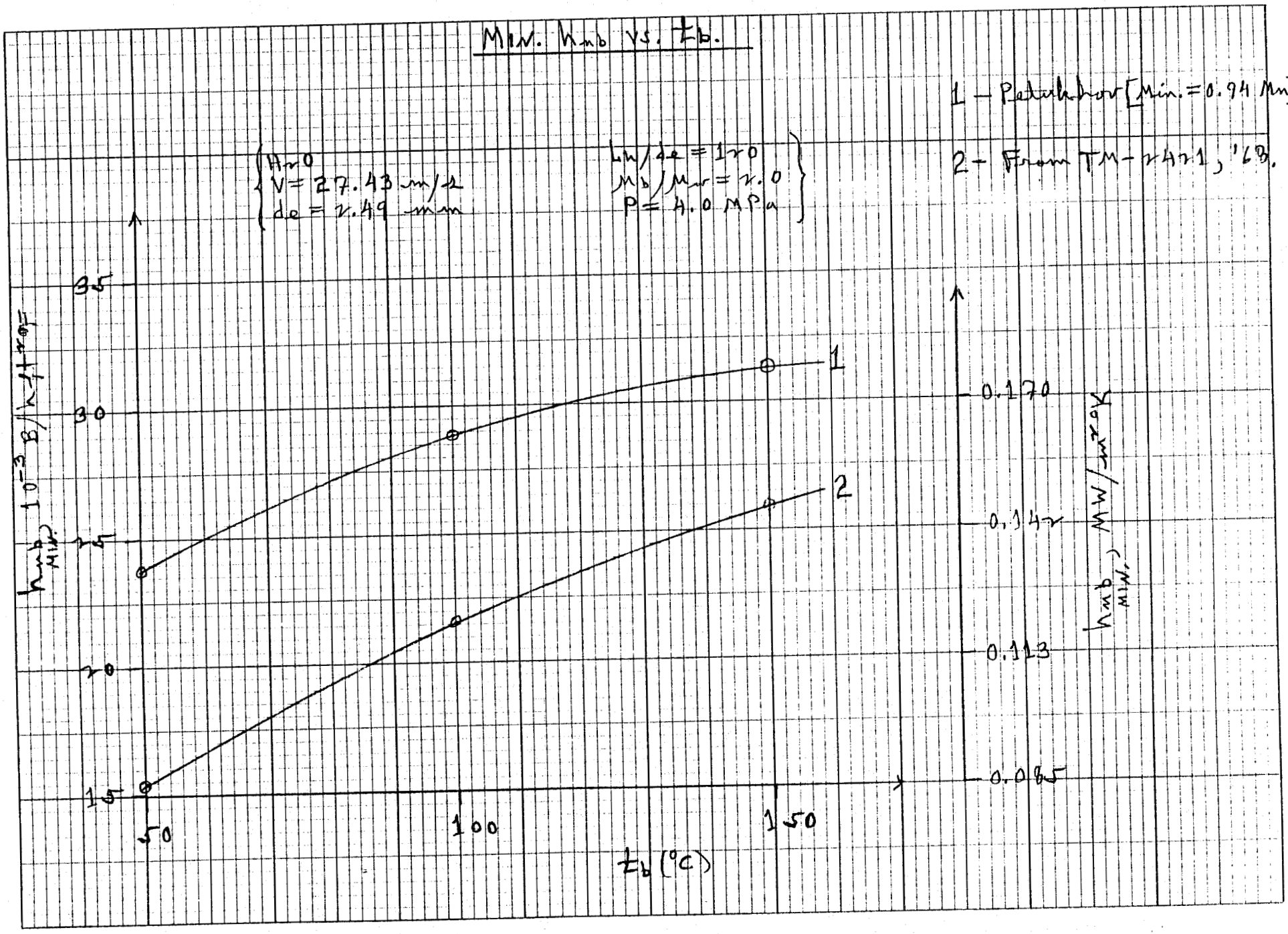

May 26, 1989

C. D. West

Correlation of Clad Oxide Data with Bulk Coolant Temperature.

At the last R&D staff meeting (May 16), you described briefly the initial results of plotting oxide growth rate vs. bulk water temperature (t_b). Data from ANS corrosion tests 7, 9, & 10 were displayed for two constant oxide thicknesses (5 and 10 μm), for which the regression curves were nearly the same. The following summarizes some (incomplete) thoughts I've had concerning this interesting correlation approach.

a. The fit of the data after including points from ANS tests 6, 8, & 11 as well as the HFIR data would obviously tell a more complete story.

b. J. C. Griess and co-workers prepared a similar plot in the second of their four ORNL reports on HFIR oxide formation. Their Fig. 7 (p. 17) of ORNL-3056 (Feb. 1961) is shown here as Fig. 1. The figure to the left is for pH = 5.0 and the one to the right for pH $\approx$ 7.0. In each case, the temperature rise rate increases approximately linearly with t_b. For the left figure, test conditions were V = 10.4 and 14.6 m/s, P = 6.2 MPa, and ϕ = 5.0 MW/m^2 (for two Al alloys, 6061 & 1100). The final correlation of oxide growth rate, based on many more data and published three years later in ORNL-3541, was expressed in terms of the oxide-water interface temperature (t_i). Using ϕ = heat flux, δ_{ox} = oxide thickness, and θ = time, Fig. 1 is a plot of $d\Delta t_{ox}/d\theta$ vs. t_b (ϕ fixed), whereas the new ANS plots are of $d\delta_{ox}/d\theta$ vs. t_b (δ_{ox} fixed). Since the oxide thermal conductivity is apparently constant, the two rates (derivatives) are related by ϕ.

c. With regard to the 10-test data collection itself (c. tests 2-11), several items are of interest. Using subscripts 6 and 2 to denote test-section positions 6 (near the outlet) and 2 (near the inlet), h = heat transfer coefficient, and Δt_f = film (boundary layer) Δt, the following average ratios characterize the data:

	ϕ_6/ϕ_2	h_6/h_2	$(\Delta t_f)_6/(\Delta t_f)_2$
All tests	1.086	1.066	1.019
Excl. Test 10	1.071	1.060	1.010

Test 10 was excluded in the second row because $(t_b)_{in}$ was 39°C (10°C lower than for the ANS reference core) and because ϕ_{max} was 12.5% higher than ϕ_{max} for the new reference core at 333 MWt. In any event, the differences in the ratios are small. Because h increases with streamwise distance along with ϕ, the average axial increase in Δt_f is only ~1%, which is just what would be expected for the case of turbulent flow and constant wall heat flux.

Note further the values of $dt_i = (t_i)_6 - (t_i)_2$ and of $dt_b = (t_b)_6 - (t_b)_2$ and of their average ratio:

	dt_i (°C)	dt_b (°C)	dt_i/dt_b
All tests	12-31	13-22	1.088
Excl. Test 10	12-22	13-22	1.052

which reflects the same result as the preceding paragraph. It seems clear that for the limited variable ranges of the subject data set, t_b and t_i are rather closely correlated.

d. In the following, I've used the same data set, characterized by a broad range of ϕ, that I used in my letter of October 7, 1988, in which I described my "new oxide interpretation." Figure 4 of that letter is shown as Fig. 2, in which a plot of $\delta_{ox}/(\delta_{ox})_G$ vs. ϕ_{max} produces a tight trend. $\delta_{ox}/(\delta_{ox})_G$ is the ratio, as before, of oxide thickness to that given by the Griess correlation. The same ratio, plotted vs. $(t_b)_{max}$ in Fig. 3, produces no trend at all. In these terms, the points are:

No.	Case	$\delta_{ox}/(\delta_{ox})_G$	ϕ_{max}, MW/m^2	$(t_b)_{max}$, °C
1.	SRP (production)	0.2	2.2	113
2.	ATR (at ~190 MWt)	0.5	~4	~100
3.	HFIR (c. tests)	1.0	6.3	121
4.	HFIR (at 100 MWt)	(1.0)	6.2	120
5.	ANSR (c. test 4)	2.7	12.7	100
6.	ANSR (des., 333 MWt)	?	15.6	122

e. As I've suggested, a "hot patch" test could be conducted with the present experimental system by laterally grooving the opposite exterior surfaces of a test section for a short axial distance. The backup plates would be modified to provide mechanical support for the grooved portion of the element. If the wall thickness of the hot patch region were, e.g., half the normal thickness, ϕ in that region would be nominally doubled. Because the side regions of minimum wall thickness are in parallel with the hot patch (or normal) zones, a correction (calculable) would reduce ϕ_{hot}/ϕ_{normal} somewhat. This test, or tests, should show clearly whether or not a localized heat flux "spike", at nearly constant t_b, affects δ_{ox} significantly.

f. Finally, the new oxide growth rate curves (1st paragraph) can be applied to the current reference core (333 MWt) to see what the implications might be <u>if</u> they indeed constitute a correlation.

Since the maximum t_b will occur at the hot-streak exit, the maximum δ_{ox} will also occur there, regardless of the local ϕ. Using average growth rates from the 2 curves available, $(\delta_{ox})_{in}$ at $t_{b,in} = 49°C$ would be 10.1 μm at 14 days, and at the average exit location ($t_b = 86.1°C$), δ_{ox} would be ~52 μm. At the hot streak exit, <u>if</u> $(t_{b,o})_{max}$ could be reduced from 122°C, the present value, to 99°C, the maximum $(\delta_{ox})_{out}$ would still be a massive 91 μm. We are basically more concerned with Δt_{ox} than with δ_{ox}, and since $\Delta t_{ox} = \frac{\phi\delta_{ox}}{k_{ox}} \propto \phi\delta_{ox}$, the outlet ϕ_{max} must be much smaller than the inlet ϕ_{max} to prevent spallation. In this case, and for a constant Δt_{ox}, $(\phi_{max})_{out}$ could be no more than 1/9 $(\phi_{max})_{in}$. One could imagine the extreme decreasing gradient of ϕ from inlet to outlet skewing the generation of heat so severely in the upstream direction that a more limiting core region might occur upstream of the exit where $t_b \rightarrow (t_b)_{out}$ while ϕ significantly exceeds the outlet value.

g. In summary, I continue to believe that we can not make a convincing "oxide case" until we have a clearer picture of the primary variables – and in particular the effect of ϕ aside from its influence on interface temperature.

W. R. Gambill

W. R. Gambill

WRG:cz

Enclosures

UNCLASSIFIED
ORNL-LR-DWG. 54148

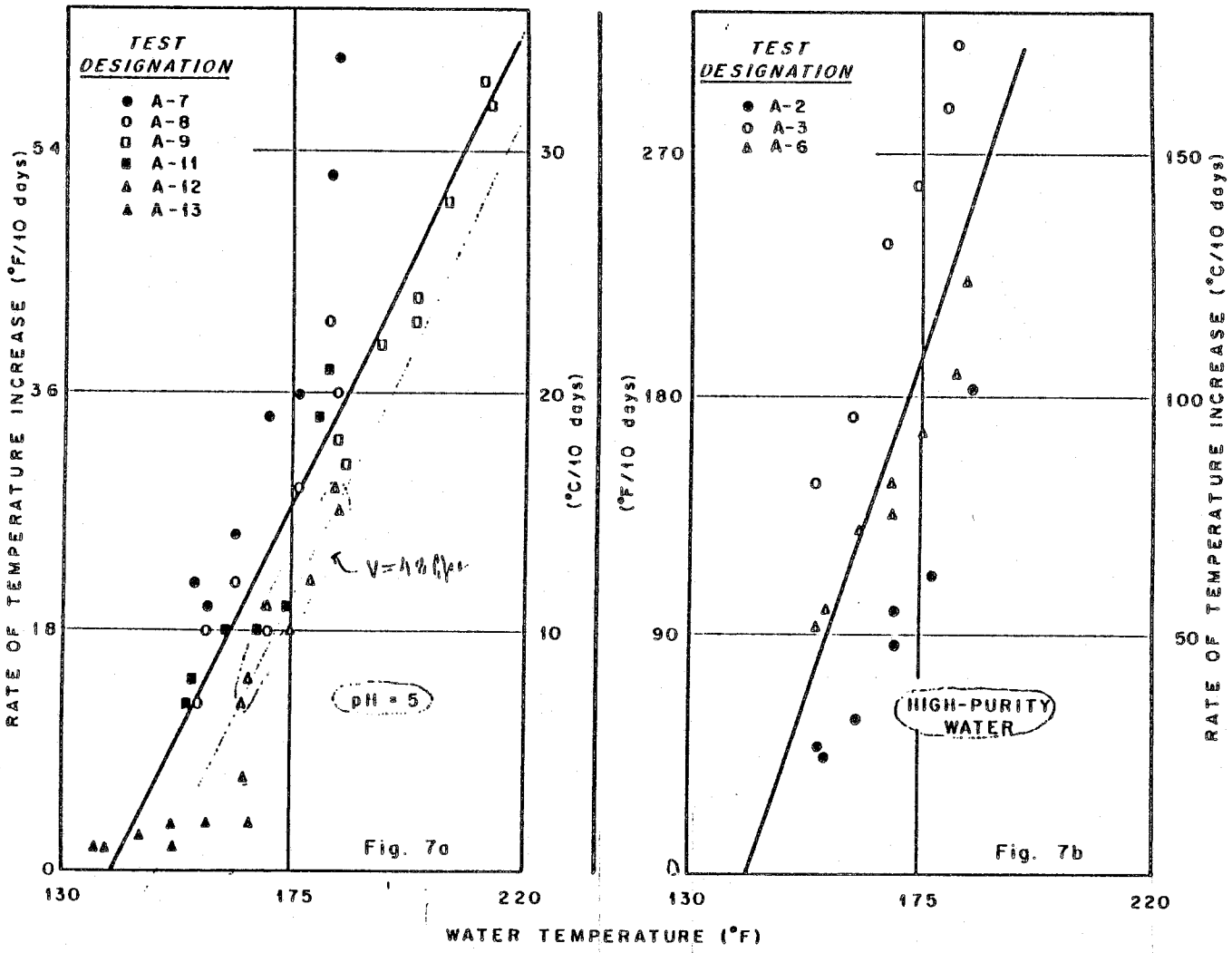

Fig. 7. Correlation of Rate of Temperature Increase and Water Temperature.

FIG. 1.

FIG. 2.

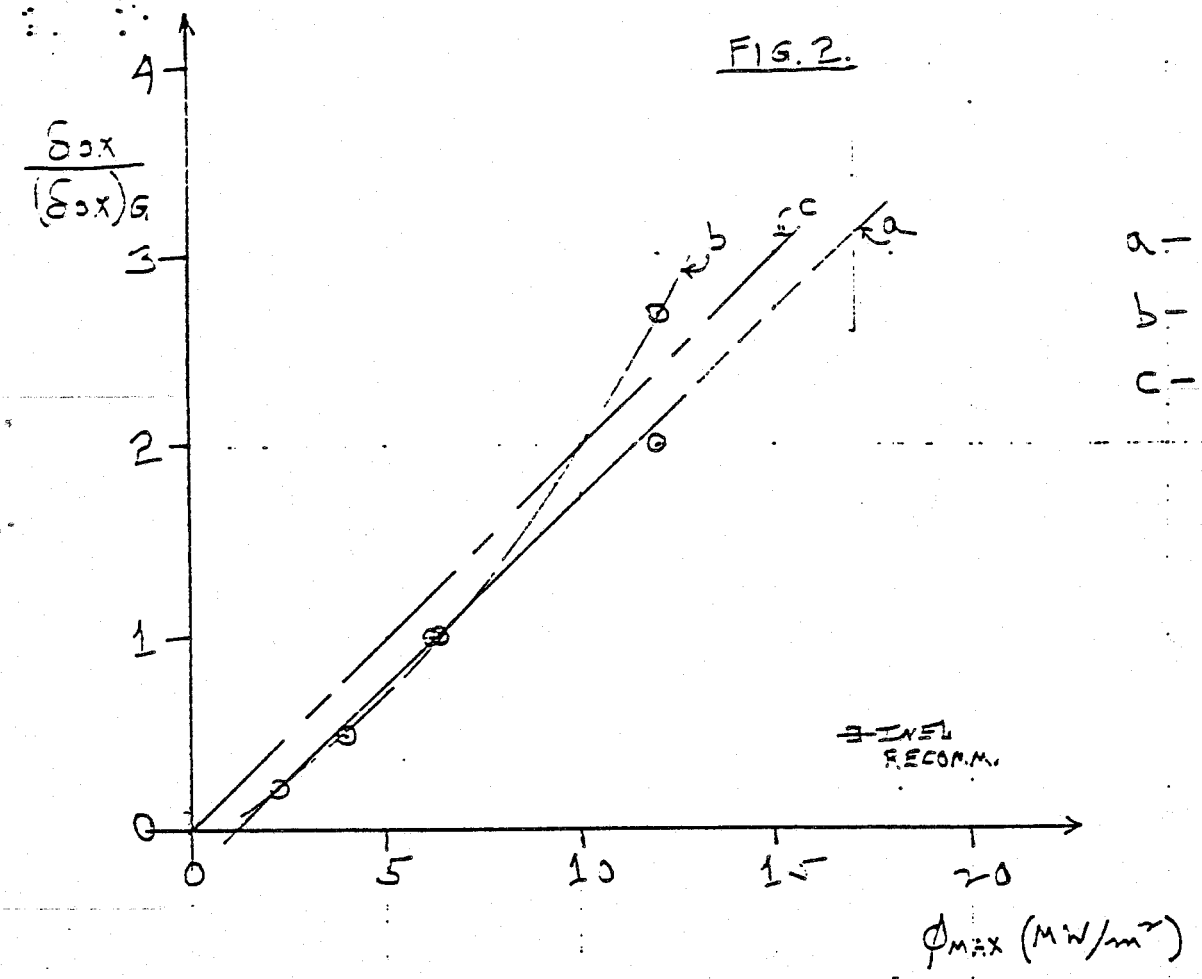

a – PROBABLE (?).

b – POSSIBLE.

c – SRL ϕ FUNCTION

FIG. 3.

WRG
5/39

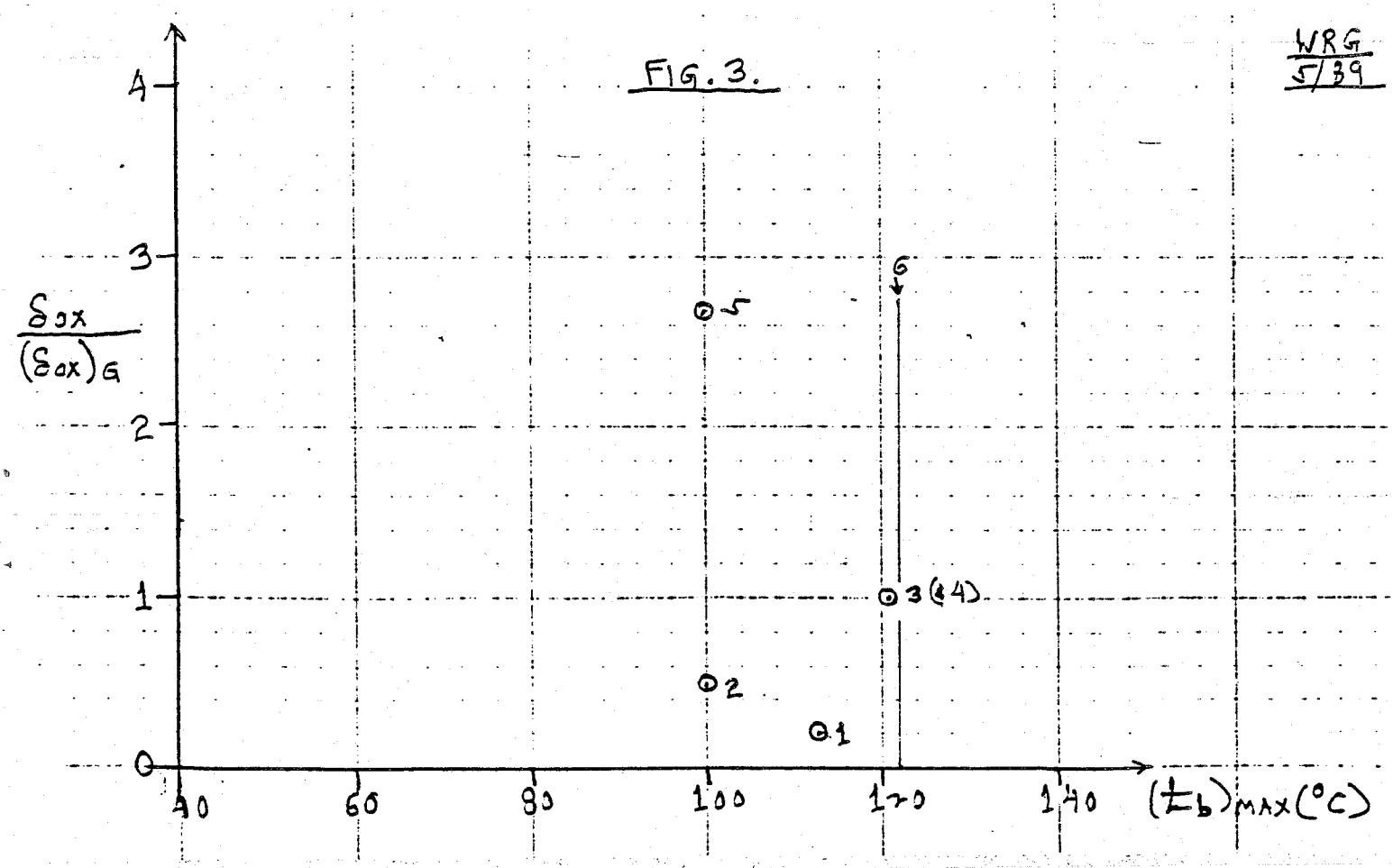

FUEL DEVELOPMENT AND EVALUATION
April 1989

G. L. Copeland

The HFIR target capsule of ANS fuels is awaiting irradiation in the first normal HFIR cycle. It now appears that the schedule will be delayed such that evaluation of the SiC temperature monitors will be in the next fiscal year. However, we still plan to delay final machining of the next fuel holders until enough monitors can be evaluated from the first capsule to assure that the irradiation temperatures are in the correct range.

The B&W subcontract is still not finalized but is about ready.

Work at ANL is proceeding on the next irradiation capsule, fabrication development, and basic studies and modeling of irradiation performance. The fabrication of fuel plates of 6061 aluminum by hot isostatic pressing is appearing less promising; however, the lower volume fractions and less severe fuel gradients in the current core design make it extremely unlikely that a lower deformation process such as this will be necessary for fabricating the plates. Initial results from two-compact plates (such as would be needed for burnable poison at the ends of each plate or some gradient schemes) appear very promising.

ANL Contribution to the ANS Monthly Report for May 1989

I. Management/Experiment Design (J. L. Snelgrove)

Owing to additional delays being experienced in bringing HFIR back to power, the schedule for irradiation of the first capsule experiment continues to slip. We will probably not have any information from the first test before next fiscal year. We will hold to our plan to have the fuel holders for the second test ready for final machining by the end of September, however.

II. Fuel Development and Fabrication (R. F. Domagala, T. C. Wiencek, and H. R. Thresh)

Hot isostatic pressing (HIP) experiments are being continued in an attempt to reproducibly bond 6061 Al to itself. Only once (two assemblies) has a HIP run resulted in a metallurgical bond of two pieces of 6061. Portions of these bonded samples have been examined metallographically, and, while the original interface is still easily discernible, there is clear evidence of some recrystallization across that interface. Other portions of the bonded samples were cold rolled in the as-HIPped condition as well as after anneals at 500°C of 24 and 72 h. Samples were rolled with the interface parallel to as well as perpendicular to the roll surfaces. Some samples separated at the original interface after as little as 9% reduction in thickness while two samples, annealed for 24 h at 500°C, were reduced 97% without failure. Such performance suggests nonuniform bonding across the mating surfaces. Modified shear test coupons were machined from other pieces of the bonded

6061 assemblies. For the first test the shear area was greater than the area in tension so that a tensile fracture resulted in the base material. The ultimate tensile strength (UTS) of the 6061 was 158 MPa (23 ksi) which compares favorably with handbook values of UTS for 6061 ranging from 124 to 310 MPa (18 to 45 ksi), depending on the thermomechanical history of the material. The HIP condition should yield a condition closest to the weakest (0-temper) state. The bonded area was unaffected by the test so we learned that its shear strength is greater than 28 MPa (4 ksi).

A second shear test sample was prepared with a smaller shear area. The result of this test was a shear failure at the bond interface at 53 MPa (7.7 ksi). An examination of the parted surfaces with the unaided eye as well as with a low-power microscope suggests an intermittent bond of perhaps 50% of the area. This would be consistent with the measured shear strength as well as the fact that some samples rolled after HIPping separated while others did not.

For comparative purposes, handbook values for the shear strength of 6061 range from 83 to 207 MPa (12 to 30 ksi) depending, as does the UTS, on the thermomechanical history.

Two additional HIP runs were conducted with e-beam welded assemblies of 6061 Al against 6061 Al. After 4 h at 500°C and 76 MPa (11 ksi), neither of the runs yielded a bonded product. We are inevitably coming to the conclusion that in spite of the fact that e-beam welding is conducted in a desirable vacuum environment, it is not the best sealing procedure. Even the tiniest discontinuity in the weld would permit the HIP atmosphere to permeate between the pieces and preclude bonding. Metallographic examination of the 6061 Al e-beam weld, in fact, did show microcracks but it is impossible to determine if they are continuous and thus allowed the gas to enter the interface.

Several more HIP runs are planned and will be described in future reports. Meanwhile, literature searching continues as do phone or letter communications initiated between us and personnel at IPS, Inc. (a HIP manufacturer), Alcoa Research Lab., ORNL, and B&W, Lynchburg. A few suggestions have been received as a result of these contacts but all personnel with whom we have communicated to date have had no specific experience with HIP bonding 6061 Al. They all agree, however, that it is a nontrivial task, probably a result of the complex nature of the oxide formed on this alloy. Further, there is virtually no way to preclude the formation of some oxide.

In order to check the accuracy of temperature measurements made with the one W+5 Re/W+26 Re thermocouple in our HIP, two special runs were conducted. One run was made at 670°C and the other at 645°C (as indicated by the W-Re thermocouple). Gas pressures were the same as for our standard practice. For each run two pieces of pure Al were contained in a small ZrO_2 crucible. The pieces of Al heated to an indicated temperature of 670°C melted but did not "flow" into a single puddle. The Al pieces heated to an indicated temperature of 645°C did not melt.

The melting point of Al is 660°C and the observations noted above give us a good measure of confidence that our indicated temperatures are probably accurate to approximately 115°C. No further tests to establish the accuracy of our temperature measurements are planned at this time.

Twin-compact miniplates fabricated by conventional picture frame techniques have been discussed in several earlier reports. Full longitudinal sections were cut, mounted and polished for metallographic examination. The transition between what was originally the compact-compact interface is smooth with no very sharp step-function in loading observed. The 6061 clad and/or the Al matrix powder appear to have flowed smoothly into any gaps. Although these plates were made using W powder as a surrogate fuel, experience to date suggests that the use of multiple compacts for conventional fabrication of plates poses no serious problems.

Twenty-one blanks for the next group of FANS (HANS) have been machined. These oversize pieces are 38 mm (1.5 in.) high and 19 mm (0.75 in.) in diameter with all three 1 mm holes drilled in the proper locations. These will be identified and stored in preparation for the next campaign.

Finally, a summary of all HIP runs conducted to date has been generated and distributed to interested personnel at ANL.

III. Other Tasks

Postirradiation Examinations (G. L. Hofman and L. A. Neimark)
No report this month.

Analytical Modeling (J. Rest, G. L. Hofman, and S. A. Zawadzki)

No report this month.

Structural Changes in Irradiated U_3Si and U_3Si_2 Determined by Neutron Scattering (R. C. Birtcher, M. Mueller and J. W. Richardson)

Powder specimens of U_3Si and U_3Si_2 have been irradiated at ANL'S Intense Pulsed Neutron Source, IPNS. The first neutron doses resulted in about 3.0×10^{-3} dpa and 4.8×10^{-6} percent burnup. Neutron scattering measurements have been made on the irradiated materials. Small changes in the lattice parameters and diffraction peak shapes have been detected. Refinement of the structure determinations is continuing; disordering, atomic distortions, and amorphization will be determined.

Ion Irradiation Simulation of Fuel Burnup (R. C. Birtcher and L. M. Wang)

The irradiation stability of amorphous materials is being investigated by a study of germanium. Ion irradiation simulation experiments on Ge have shown that Ge exhibits the same basic rapid swelling characteristics as U_3Si. During 1.5-MeV Kr-ion irradiation at room temperature Ge becomes amorphous, develops voids and then swells at

a high rate. The microstructure during the rapid swelling develops the appearance of a sponge. The fibers in the sponge grow during continuing irradiation. An initial test indicates that Ge amorphization may be weakly suppressed by irradiation at temperatures above the amorphization limit.

ATTACHMENT 6

Internal Correspondence

MARTIN MARIETTA ENERGY SYSTEMS, INC.

B.H.Montgomery
D.L.Selby

J.A.Johnson

June 5, 1989

Monthly Activities, May 1989

ANS Corrosion Test Loop

R.E.Pawel
M.T.McFee
S.P.Baker
J.F.King
J.D.Hudson
R.R.Leedy
G.L.Yoder
B.H.Montgomery
A.V.Blalock
J.D.McNabb
L.D.Chitwood
O.B.Cavin

1. The basis of our most recent test, CTEST No.11, was to examine further the influence of coolant temperatures on the corrosion of the 6061-Al specimen. For approximately the same average heat flux as in CTEST No.4, we used a lower inlet coolant temperature in combination with a lower coolant velocity in order to achieve the same interface temperature in mid-specimen. As noted in the previous monthly report, for this test we anticipated a lower rate of oxidation than that observed in CTEST No.4 due to water conditions now favorable to the formation of the protective iron-rich layer.

The test was begun on May 3, 1989 with the following loop parameters:

Coolant pH	= 5.0
Average Heat Flux	= 11.9 MW/m^2
Coolant velocity	= 19.2 m/s
Mid-spec coolant temp	= 55°C
(inlet coolant temp)	= 38.5°C
Inlet coolant pressure	= 3.7 MPa

The test was completed on May 18 after almost 360 hours of operation. Despite the equivalence of the heat flux and interface temperatures (at one time considered to be the principal variables), the rate of film buildup in this experiment was as predicted: much less than that of CTEST No.4. The film thicknesses at the three reference thermocouple positions calculated from tear-sheet data using the newest OXCAL version (OXCAL-F) are shown in Figure 1. Even at the hot (outlet) end of the specimen, the film thicknesses were comparatively small. The coolant temperatures are clearly exerting an effect on the oxidation process.

2. Because of the importance of confirming and further defining the circumstances under which the iron-rich layer forms, CTEST No.12 will be conducted under conditions of high pH and coolant water temperatures (pH 6, T_{ci}=80°C, nominal CTEST No.3 parameters). This test specimen should therefore not exhibit the iron-rich layer, and the oxidation rate should be relatively rapid. The development of oil leaks in the Loop's main pump system has led to a delay in startup for this test until replacement seals are installed and the water system is again found to be satisfactory for operation. The new anticipated startup date is on/about June 12.

3. An experiment in the Corrosion Test Loop basically results in a set of measurements of the temperature increases along the aluminum test piece as a result of oxide build up on the main heat-transfer surface to the coolant water stream. From these measurements, and known values of certain other loop operation parameters, the oxidation process is characterized in terms of several calculated system variables. Because of the geometry of the test specimen, and because the temperature and properties in the test zone vary with position and time, a somewhat intricate calculation scheme is necessary.

To accomplish the desired calculations, two computer programs have been developed. ANSDAT, written by G.L.Yoder, operates directly with the Loop's DAS output to calculate the desired quantities. OXCAL, written by R.E.Pawel, performs a virtually identical function except that it presently operates in a "batchwise" data input mode. Both programs have been subject to modification during the past year or so, particularly in the details of the film thickness calculation. For example, OXCAL can now compute film thicknesses (or film temperature drops) on the basis of six different assumptions or judgments regarding the calculation strategy.

While the results of the calculations for the two programs are not identical, the agreement is considered very satisfactory and, because they were constructed independently, constitutes a realistic check on the mechanical correctness of each. Tables I and II are submitted as examples of typical output from these programs from two recent experiments. Four calculated quantities are listed for three thermocouple positions along the specimen (at x=L/6, L/2, and 5L/6) at three times during the test: near the startup, at mid-test, and near the end. The agreement in the listed quantities is excellent for CTEST No.9, less so, especially for the film thickness values, for CTEST No.10 mainly because of differences in the assignment of "zero time" for this experiment. At this time, part of the disparity in interface temperatures is thought to involve the fact that each program uses a different data base for the properties of water in calculating the heat transfer coefficient.

Both of these programs were utilized this month to generate data from which the rate of film growth at various film thicknesses could be determined. Various preliminary "correlations" of these rates were made and it is clear from these that several process parameters are effective in determining the oxidation kinetics behavior. Additional analyses are continuing.

As part of the above sequence of analysis, the data from CTESTS No.3 through No.10 were reexamined using the latest film thickness computation scheme from OXCAL. Simply, this particular computation assigns a film thickness of 2 m at each point on the specimen at time zero, computes "closure errors" for calculated temperatures across the test piece that are normalized with respect to the local heat fluxes, and then carries these correction terms through all subsequent calculations. This scheme is equivalent to the one presently in use in ANSDAT. Since in previous monthly reports we have occasionally introduced rate curves for these tests calculated via different bases, a complete set computed on the above basis is now presented for information and comparison purposes. Figures 2 through 9 are this collection of data.

REP. 6/5/89

R.E.Pawel, 4500-S, T-32, MS-6156, 4-5138

REP/wp

TABLE I

A COMPARISON OF THE ANSDAT AND OXCAL-F PROGRAM RESULTS

CALCULATIONS FOR ANS CTEST No.9

Time:	Calculated Parameter	ANSDAT pos.2	ANSDAT pos.4	ANSDAT pos.6	OXCAL-F pos.2	OXCAL-F pos.4	OXCAL-F pos.6
30 hrs:	Coolant Temp, °C	61.1	69.7	78.0	61.0	69.3	77.6
	Heat Flux, MW/m^2	11.6	11.9	12.1	11.6	12.0	12.2
	Interface Temp, °C	137.4	148.0	156.5	137.6	145.3	152.6
	Film Thickness, μm	4.0	4.9	5.8	3.9	4.8	5.7
131 hrs:	Coolant Temp, °C	61.2	69.9	78.3	61.0	69.5	78.0
	Heat Flux, MW/m^2	11.3	12.1	12.9	11.3	12.1	12.9
	Interface Temp, °C	135.7	149.4	161.4	135.8	146.4	157.1
	Film Thickness, μm	9.1	13.3	17.7	9.1	13.3	17.7
221 hrs:	Coolant Temp, °C	61.2	70.0	78.4	61.1	69.6	78.1
	Heat Flux, MW/m^2	11.0	12.1	13.3	11.0	12.1	13.3
	Interface Temp, °C	134.3	150.3	164.6	134.2	147.0	160.2
	Film Thickness, μm	12.7	19.5	25.9	12.7	19.5	26.1

TABLE II

A COMPARISON OF THE ANSDAT AND OXCAL-F PROGRAM RESULTS

CALCULATIONS FOR ANS CTEST No.10

Time:	Calculated Parameter	ANSDAT pos.2	ANSDAT pos.4	ANSDAT pos.6	OXCAL-F pos.2	OXCAL-F pos.4	OXCAL-F pos.6
30 hrs:	Coolant Temp, °C	44.7	55.6	66.1	44.6	55.1	65.6
	Heat Flux, MW/m^2	15.0	15.4	15.8	15.0	15.3	15.7
	Interface Temp, °C	148.8	159.8	169.7	149.2	156.5	165.1
	Film Thickness, μm	4.1	4.2	4.6	2.8	3.2	3.9
141 hrs:	Coolant Temp, °C	45.0	56.3	67.2	44.8	55.8	66.7
	Heat Flux, MW/m^2	14.7	15.7	17.5	14.5	15.5	17.2
	Interface Temp, °C	147.4	162.8	181.3	146.2	157.8	174.6
	Film Thickness, μm	6.2	8.8	14.0	5.4	8.4	13.9
261 hrs:	Coolant Temp, °C	45.6	57.0	68.0	45.5	56.5	67.5
	Heat Flux, MW/m^2	14.1	15.7	18.7	13.7	15.2	18.1
	Interface Temp, °C	143.9	163.4	189.4	141.7	157.0	180.8
	Film Thickness, μm	8.2	13.5	22.3	7.9	13.7	22.8

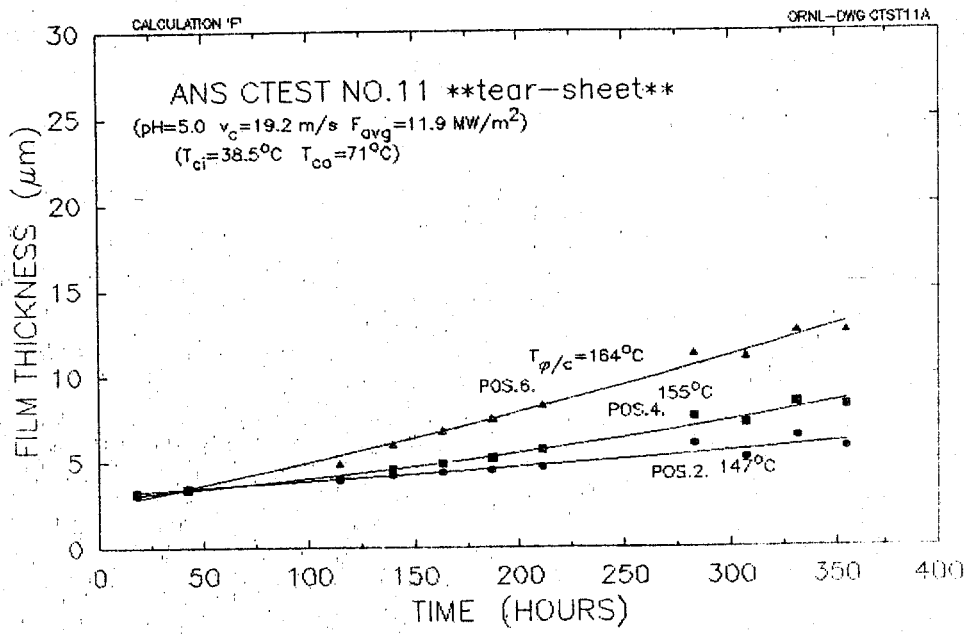

FIG.1. CALCULATED FILM GROWTH FOR CTEST No.11. (Tear-Sheet Data)

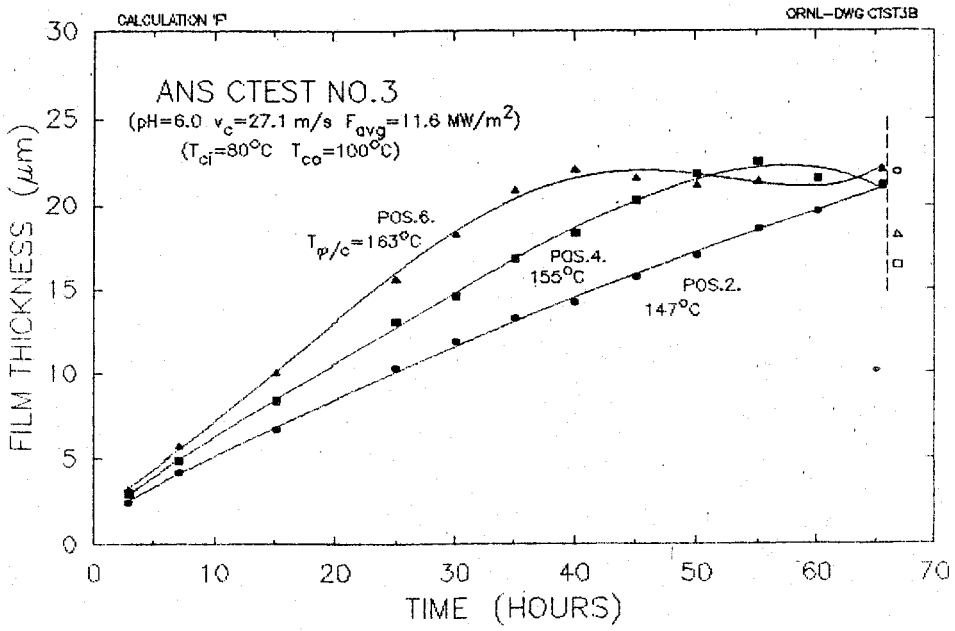

FIG.2. CALCULATED FILM GROWTH FOR CTEST No.3.

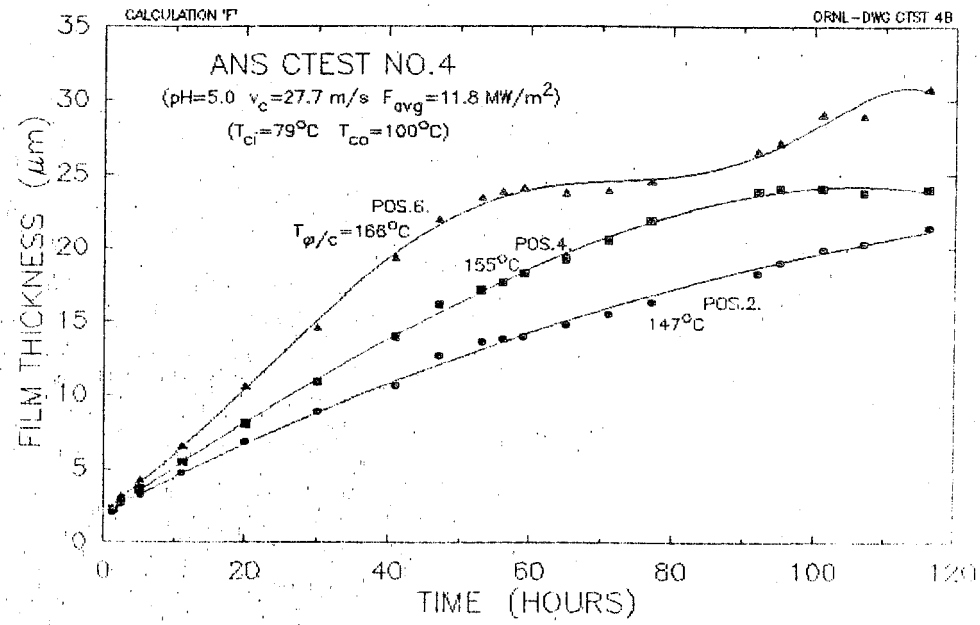

FIG.3. CALCULATED FILM GROWTH FOR CTEST No.4.

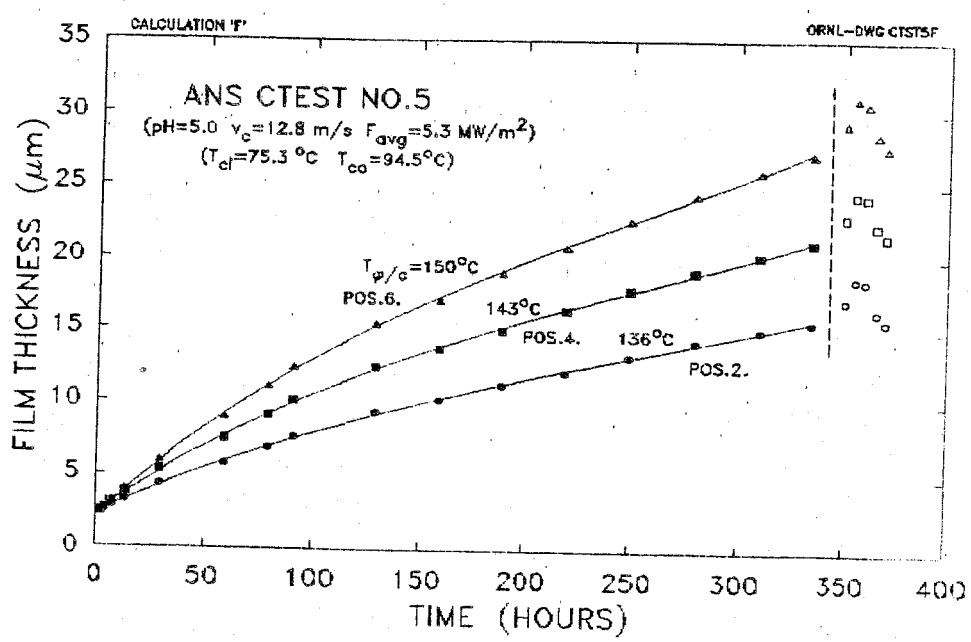

FIG.4. CALCULATED FILM GROWTH FOR CTEST No.5.

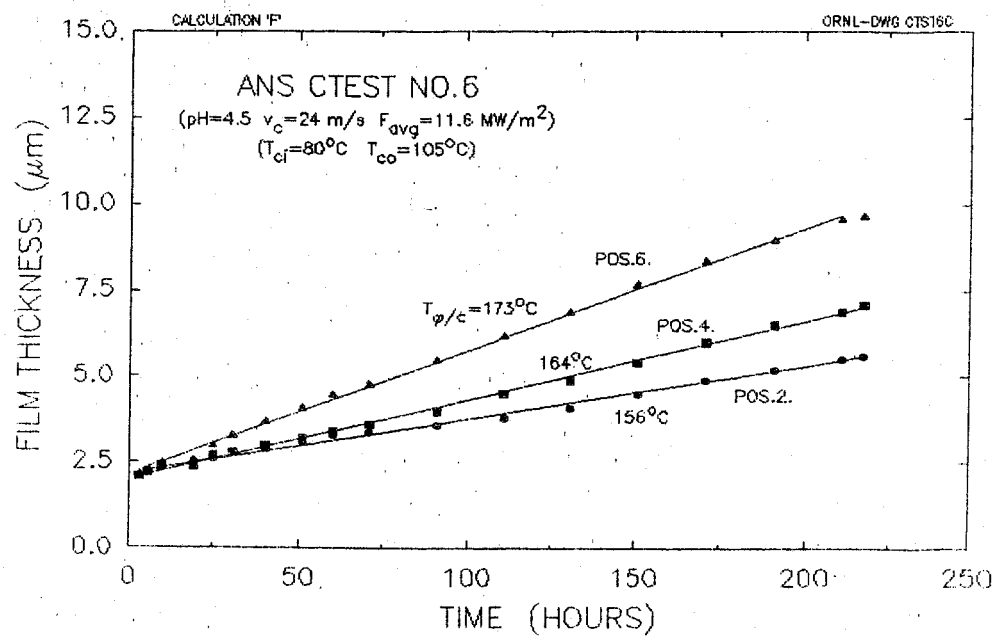

FIG.5. CALCULATED FILM GROWTH FOR CTEST No.6.

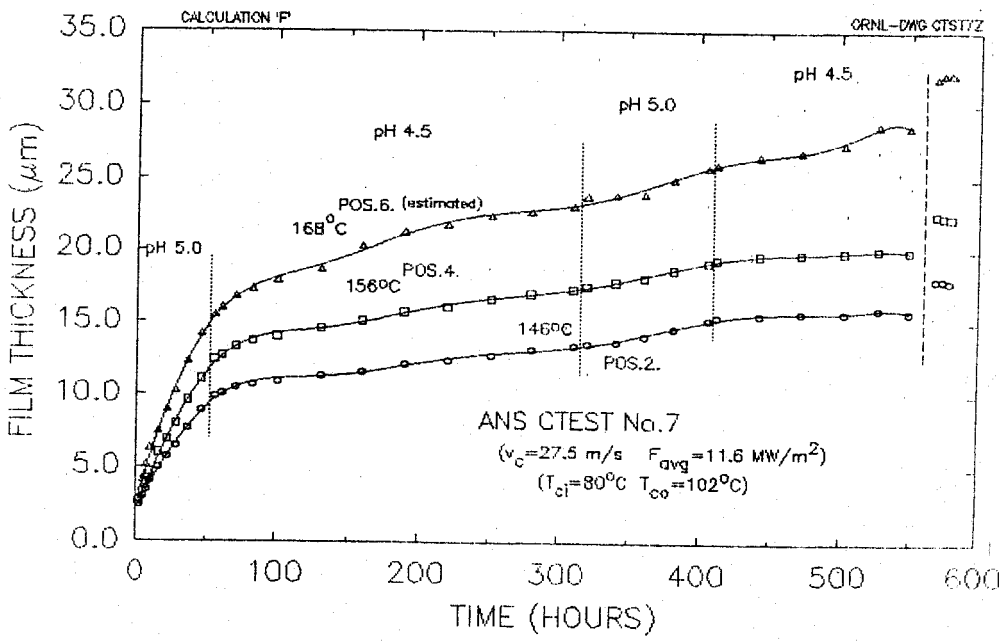

FIG.6. CALCULATED FILM GROWTH FOR CTEST No.7.

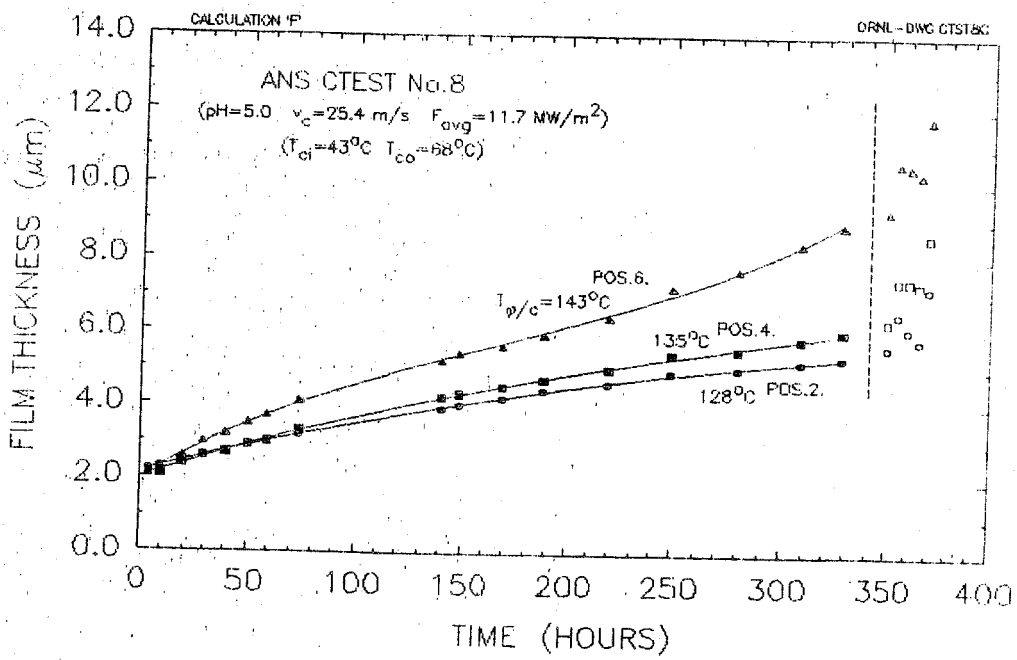

FIG.7. CALCULATED FILM GROWTH FOR CTEST No.8.

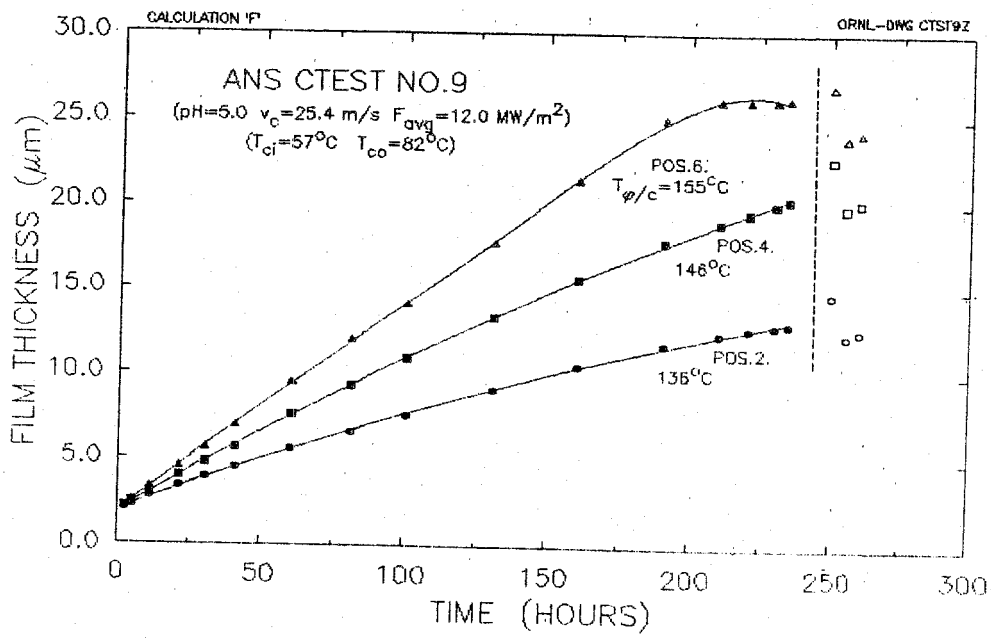

FIG.8. CALCULATED FILM GROWTH FOR CTEST No.9.

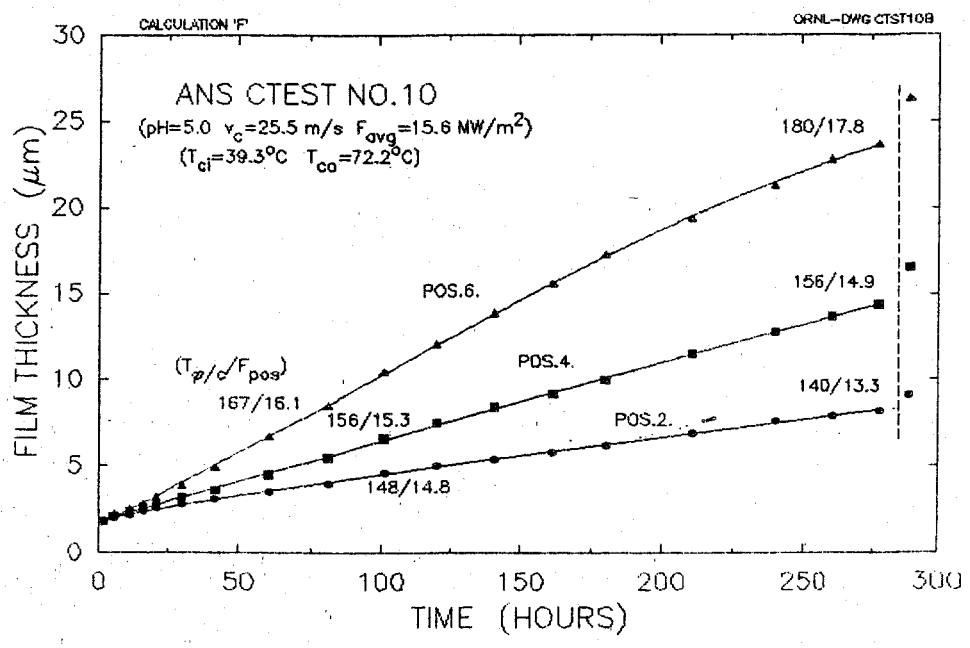

FIG. 9. CALCULATED FILM GROWTH FOR CTEST No. 10.

ATTACHMENT 7

ANS Progress Report for the Month of May 1989

Limitations of "Only Radial Grading" to Improve the Thermalhydraulic Performance of the Core

Felix C. Difilippo

The thermalhydraulic performance of the offset 67.4 L core (our latest preliminary design) was computed with detailed power distributions from BOLD-VENTURE calculations. The calculations assumed a nominal core with no fabrication defects and correlation without bias, i.e., these are nominal results and were no intended to include uncertainties. The key parameter of the calculations is the oxide correlation; we have used the correlation proposed by W. R. Gambill which depends explicitly on the heat flow.

Two cases are shown: flat fuel and radial grading only optimated at time t = 7 days. The neutronic calculations include burnable poison and control rods movement. The natural boron burnable poison is located in both end caps for the upper core and in the upper end cap for the bottom core. Table 1 indicates that a reasonable flattening of the power distribution was obtained for the axially averaged power densities. [Note: There was only one iteration.]

Table 1
Axially Averaged Power Densities[a] (Mw/L)

Upper core

	Radial Node[b]							
Fuel	1	2	3	4	5	6	7	8
Flat	5.06	4.47	4.29	3.15	3.38	5.43	6.38	7.52
Graded	4.49	4.46	4.52	4.59	4.83	5.31	5.55	5.83

Lower Core

	Radial Node							
Fuel	1	2	3	4	5	6	7	8
Flat	4.63	4.32	4.20	3.97	4.17	6.49	7.34	8.21
Graded	5.15	5.18	5.25	5.33	5.48	5.99	6.13	6.32

[a]At 7 days.

[b]Equally spaced nodes.

The list of figures show the results of the thermalhydraulic calculations as functions of time; we show only the hottest channel at each time step (see Figs. 1 and 2 for definitions of symbols).

Figure Captions

Fig. 1. Flat fuel distribution: axial heat flow.

Fig. 2. Radially graded fuel distribution: axial heat flow.

Fig. 3. Flat fuel distribution: bulk coolant outlet temperature, radial profile.

Fig. 4. Radially graded fuel distribution: bulk coolant outlet temperature, radial profile.

Fig. 5. Flat fuel distribution: temperature differential across the oxide layer.

Fig. 6. Radially graded fuel distribution: temperature differential across the oxide layer.

Discontinuities in the heat flow are a numerical artifact of the space-dependent cross sections.

In conclusion, Fig. 6 shows the necessity of axial grading to remedy the effects of the strong axial gradient of the power distribution.

D3(2)

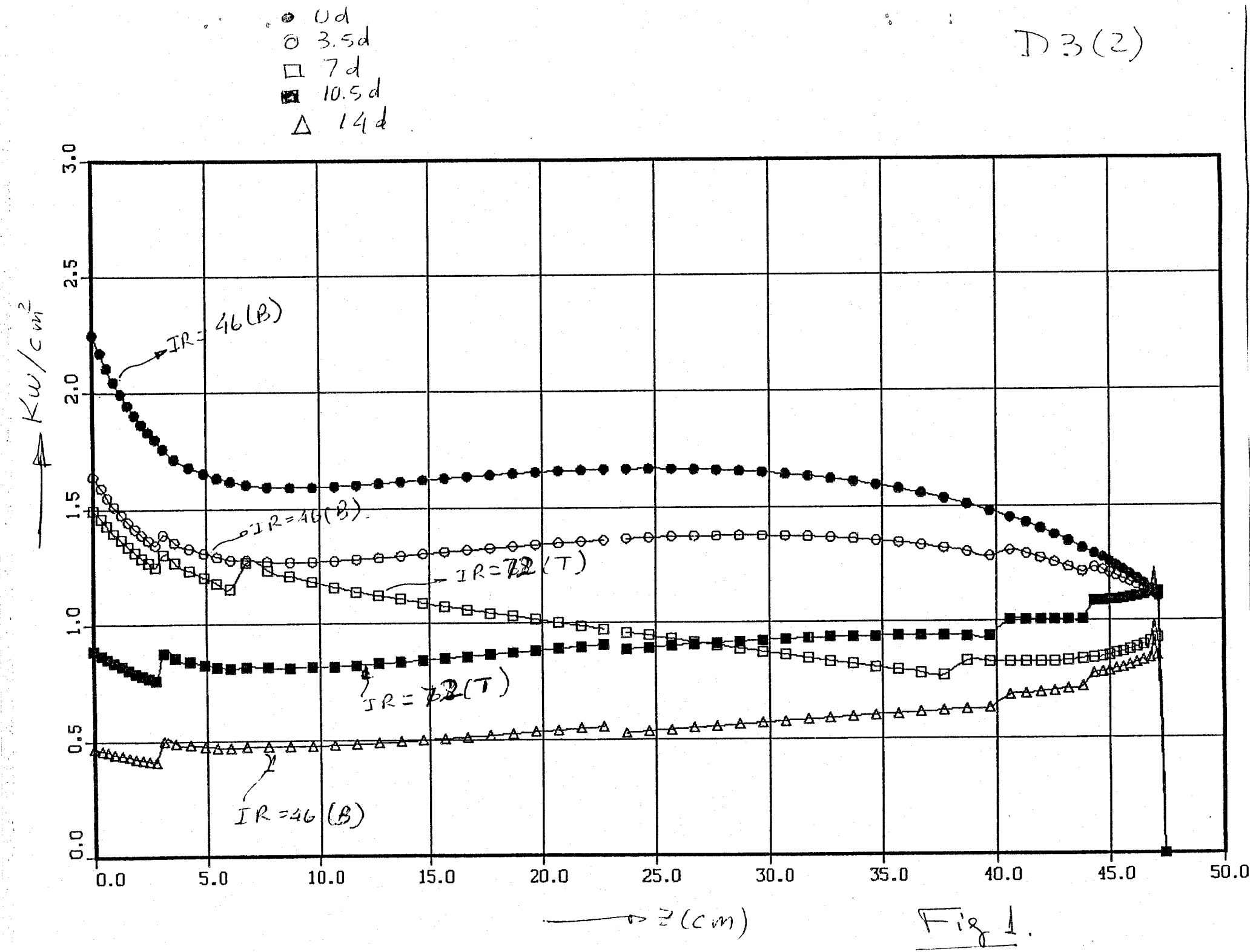
0d
3.5d
7d
10.5d
14d
KW/cm²
3.0
2.5
2.0
1.5
1.0
0.5
0.0
0.0
5.0
10.0
15.0
20.0
25.0
30.0
35.0
40.0
45.0
50.0
IR = 46 (B)
IR = 46 (B)
IR = 72 (T)
IR = 72 (T)
IR = 46 (B)
Z (cm)

Fig 1.

D5(2)

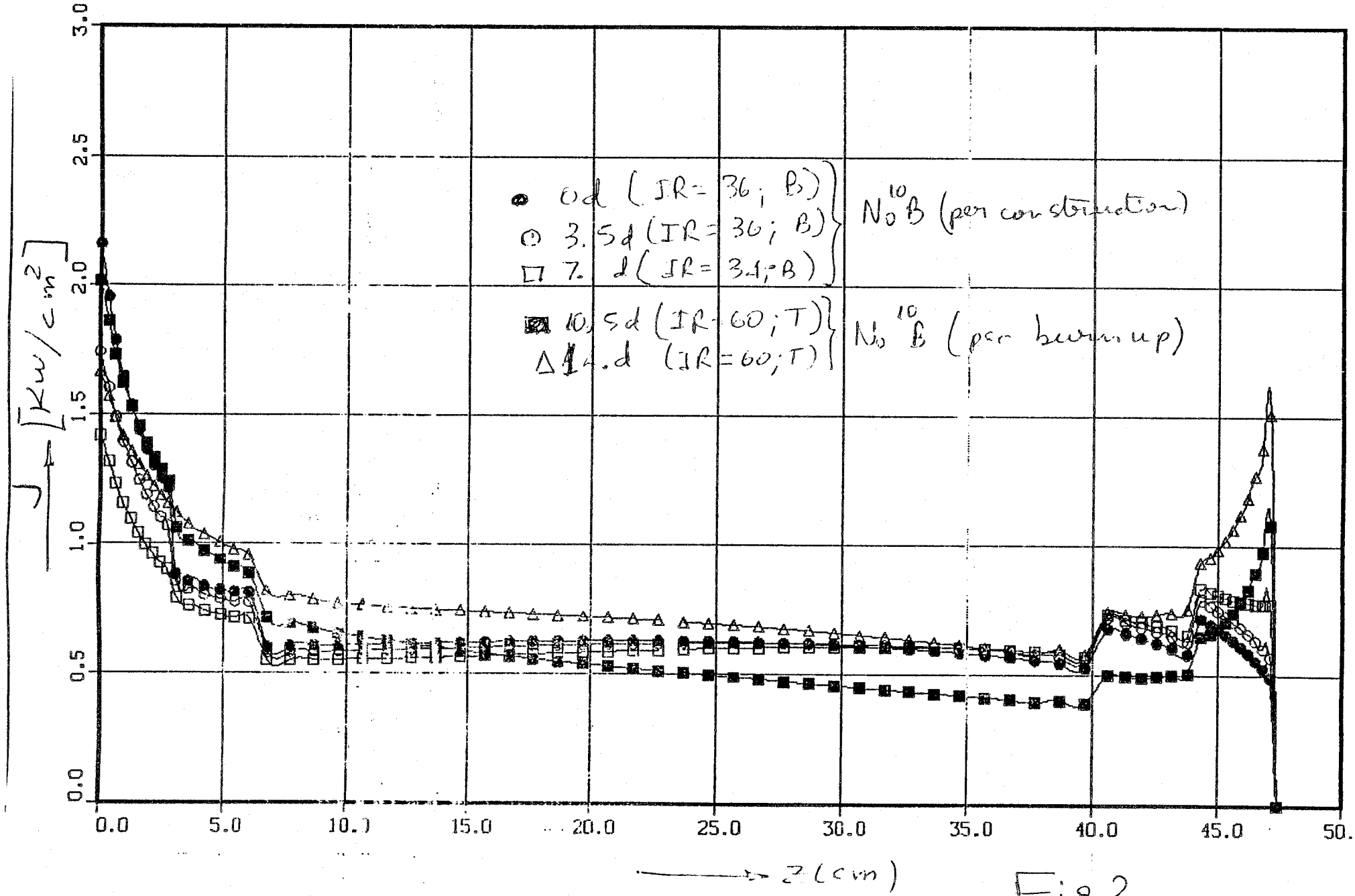
3.0
2.5
2.0
1.5
1.0
0.5
0.0
J → [Kw/cm²]
0.0
5.0
10.0
15.0
20.0
25.0
30.0
35.0
40.0
45.0
50.
→ z (cm)
0d (IR = 36; B)
3.5d (IR = 36; B)
7. d (IR = 3.1; B)
No 10B (per construction)
10.5d (IR = 60; T)
14.d (IR = 60; T)
No 10B (per burn up)

Fig 2

D3(2)

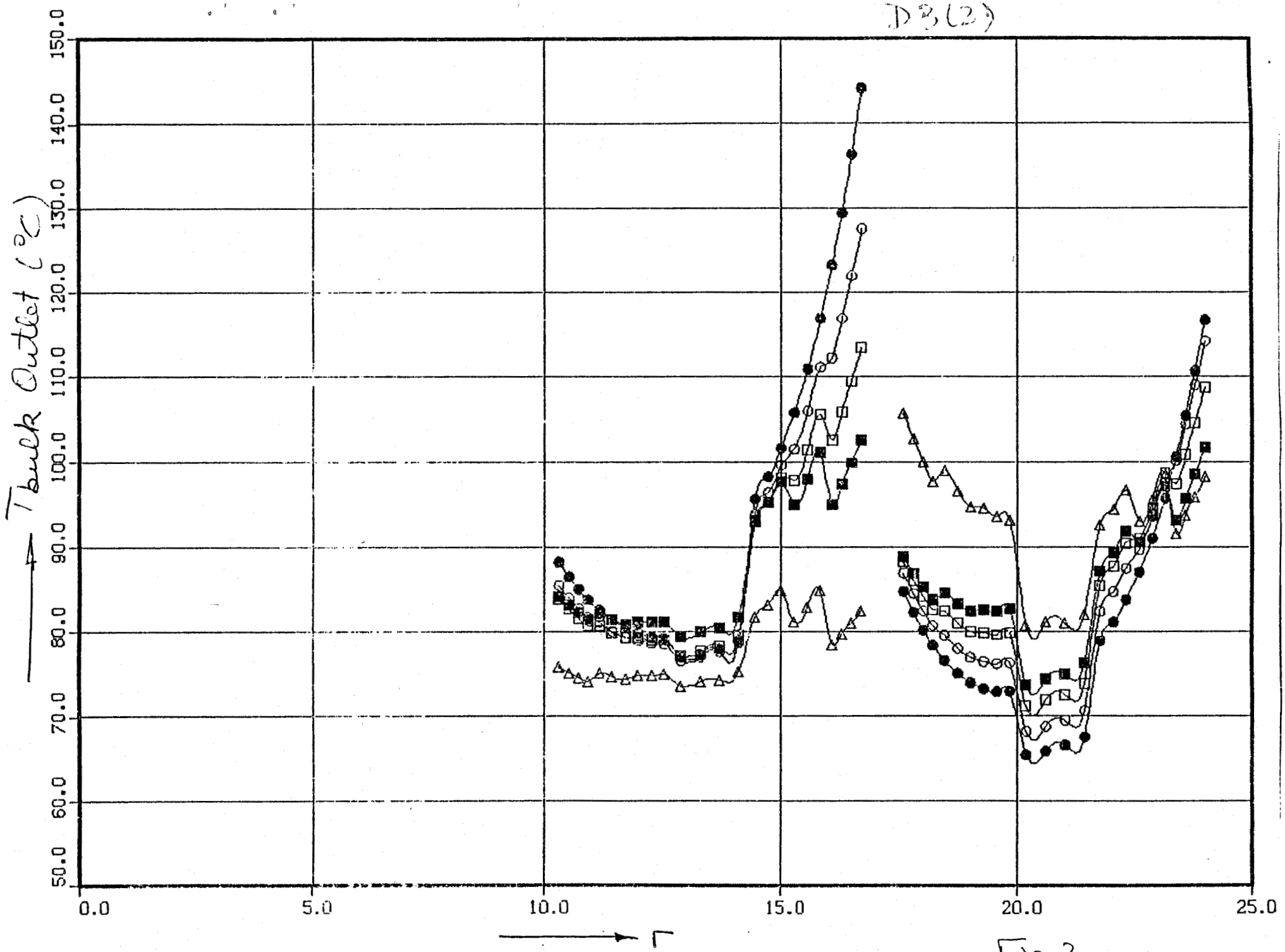
150.0
140.0
130.0
120.0
110.0
100.0
90.0
80.0
70.0
60.0
50.0
0.0
5.0
10.0
15.0
20.0
25.0
Tbulk Outlet (°C)
r

Fig 3

D5(3)

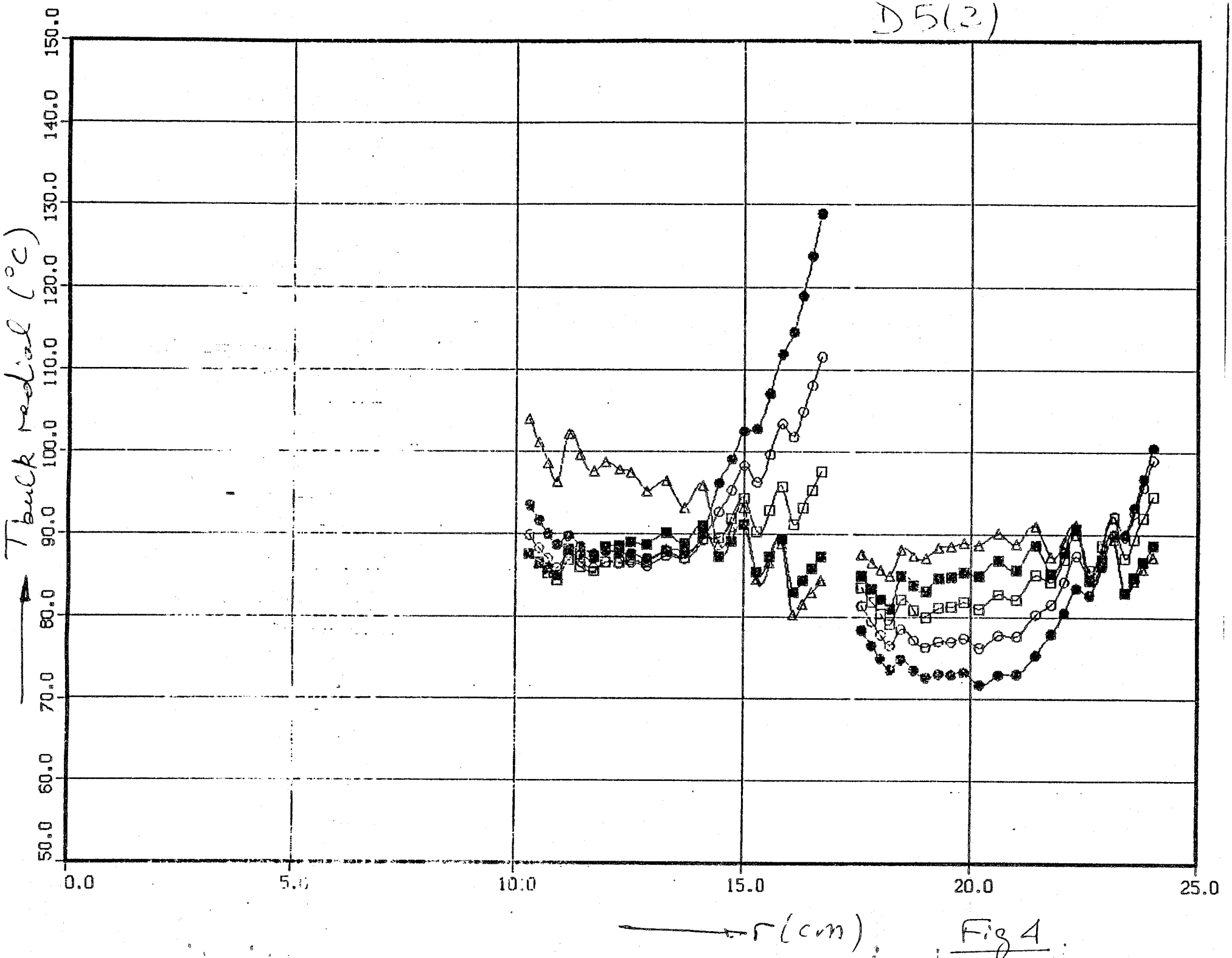
150.0
140.0
130.0
120.0
110.0
100.0
90.0
80.0
70.0
60.0
50.0
0.0
5.0
10.0
15.0
20.0
25.0
Tbulk radial (°C)
r (cm)

Fig 4

D3(2)

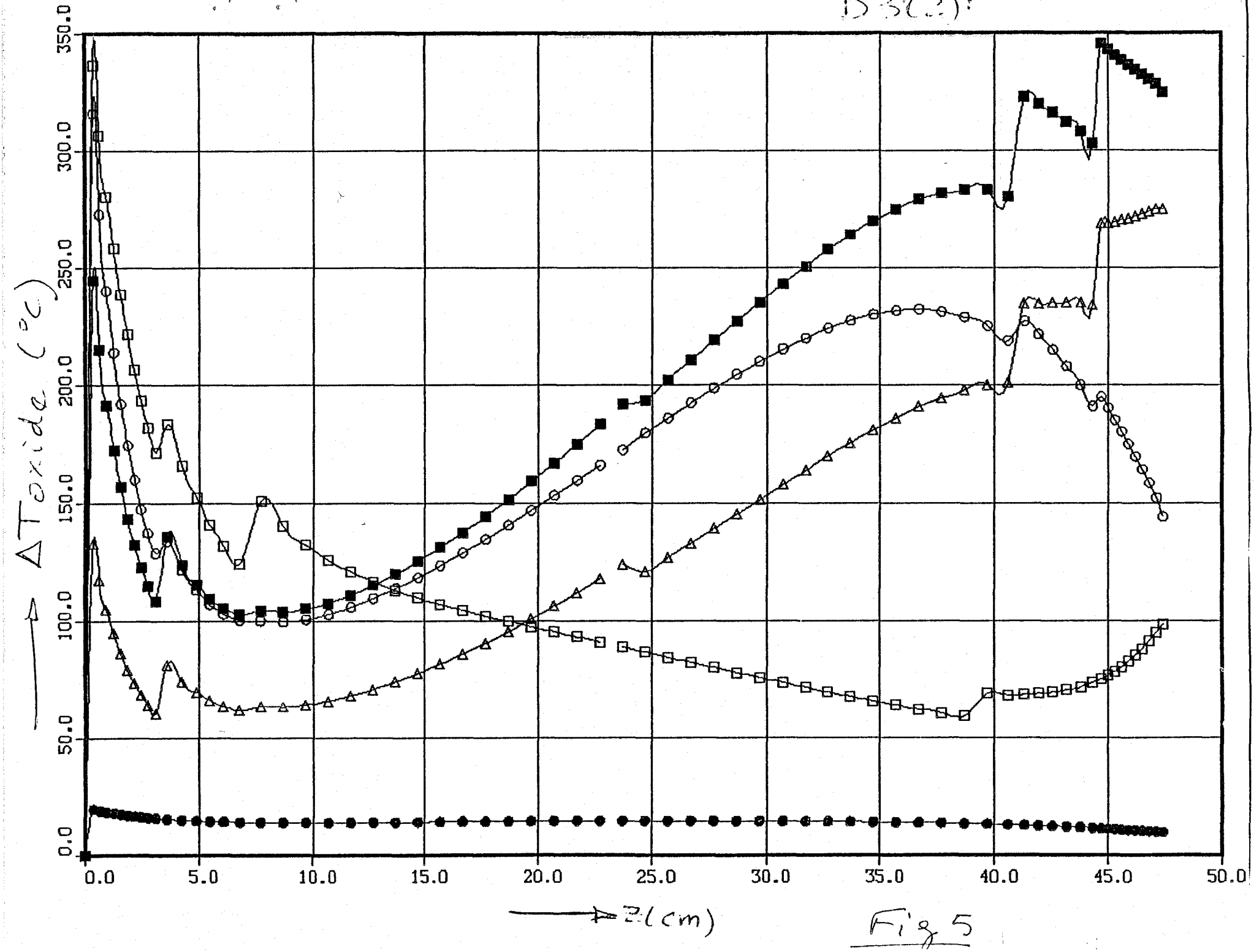
350.0
300.0
250.0
200.0
150.0
100.0
50.0
0.0
0.0
5.0
10.0
15.0
20.0
25.0
30.0
35.0
40.0
45.0
50.0
ΔT oxide (°C)
z (cm)

Fig 5

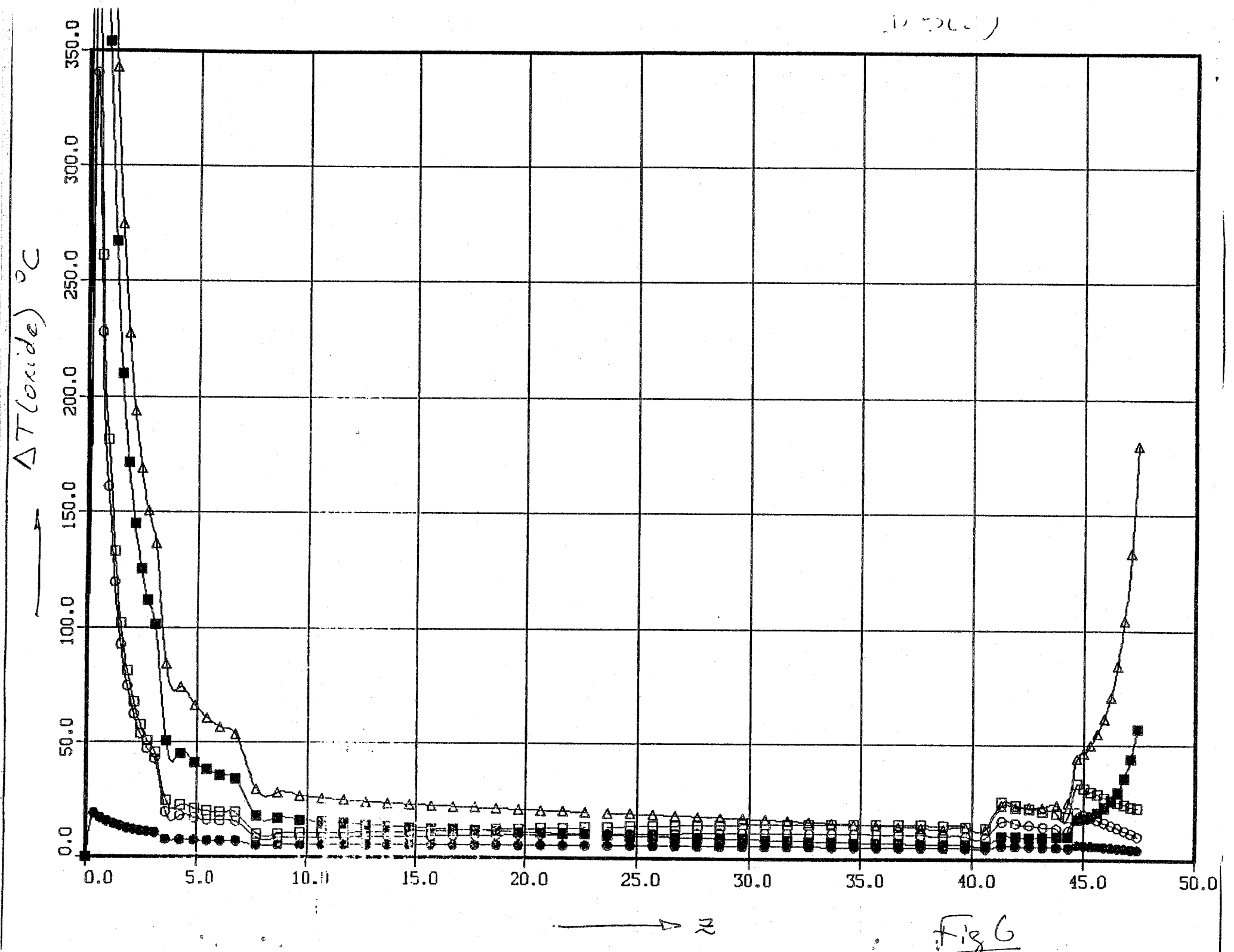
ΔT (oxide) °C
350.0
300.0
250.0
200.0
150.0
100.0
50.0
0.0
0.0
5.0
10.0
15.0
20.0
25.0
30.0
35.0
40.0
45.0
50.0
z

Fig 6

ATTACHMENT 8

Internal Correspondence

MARTIN MARIETTA ENERGY SYSTEMS, INC.

June 13, 1989

J. A. Johnson

April Monthly Progress Report for Structural Analysis Activities on ANS

1. Structural Stability of Involute Fuel Plates (R. C. Gwaltney, C. R. Luttrell, W. F. Swinson, and G. T. Yahr)

Stability of the fuel plates at the 27.4 m/s flow velocity planned for the ANS is a prime consideration. It was reported in the March progress report that the January 28, 1989, ANS reference core is marginal with regard to the stability of the fuel plates. That conclusion was reached on the basis of applying a factor of safety of 1.5 to the calculated critical velocity by the Miller approach. The fuel plates will be welded to the side plates intermittently. Earlier studies on the effect of intermittent weld attachment indicated a reduction in calculated critical velocity to 80 percent of the calculated critical velocity for a plate continuously attached. This effect was neglected in the March evaluation of the January 28 ANS reference core. The allowable maximum flow velocity should be determined by multiplying the calculated Miller velocity by 0.8 to account for intermittent welds and also dividing it by a safety factor of 1.5. Revised calculations are shown in Table 1 for the ILL, HFIR, and January 28 ANS reference cores. Note that the allowable maximum flow velocities obtained by applying both the weld reduction factor and the factor of safety to the calculated Miller velocity are above the reactor flow velocities for the successfully operated ILL and HFIR cores, but they are not for the January 28 ANS reference core.

A parameter study was run to determine how much the annular widths of the ANS fuel elements would have to be reduced to raise the allowable maximum velocities for both the upper and lower elements above 27.4 m/s. The inside radius of the lower element was held constant at 102 mm and the side plate was 7 mm thick for all the cores. The results of the parameter study are given in Table 2. An allowable flow velocity in both the upper and lower elements slightly higher than the required flow velocity of 27.4 m/s is achieved with annular widths of 54 and 58 mm for the upper and lower elements, respectively. An increase in core length of 25 percent would provide a stable core with the same volume of fuel as the reference core. A comparison of the dimensions of this new core and the January 28 ANS reference core is given in Table 3. Further evaluation of potential advantages and disadvantages of this new core is required.

2. <u>ANS Materials Characterization</u> (D. J. Alexander)

A possible source of additional irradiated 6061-T6 material has been identified. Ken Thoms has spoken with officials at the University of Missouri who are considering replacing components of the University of Missouri Research Reactor (UMRR). These vessels have been irradiated to levels of interest to the ANS program and at temperatures close to those at which the ANS will operate. Further details are given in the Memorandum of Conversation from Ken Thoms, May 23, 1989.

The two vessels would offer a much better source of material than the small clamshell specimen holders from a HFIR irradiation capsule which are going to be tested. The much larger size would allow the specimens to be extracted which should satisfy the validity requirements for fracture testing, thus giving much more useful data. In addition, the process of testing the specimens would be greatly simplified. If the expenses associated with transportation and specimen manufacture are not prohibitive, this source of material should be used rather than attempting to test the clamshell specimen holders.

On May 30 a brief presentation of the irradiation plan was presented at the biweekly Task Group Leaders Meeting. Ted Ryan stated that we should consider doing some irradiations and tests of material for the cold source. No such testing had been planned, although some funding was included for possible irradiations and testing. These tests would necessitate irradiations, storage, and testing at cryogenic temperatures, perhaps using liquid nitrogen rather than liquid hydrogen. These possibilities are being considered.

G. T. Yahr

G. T. Yahr, 9204-1, MS-8051 (4-0716)

GTY:dw

cc: J. M. Corum
D. L. Selby
C. D. West

Table 1. Critical flow velocities for involute plate reactor cores

	ILL	HFIR		ANS Ref. (1-28-89)	
		Inner	Outer	Lower	Upper
Reactor flow velocity (m/s)	15.5	15.5	15.5	27.4	27.4
Critical flow velocity (m/s)					
1. Miller analogy					
(a) Fixed edges and no safety factor	68.1	49.8	47.1	42.8	41.5
(b) Intermittent edge attachment with safety factors	36.3	26.6	25.6	22.8	22.1
2. Dynamic pressure					
(a) Deflection limited	69.8	44.4	50.5	40.3	45.3
(b) Stress limited	35.0	21.9	27.9	21.0	26.2
3. Fluid elastic excitation	26.2	15.6	19.8	14.2	17.5

Table 2. Parametric study to determine stable ANS core for flow rate of 27.4 m/s

Case	Element	Involute radius (mm)	Outer radius (mm)	Annulus width (mm)	Critical velocity (m/s)				
					Miller		Dynamic pressure		Fluid elastic excitation
					Calculated	Allowable	Deflection	Stress	
Reference	Upper	175	241	66	41.5	22.1	45.3	26.2	17.5
Reference	Lower	102	168	66	42.8	22.8	40.3	21.0	14.2
2	Upper	166	223	57	49.1	26.2	57.3	33.3	23.4
2	Lower	102	159	57	52.9	28.2	54.5	27.6	19.8
3	Upper	169	229	60	46.4	24.7	53.0	30.6	21.2
3	Lower	102	162	60	49.4	26.3	49.2	25.2	17.6
4	Upper	172	235	63	43.9	23.4	49.0	28.2	19.2
4	Lower	102	165	63	46.0	24.5	44.5	23.1	15.8
5	Upper	167	221	54	51.8	27.6	61.9	35.1	26.2
5	Lower	102	160	58	51.7	27.6	52.6	26.7	19.0

Table 3. Dimensional comparison of January 28, 1989, reference core and new stable core

	Reference core	New core
Lower element		
Involute radius	102 mm	102 mm
Outer radius	168 mm	160 mm
Annular area	0.056 m^2	0.048 m^2
Heated length	0.474 m	0.594 m
Plate length	0.494 m	0.614 m
Upper element		
Involute radius	175 mm	167 mm
Outer radius	241 mm	221 mm
Annular area	0.086 m^2	0.066 m^2
Heated length	0.474 m	0.594 m
Plate length	0.494 m	0.614 m
Flow area in coolant channels	0.071 m^2	0.057 m^2
Total core height	1.038 m	1.278 m

Design Calculations for the ANS Cold Source

D. L. Henderson, R. A. Lillie, and R. G. Alsmiller, Jr.

Two-dimensional cold source calculations were performed to investigate the performance of a combined liquid nitrogen-15 (LN_2) and liquid deuterium (LD_2) cold source configuration. Interest in combined LN_2 and LD_2 systems is motivated by the possibility of a reduction in the LD_2 inventory and a reduction in the total heat absorbed by LD_2. Figure 1 depicts the cold source geometry and indicates the position of the LN_2 layer (LN_2 is substituted for LD_2). Two cases with different thicknesses of LN_2 are examined. The first case has a 23.7 mm thick LN_2 layer and the second case a 35.6 mm layer. Calculations have been carried out for a cavity length of 190 mm and radius of 83.1 mm. The cavity region is denoted the gaseous deuterium region in Fig. 1. The method of calculation has been described in Ref. 1 and the neutron boundary source spectrum (Maxwellian treatment) in Ref. 2. The cross section data used are from the 39 neutron group ANSL-V library [3] that was developed for the Advanced Neutron Source project. The nitrogen-15 cross section data contained in the library were modified below 50 meV to account for diatomic liquid scattering effects (Ref. 4 and references sited therein). The results given below are very preliminary as the liquid deuterium and liquid nitrogen-15 cross section data sets require verification and could require additional modifications.

Figure 1 presents a comparison of the calculated angular neutron leakages at 0° into an 83.1 mm radius guide tube. The comparison is between the 190 mm cavity – liquid deuterium results (discussed in Ref. 2) and the 190 mm cavity – 23.7 mm thick liquid nitrogen-15 layer results for the wavelength range 0.05 to 1.22 nm. Replacing 23.7 mm of LD_2 with LN_2 causes a slight increase in the angular neutron leakage for wavelengths between 0.128 and 0.981 nm. Figure 2 displays the same comparison but with curves drawn through the wavelength group midpoints. Table 1 presents a comparison between the 190 mm cavity – liquid deuterium – 23.7 mm thick and – 35.6 mm thick liquid nitrogen-15 layer results. One notes that above 5.02 nm the 35.6 mm thick LN_2 layer results are slightly below the 23.7 mm results.

In general, the above results indicate that the angular neutron leakage spectrum is not substantially affected by the replacement of a small layer of LD_2 by LN_2. The results calculated are sufficiently interesting to warrant further investigations into combined LN_2 and LD_2 cold source configurations. As mentioned above, the results presented are quite preliminary and caution is advised in their usage.

Table 1

Comparison of Neutron Leakage Per Unit Wavelength from Spherical Cold Source

(Angle from Cold Source Centerline = 0°, Cold Source Radius = 190 mm, Cavity Length = 190 mm)

Neutron Energy Group	Wavelength [nm] High	Low	Midpoint	Neutron Leakage Per Unit Wavelength [neutrons/s/sterad./nm] All LD_2	LD_2+23.7 mm LN_2	LD_2+35.6 mm LN_2
15	2.15-2	1.65-2	1.90-2	1.87+16	1.88+16	1.88+16
16	2.51-2	2.15-2	2.33-2	1.61+16	1.61+16	1.61+16
17	2.86-2	2.51-2	2.68-2	1.45+16	1.45+16	1.46+16
18	3.27-2	2.86-2	3.06-2	1.49+16	1.48+16	1.48+16
19	3.73-2	3.27-2	3.50-2	1.43+16	1.42+16	1.41+16
20	4.13-2	3.73-2	3.93-2	1.30+16	1.29+16	1.29+16
21	4.54-2	4.13-2	4.33-2	1.15+16	1.15+16	1.16+16
22	4.98-2	4.54-2	4.76-2	1.29+16	1.25+16	1.28+16
23	5.51-2	4.98-2	5.25-2	1.23+16	1.20+16	1.28+16
24	6.17-2	5.51-2	5.84-2	2.26+16	2.14+16	2.38+16
25	7.11-2	6.17-2	6.64-2	4.87+16	4.71+16	5.24+16
26	8.87-2	7.11-2	7.99-2	9.37+16	9.60+16	1.05+17
27	1.28-1	8.87-2	1.08-1	2.25+17	2.26+17	2.33+17
28	1.65-1	1.28-1	1.47-1	2.30+17	2.38+17	2.42+17
29	2.86-1	1.65-1	2.26-1	1.52+17	1.67+17	1.71+17
30	4.29-1	2.86-1	3.58-1	1.27+17	1.34+17	1.33+17
31	5.02-1	4.29-1	4.65-1	9.72+16	9.95+16	9.73+16
32	5.61-1	5.02-1	5.31-1	7.08+16	7.17+16	6.97+16
33	6.17-1	5.61-1	5.89-1	5.31+16	5.34+16	5.16+16
34	6.74-1	6.17-1	6.46-1	3.94+16	3.95+16	3.81+16
35	7.51-1	6.74-1	7.13-1	2.82+16	2.82+16	2.71+16
36	8.44-1	7.51-1	7.97-1	1.86+16	1.85+16	1.78+16
37	9.81-1	8.44-1	9.12-1	1.10+16	1.10+16	1.05+16
38	1.22	9.81-1	1.10	5.06+15	5.03+15	4.83+15
39	9.05	1.22	5.13	1.29+14	1.29+14	1.24+14

References

1. R. A. Lillie and R. G. Alsmiller, Jr., July 1988 ANS Monthly Progress Report, Attachment 12.
2. R. A. Lillie, March 1989 ANS Monthly Progress Report, Attachment 8.
3. J. W. Arwood et al., "Preparation and Benchmarking of ANSL-V Cross Sections for Advanced Neutron Source Reactor Studies," *Trans. Am. Nucl. Soc.* **55**, 615 (1987).
4. D. L. Henderson, "Preliminary ANS Reactor Cold Source Gain Factor Calculations for Liquid Deuterium and Liquid Nitrogen-15," ORNL/TM-10824 (1988).

Fig. 1 Cold Source Two-Dimensional R-Z Model

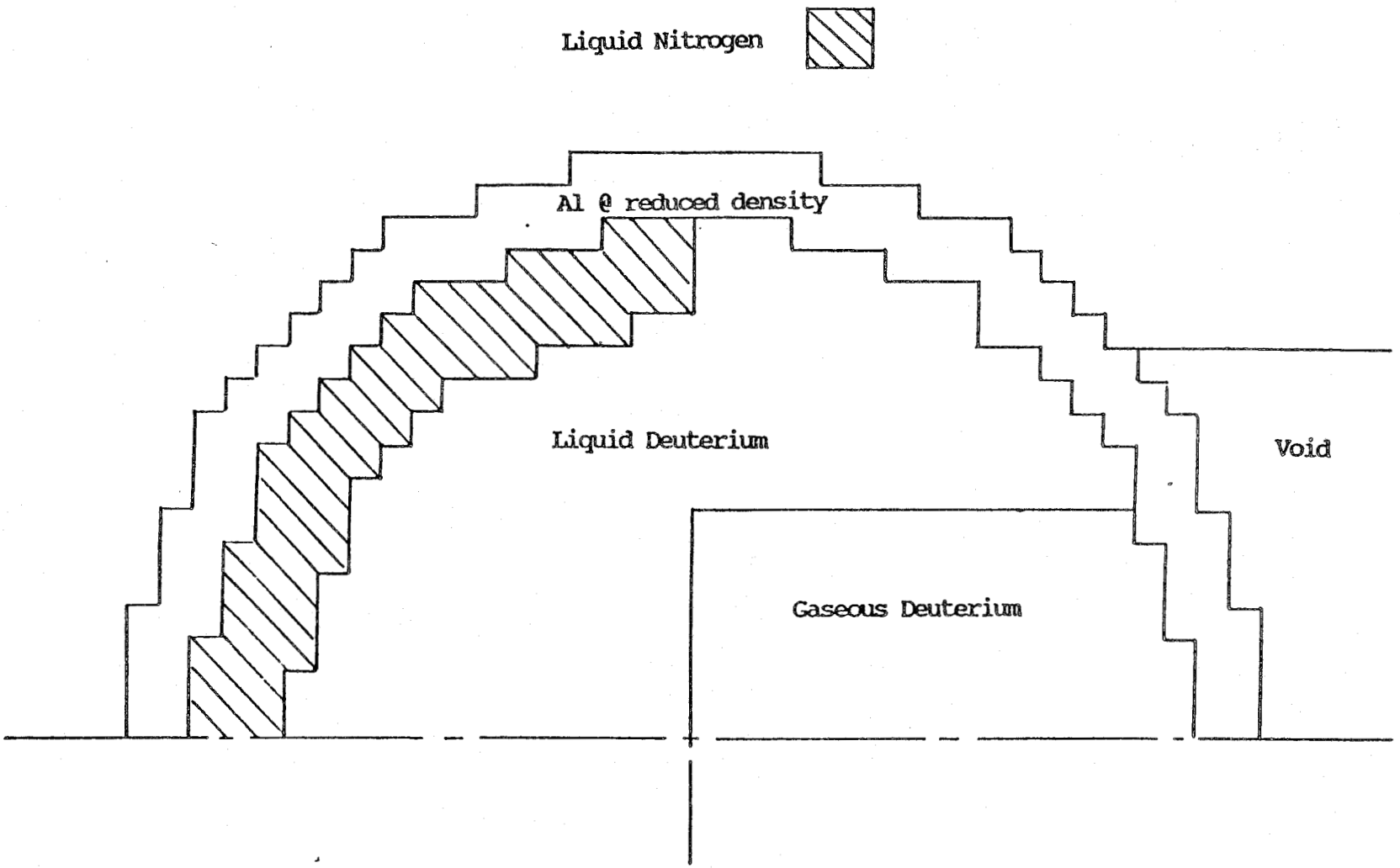

Fig. 2

Neutron Angular Leakage per unit Wavelength

(Cold Source centered at 748 mm,
Cold Source radius = 190 mm,
LN thickness = 23.7 mm,
Void Tube radius = 131 mm,
Cavity radius = 83.1 mm,
Neutron guide radius = 83.1 mm,
Angle from centerline = 0 Degree)

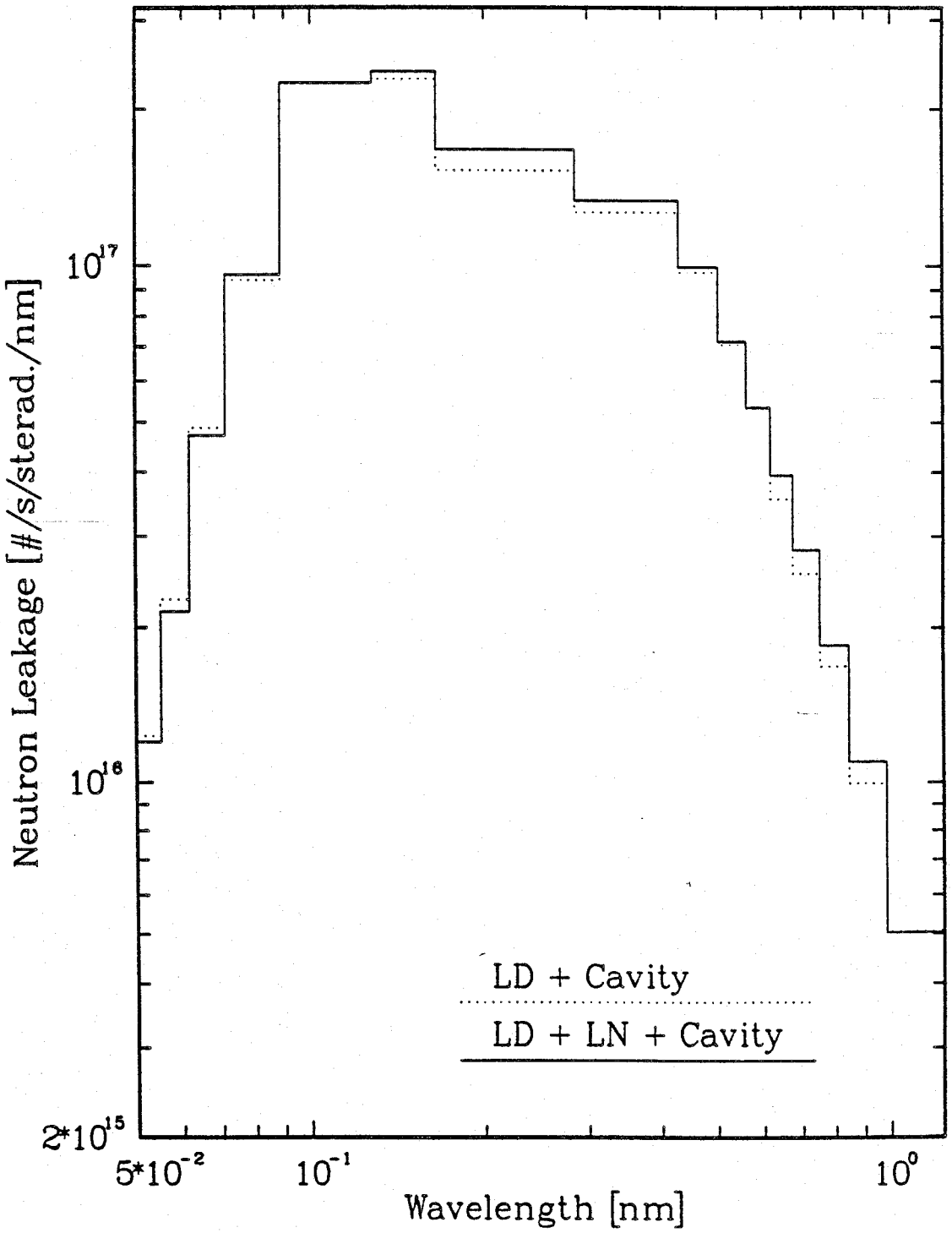

Fig. 3

Neutron Angular Leakage per unit Wavelength

(Cold Source centered at 748 mm,
Cold Source radius = 190 mm,
LN thickness = 23.7 mm,
Void Tube radius = 131 mm,
Cavity radius = 83.1 mm,
Neutron guide radius = 83.1 mm,
Angle from centerline = 0 Degree)

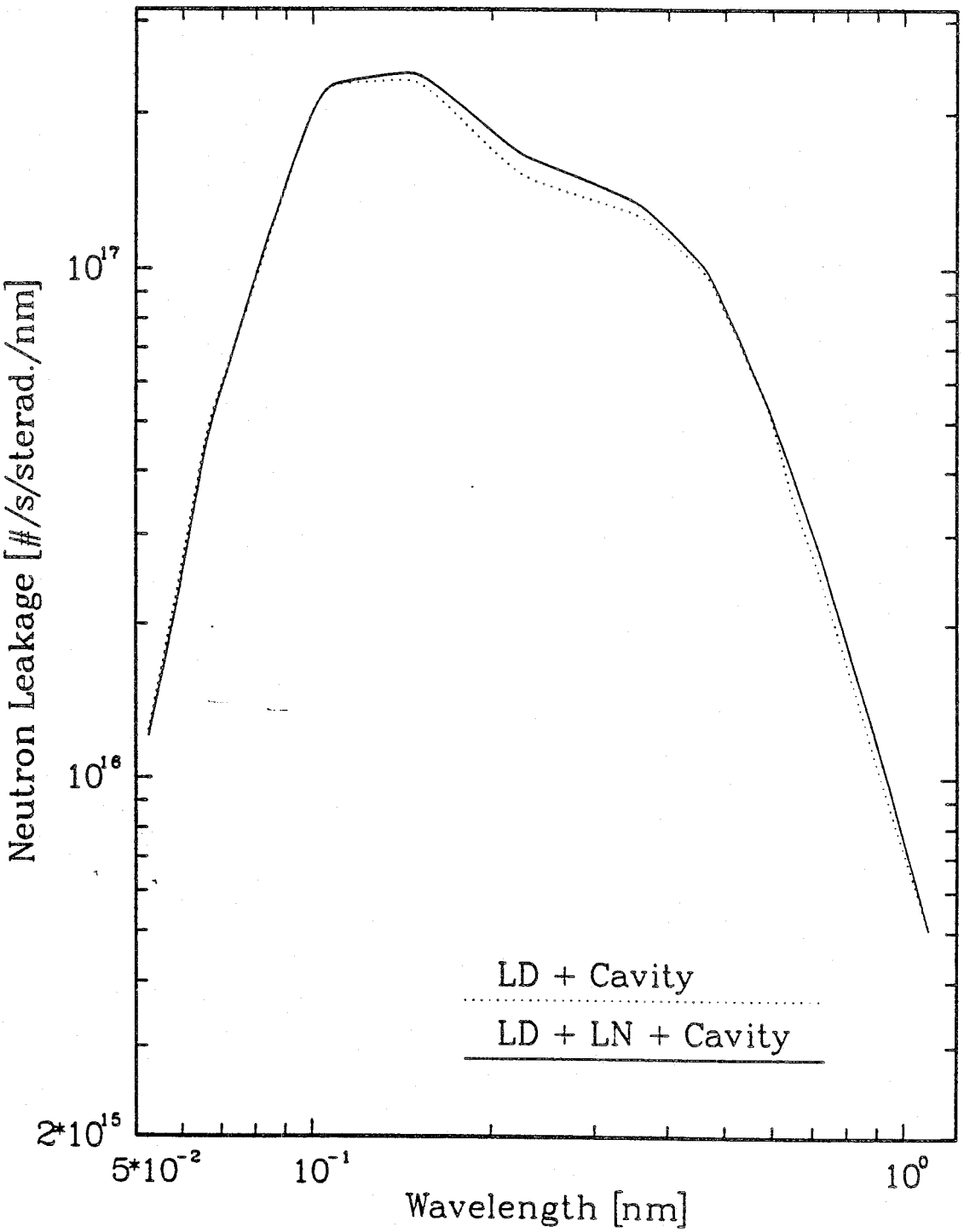

ATTACHMENT 10

Internal Correspondence

MARTIN MARIETTA ENERGY SYSTEMS, INC.

June 19, 1989

J A Johnson

WBS 1.1.9: Monthly Progress Report on Neutron Science Tasks for May, 1989

1. Neutron Multidetectors

As a first step in the ANS neutron multidetector R&D program, a survey of current detector capabilities and limitations has been undertaken by S. A. McElhaney of I&C Division. A questionnaire directed to 47 neutron laboratories worldwide led to detailed information on existing installations and current R&D programs at 23 different laboratories. Detector types identified include gaseous electronic, scintillation, semiconductor, video imaging, foil, image plate and photographic detector systems.

The ideal position-sensitive detector (PSD) should have a high efficiency (ϵ >80%), high countrate capability (>10^5 s^{-1}), good spatial resolution in two dimensions (<5 mm), short deadtime (<1 μs), inherently small γ-sensitivity and low electronic noise. In addition, a PSD should be stable, reliable, robust (especially with respect to possible "burning" by a direct beam), and comparable in cost to any other major spectrometer component. No currently available PSD can meet all of these requirements.

The gaseous electronic detectors provide high efficiency, good resolution, reliability, and excellent background rejection. They have problems, however, with timing, limited countrate capability, and expense. Currently, ORDELA, Inc. is working on a new encoding method for 1-D PSD's which should increase the countrate capability to 10^5 s^{-1} per pixel. Another effort showing promise is coupling of gaseous detectors with solid state devices, being developed at ILL. This design seeks to combine the attributes of a gas with the excellent timing and spatial resolution offered by solid state technology. In the future, continuing efforts by CERN and others to improve on existing multi-wire proportional counters (such as avalanche chambers) may provide further advances translatable to thermal neutron PSD's.

Scintillation detectors are currently receiving the most development work around the world. They offer the possibility of high spatial resolution, good efficiency (usually optimised at a given energy), high countrates, and short dead time. However, they suffer from a high γ-sensitivity. Many laboratories, including RAL, KFA, LANL, and ANL are actively pursuing the development of scintillation detectors and addressing the γ-sensitivity problem. Developers at RAL have returned to investigating the ^{6}Li/ZnS combination as a way to reduce the γ contribution, while KFA is investigating other ^{6}Li possibilities, such as ^{6}LiI, ^{6}LiH, and ^{6}LiD.

The application of imaging systems and foil detectors will depend on developments to overcome

limiting problems, such as low efficiency. The growing semiconductor industry effort shows great promise for PSD's at the resolution levels and countrates needed for SANS. This is a new field, however, and problems associated with γ-sensitivity and cost must still be addressed, although the possibility of mass production of devices should bring the cost down long term. A full report on the survey will be forthcoming this Fall.

2. Detector Shielding Calculations

The assessment of neutron transport calculations for the design of detector shielding is now being undertaken by the Brookhaven Group led by J F Carew, and initial computation of the shield neutron attenuation is underway. An existing ANISN 69-group one-dimensional model of the BNL HFBR core is being extended to include the vessel and the thermal and biological shields for use in determining the neutron detector ambient background spectrum in the neighbourhood of the H-7 and H-8 spectrometers. In addition, an ANISN model and cross-section database for the proposed ANS detector configuration (see April 1989 Monthly Report) is being constructed for the shield flux attenuation calculations. The H-7/H-8 neutron spectrum determined from the HFBR ANISN model will be used initially as the (typical) neutron flux background spectrum for input to the ANSISN detector shield calculations.

3. Topical Reports on the ANS

The second issue of **TRans** is attached.

4. Comparison of Beam Tube Designs at Saclay and ILL

For many types of thermal neutron scattering experiments, focussing monochromator techniques are able to provide gains of about a factor of 4 in flux on the sample, compared with that obtained using conventional (flat) monochromators. Many of these techniques were developed at the ILL, where (ironically) *optimal* use of focussing is often not possible, however, because the beam tube geometry, which was designed before focussing became commonplace, restricts the illumination available to a monochromator. Some of the lessons learned have been implemented in the design of the beam tubes at the new Saclay reactor, with the result that beam fluxes per source neutron are higher at Saclay than at ILL.

An analysis of the reasons for this flux gain is attached. It shows that, while a useful gain is available for "easy" experiments, there is *no* gain in practice for experiments which push the state-of-the-art; we expect the latter types of experiment to dominate at the ANS. The physical reason for this is that the flux gain is achieved by an increase in divergence, which usually needs to be removed again by collimation for high resolution work. In this case, the extra flux is actually delivered towards the spectrometer as *noise* rather than signal, and we would have been better off without it. These results are being studied to produce new

designs which provide real gains at high resolution in the ANS beam tube configurations, together with ways of relaxing the in-pile collimation for those experiments which can take advantage of higher flux produced by increased beam divergence.

5. Second-floor Beam Room

The nuclear and fundamental physics community has responded to a recent ANS questionnaire with a number of suggestions for beams and instruments. An important result of this response is that we are now able to begin more detailed conceptual layout studies of the second-floor beam room. Instruments on the second level must be able to use inclined beams or guides, which precludes most types of neutron scattering instruments (because of the mixing of horizontal and vertical divergences), but there are four classes of instrument currently proposed which could profitably be installed at this level:

(i) Very cold neutron (VCN) physics
(ii) Ultracold neutron (UCN) physics
(iii) Isotope separation on-line (ISOL)
(iv) Depth profiling station

The best current method of UCN production is to use a neutron turbine to Doppler-shift the energy of a VCN beam to lower values, because a VCN beam can be transported through sufficiently thin windows with absorption losses only, whereas a UCN beam will be totally reflected at all angles by likely window materials. Thus both the VCN and UCN beams will interface to the reactor *via* VCN guides having a typical cutoff wavelength of order 7 nm. To maximize solid angle, and to minimize window material, it is proposed to base the design on the current ILL concept, in which the VCN guide actually starts *inside* the top of the cold source, so that only a relatively thin cryogenic window intervenes. The attached sketches show how this might be achieved; since there will be two identical cold sources, two VCN guides are envisaged, one of them feeding a UCN convertor. The many safety questions raised by this configuration will require careful study.

The ISOL facility requires a thermal beam. It comprises an electromagnetic fission-product separator (with appropriate hot target handling capabilities) similar to the PN1 installation at ILL, and may be followed by a small accelerator and ion-transport lines to carry ion beams to adjacent work-stations. This would add a major new capability to the ANS, and would be of interest to conventional ion-beam researchers in materials science, as well as to nuclear physicists specifically studying neutron-rich nuclides. One concept is to base the separator design on a variation of PN1, which is sited on a horizontal beam and bends upward, by using an inclined beam and bending into the horizontal plane.

The depth profiling station is situated on an inclined cold neutron beam or guide. Unlike the prompt-γ stations, which have been situated in the low γ-background of the guide hall, depth-profiling involves charged particle detection and so is not inherently γ-sensitive, allowing siting on the second level.

Sketches of how these instruments might be configured are attached.

John B. Hayter, FEDC, MS-8218 (6-9300)

JBH:jh

Attachments:

ILL/Saclay Beam Tube Comparison
Second-floor Instrument Conceptual Layout
TRans for April, 1989

Comparison of Beam Tube Designs at Saclay and ILL

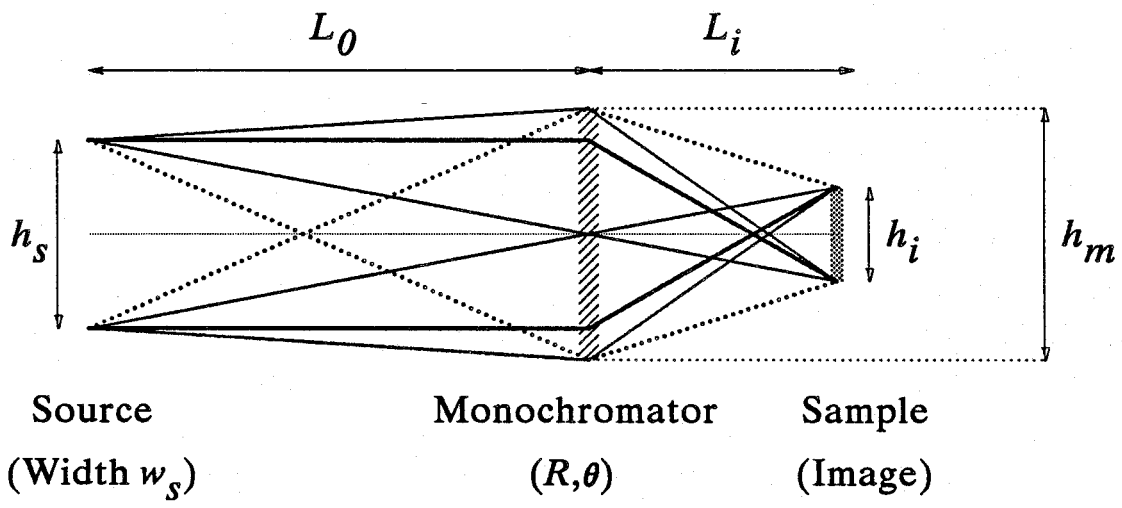

SACLAY

h_s = 150 mm
w_s = 80 mm
$L_0 \approx$ 4500 mm
$L_i \approx$ 700 mm

ILL

$h_s \approx$ 125 mm

$L_0 \approx$ 6250 mm
$L_i \approx$ 700 mm

The solid angle of the source, Ω, viewed by the sample is thus

$$\Omega = h_s w_s / L_0^2 = 5.9 \times 10^{-4} \text{ str}$$

$$\Omega = \pi (h_s / 2L_0)^2 = 3.1 \times 10^{-4} \text{ str}$$

which leads to a gain factor (per source neutron) of 1.9 in favor of Saclay, if *flux alone* is considered.

To see whether or not this corresponds to a genuine gain factor in a real experiment, however, we need to consider typical experimental conditions:

SACLAY	ILL

Horizontal divergence

$2a_h = 1.80 \times 10^{-2}$ (1.03°) $\qquad$ $2a_h = 1.54 \times 10^{-2}$ (0.88°)

Take $2a_h = 1.3 \times 10^{-2}$ *(0.75°)*
and Sample Height = Image Height (h_i)

$h_i = 23$ mm $\qquad$ $h_i = 14$ mm

$$I_{rel} = 2a_h h_m h_s / L_0 \quad s^{-1}$$

$I_{rel} = 2.60 \times 10^{-4}\, h_m$ $\qquad$ $I_{rel} = 4.33 \times 10^{-4}\, h_m$

Beam exits are the same height in the two designs, so we may take the monochromator height, h_m, to be the same in the two cases. In the case given above, where it is assumed that the sample is larger than the size of the image of the beam, there is still a factor of 1.67 in favor of the Saclay design. For many state-of-the-art experiments, however, adequate quantities of sample are not available. (A current example is provided by high-T_c superconductors, which are frustratingly difficult to crystallize.) For a sample smaller than the ILL beam image, the ILL design regains a factor 23/14, leaving effectively no difference between the two designs.

There are two lessons for ANS beam tube design. In the vertical plane, both source and exits heights should be maximized together, to the extent allowed by vertical divergence at the sample. In the horizontal plane, the source must subtend adequate solid angle from the sample, but the exit width need only correspond to the sample (not monochromator) size.

WBS 1.3.4
COLD SOURCE ASSEMBLY

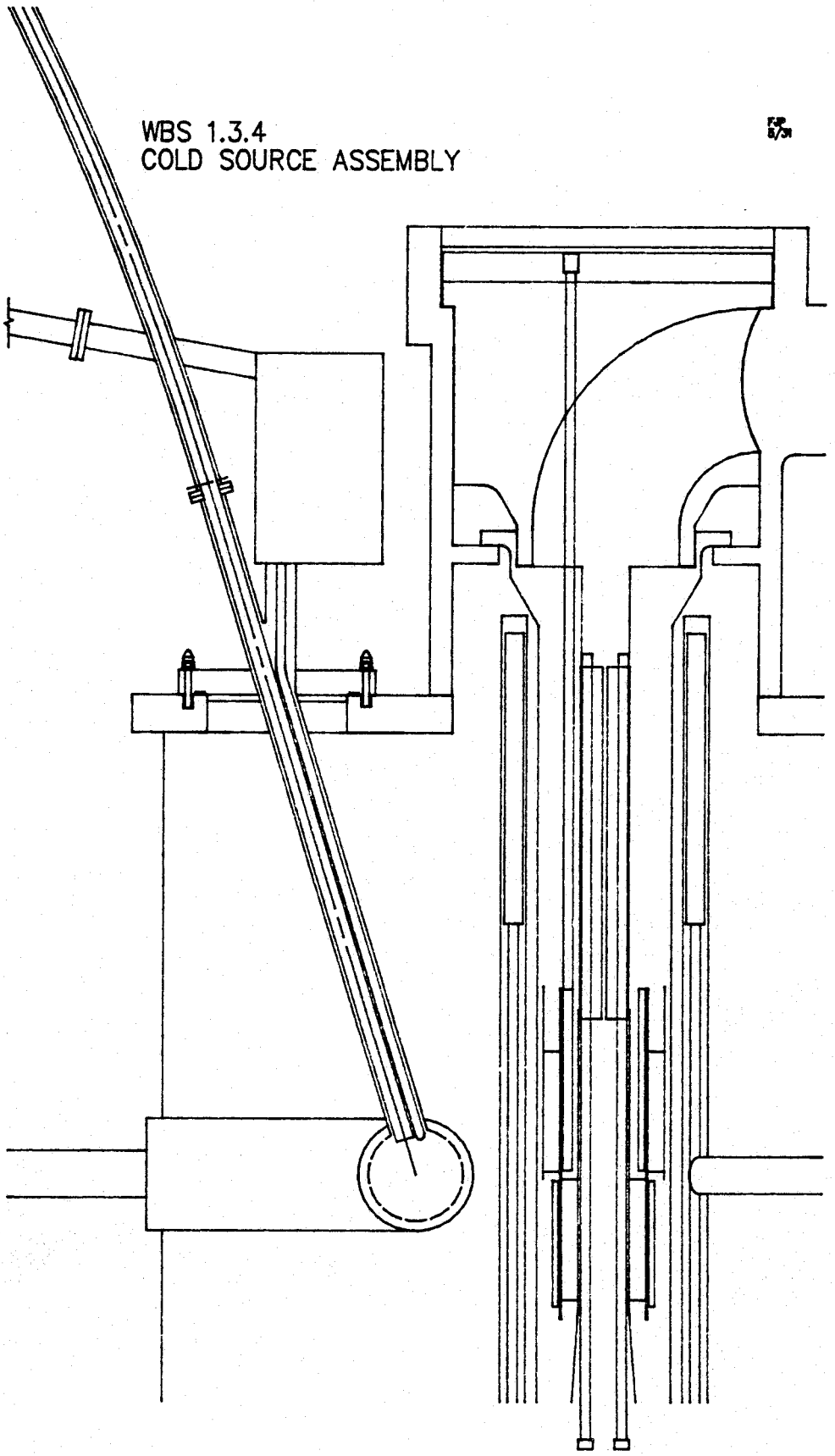

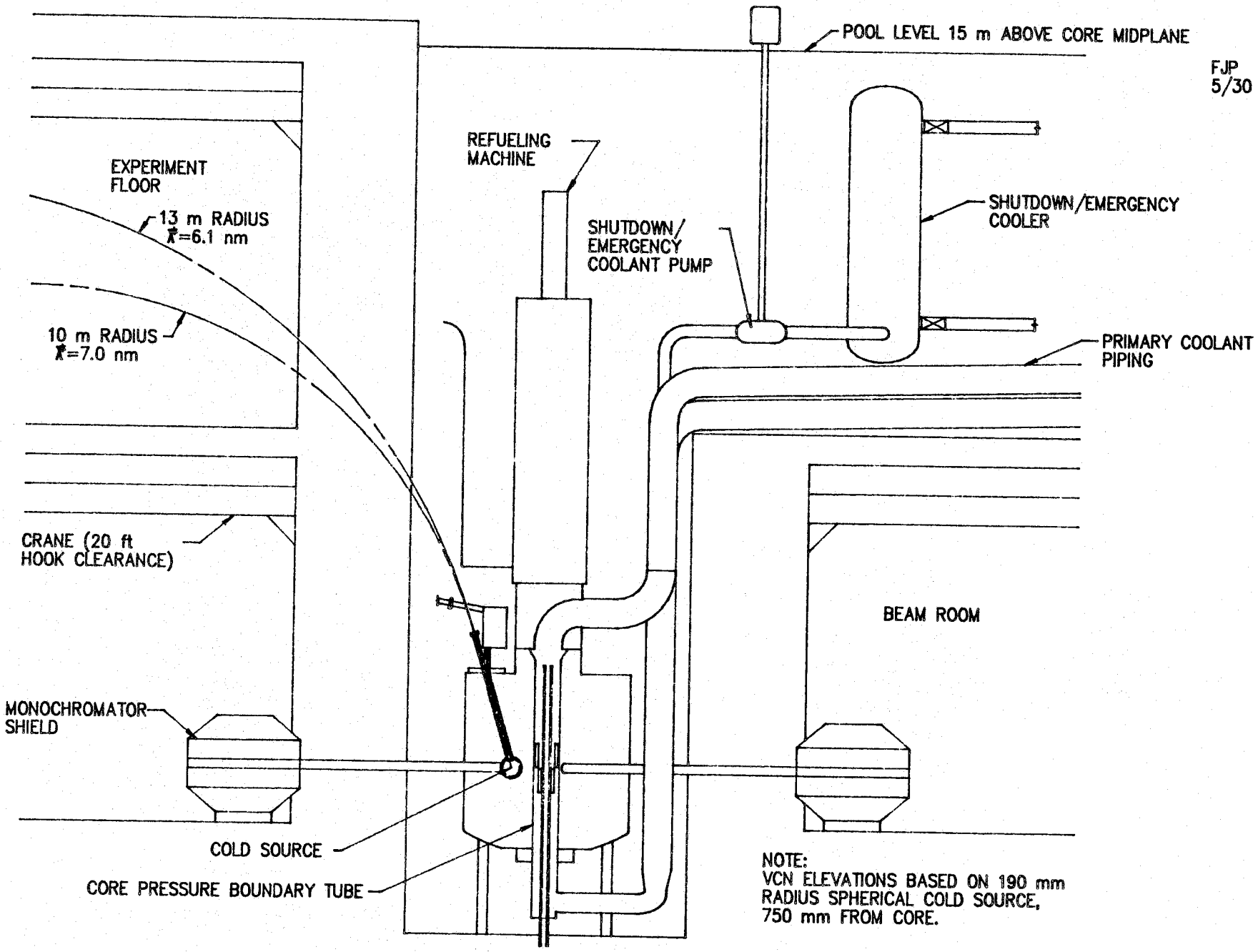
POOL LEVEL 15 m ABOVE CORE MIDPLANE
FJP
5/30
REFUELING
MACHINE
EXPERIMENT
FLOOR
13 m RADIUS
λ=6.1 nm
SHUTDOWN/
EMERGENCY
COOLANT PUMP
SHUTDOWN/EMERGENCY
COOLER
10 m RADIUS
λ=7.0 nm
PRIMARY COOLANT
PIPING
CRANE (20 ft
HOOK CLEARANCE)
BEAM ROOM
MONOCHROMATOR
SHIELD
COLD SOURCE
CORE PRESSURE BOUNDARY TUBE
NOTE:
VCN ELEVATIONS BASED ON 190 mm
RADIUS SPHERICAL COLD SOURCE,
750 mm FROM CORE.

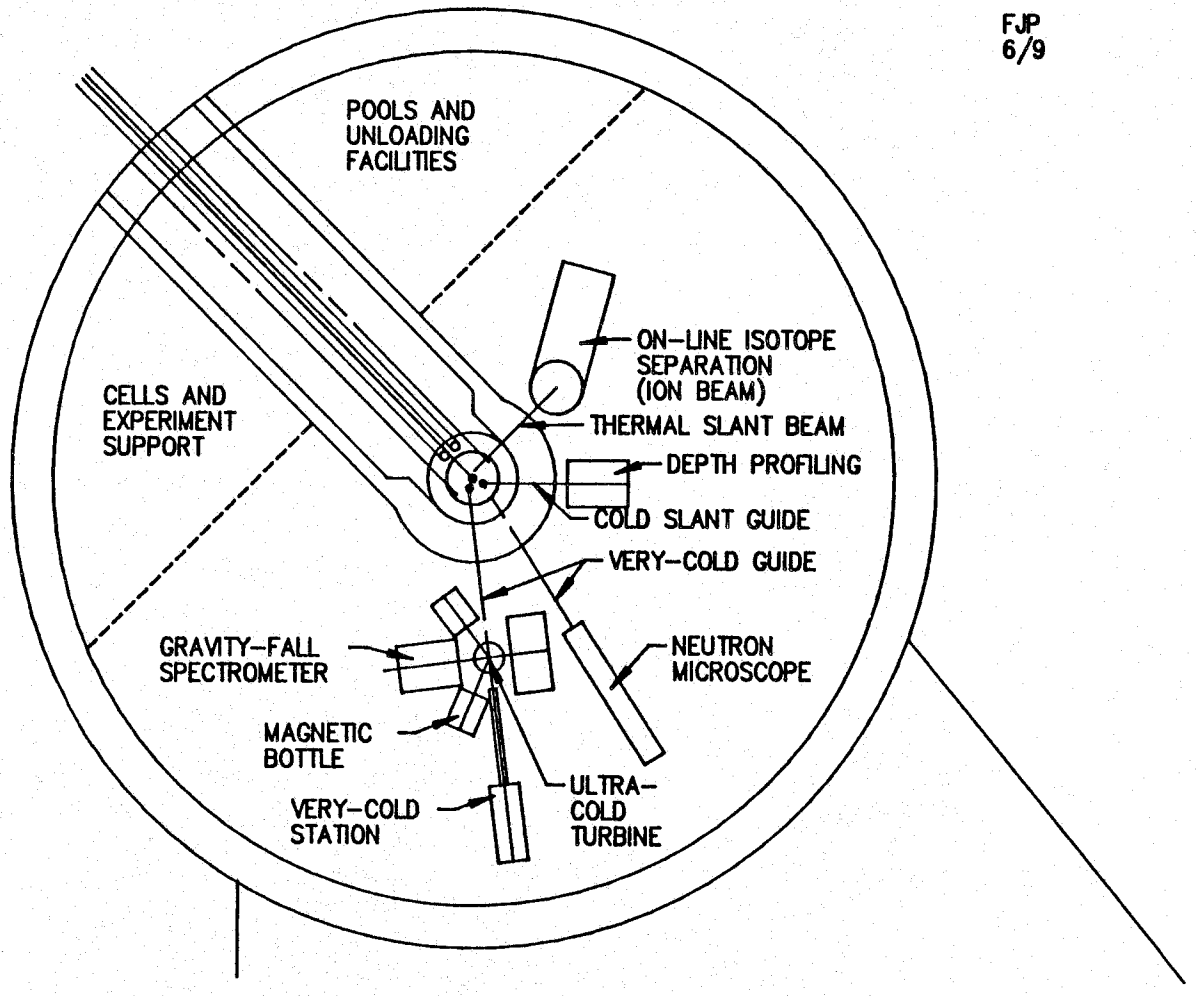
POOLS AND
UNLOADING
FACILITIES
CELLS AND
EXPERIMENT
SUPPORT
ON-LINE ISOTOPE
SEPARATION
(ION BEAM)
THERMAL SLANT BEAM
DEPTH PROFILING
COLD SLANT GUIDE
VERY-COLD GUIDE
GRAVITY-FALL
SPECTROMETER
NEUTRON
MICROSCOPE
MAGNETIC
BOTTLE
VERY-COLD
STATION
ULTRA-
COLD
TURBINE

TOPICAL REPORTS ON THE ADVANCED NEUTRON SOURCE

no 2, april 1989

ANS Reference Core Design

A project milestone has been met by the completion of preconceptual nuclear and thermal-hydraulic design work on the ANS reference core. The main features of the new design, which is still axially split and is cooled, reflected and moderated by heavy water, are shown opposite and in the table overleaf. One of the most noteworthy features is the provision of a separate coolant stream for each of the two annular elements; this new arrangement, which evolved from the flow divertor concept proposed last year to enhance cooling capacity and reduce water temperature, is combined with an upflow coolant direction which promotes a smooth and relatively rapid transition from forced to natural convective cooling.

Careful optimization of the fuel element dimensions and neutronics has produced a design with more than twice the volume of the reference split core presented at the February 1988 *Core Comparison Workshop*, leading to very much higher thermal-hydraulic margins. The adoption of such a design reflects the project's policy of making safety considerations a major design driver and is also responsive to the advice tendered by the group (chaired by J. M. Hendrie) who reviewed ANS design and R&D work on behalf of the Basic Energy Sciences Advisory Committee late last year.

For given thermal-hydraulic limits on power density, the improved cooling system and the larger active volume allow this core to accept a higher power level than previous reference core designs. The neutronic characteristics are such that a high rendement* is maintained despite the increased core volume; the doubling of core volume has been achieved with a loss of only about 15% in rendement.

The fuel elements have a much smaller radial thickness than previous split core designs. As

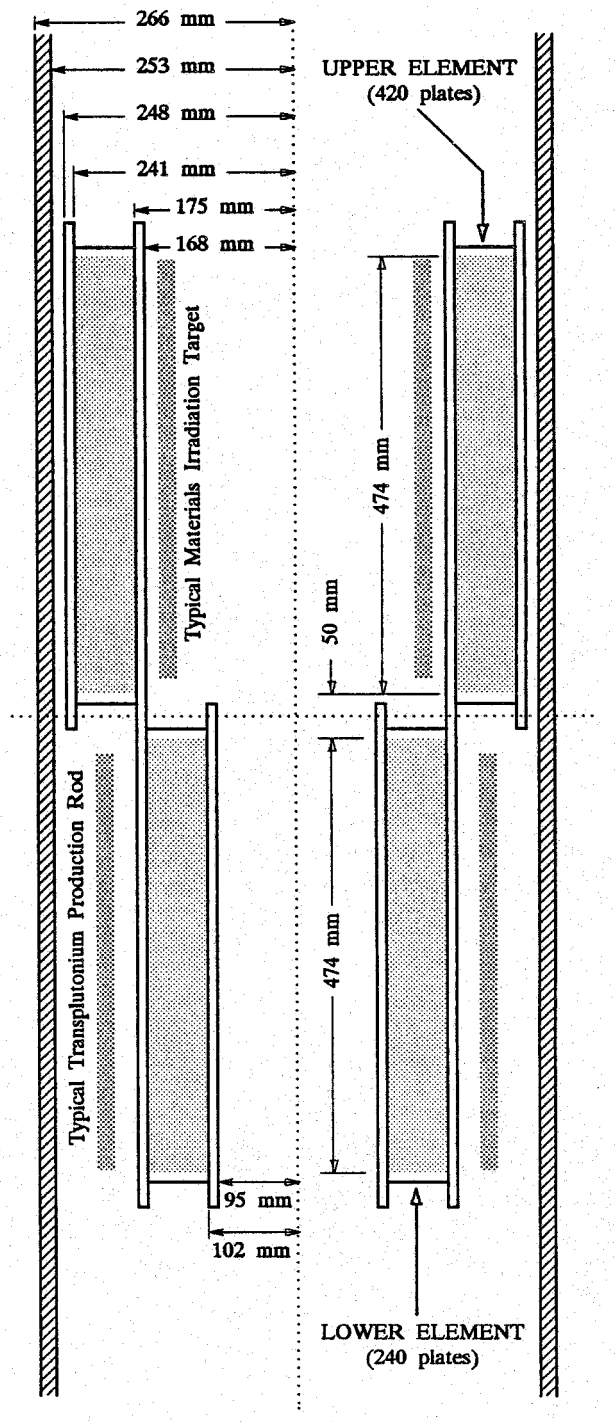

Rendement is the ratio of neutron flux in the reflector to the neutron production rate in the core.

PRECONCEPTUAL CORE DESIGN DATA

Configuration	
Number of elements	2
Geometry	Split core
Element alignment	Coaxial
Coolant flow	Upflow
Flow path	Coaxial
Fuel plate geometry	Involute
Core Dimensions	
Fueled volume	67.4 L
Heated length per element	474 mm
Flow area in coolant channels	0.071 m^2
Span of outer element plates	83 mm
Span of inner element plates	97 mm
Fuel loading per element	9 kg
Thermal-Hydraulic Conditions	
Inlet pressure	3.7 MPa
Inlet temperature	49°C
Flow velocity in element	27.4 $m.s^{-1}$
Mass flow in core	1950 $kg.s^{-1}$
Power in core*	350 MW
Power density*	5.2 $MW.L^{-1}$
Bulk outlet temperature*	88°C
Core Physics	
Reactivity at start of cycle	1.26
Rendement at 14 days†	3.26
Peak thermal flux*†	8.5×10^{19} $m^{-2}.s^{-1}$
Average fuel burnup	30%
Thermal:fast ratio at the thermal flux peak	100:1
Control Elements	
Control and shutdown rods	4 inside core
Independent shutdown rods	8 outside core
Materials	
Fuel	U_3Si_2
Enrichment	93%
Coolant	D_2O
Structure	6061-T6 Al
Control elements	Hf
Burnable poison	B_4C

*At incipient boiling limit
†Unperturbed

a result, there is less self-shielding, and less than 18 kg of ^{235}U are needed, compared with more than 25 kg in some earlier designs. As well as offering higher efficiency, the relatively narrow plates will also be much more stable at high coolant velocities.

The thermal-hydraulic parameters will be refined as further design details, such as fuel grading, are incorporated. In particular, the exact value of the thermal hydraulic limit depends on the conditions of oxide growth on the aluminum-clad fuel plates. Recent experimental results from the ANS heated water test loop imply that the Griess correlation and the INEL data from the Advanced Test Reactor underestimate the rate of oxide growth under ANS heat-flux conditions: the ANS loop was constructed to check this very possibility. If these results are confirmed, the power in this core design may be limited to about 300 MW (fission), a reduction of 14%. However, in that case, the core emerging from the conceptual design would be reoptimized, so that the reduction in the thermal neutron flux would be somewhat less than 14%.

Preliminary neutronics calculations indicate that the spectra at both the materials irradiation and transplutonium production positions have very desirable characteristics, while the introduction of the targets has <2% impact on the thermal flux in the reflector.

° ° °

Next issue: *Beam and Instrument Layout*

TRans is edited by

John B. Hayter
Oak Ridge National Laboratory
FEDC
PO Box 2009
Oak Ridge, TN 37831-8218

Oak Ridge National Laboratory is operated by Martin Marietta Energy Systems, Inc., under Contract No. DE-AC05-84OR21400 with the United States Department of Energy.

ATTACHMENT 11

Preliminary considerations on some transport characteristics of the final preconceptual design core

T. Nishigori

In preparation for the beam tube analysis, a DORT fixed source calculation has been completed for an offset core with radially graded fuel. Also, a DORT eigenvalue calculation has been carried out to see the adequacy of the fixed source calculation, in which the neutron production distribution is replaced by a fixed source obtained in the diffusion approximation. The calculational procedure is shown in Fig. 1. The basic cross section set is ANSXSLB1 with 15 neutron and 18 gamma energy groups; it lacks Ni and B-11, and takes no account of the spatial dependence of the U-235 cross sections. The following results should therefore be considered preliminary. The geometrical model and a fission neutron distribution were taken from the BOLD-VENTURE calculation designated D5 by Difilippo. The fuel is graded radially, control rods are withdrawn, and boron is placed in the endcaps. The fine mesh intervals are 121X230 in r-z geometry, the Sn order is 10, and the convergence is to 10^{-3} for local quantities.

The results for the k-eff are as follows:

BOLD-VENTURE (Case D5)	0.9915
DORT fixed source	0.9550 (-3.7%)
DORT k-calculation	0.9624 (-2.9%).

Here, the reactivity in the fixed source calculation was calculated by

$$k\text{-eff} = P / (A + L)$$

(see Table I), where the total production rate P was obtained by restarting DORT with the fission calculation option switched on (i.e., NOFIS=1). Both the transport calculations underestimate the reactivity by about 3%. The reason for this is seen from the balance table (Table I), which shows that the transport calculations give rather low production rates. The production cross section of U-235 should therefore be carefully examined by taking proper account of the spatial dependence of the energy collapsing spectrum. The absorption rates, on the other hand, give a much closer agreement; the small difference of this order is what we expect in comparison of k-eff between the transport and diffusion calculations (see Y.Y. Azmy and F.C. Difilippo, in Proc. Topl. Mtg. Reactor Phys., Jackson, Wy, Sept. 1988). Note, however, that this difference is partly due to the lack of the Ni and B-11 cross sections, which decreases the absorption rate. Note also that the transport calculations give much larger leakage rates. This is due to a large axial leakage, which cannot be dealt with by the isotropic diffusion calculation.

The results for the peak thermal flux are as follows:

BOLD-VENTURE	0.747×10^{20} n/m²s	(below 0.625 eV)
DORT source	0.898	
DORT k-calc.	0.915,	

where the upper boundary of the thermal energy range is 0.625 eV. A correction has been made for the difference in the upper energy boundary (0.65 eV in the diffusion calculation and 3.05 eV in the transport calculation) by assuming an 1/E spectrum

$$\phi(E) = 1.73 \times 10^{18} / E \qquad (n/m^2 \cdot s \cdot eV),$$

where the coefficient was determined by the value of the flux in the 14th energy group (3.05 to 10 eV) at the peak location in the DORT k-calculation; it was confirmed by the fact that the corresponding coefficients are 1.77×10^{18} and 1.67×10^{18} at the 13th and 12th energy groups (up to 100 eV), respectively. The discrepancy of about 20% arises from the different calculational methods and the different cross section sets. Figure 2 shows the radial thermal flux distribution at the peak location (axial interval of -15.2 cm to -14.2 cm below the midplane), obtained in the DORT k-calculation. The result of the DORT fixed source calculation differs from this by a few % in the thermal flux and about 10% in the fast flux.

The 2D structure of the thermal flux distribution obtained in the DORT k-calculation is shown in Fig. 3, where the fluxes, normalized to 10 at the peak location (marked by X), are shown with respect to the radial and axial mesh numbers. The fuel region uses very fine meshes, and is shown magnified in the figure. The boundary of the region where the flux exceeds 80% of the peak value is indicated by a thick line. A closer look around this region is given in FIg. 4 for the DORT k- and fixed source calculations. The corresponding peak location and the region boundary (arrow mark) in the VENTURE result are also shown. The distance of the two peak locations is radially 1.3 cm and axially 3.0 cm. The region of flux $\geqslant$ 8 slightly extends downward in the DORT k-calculation. The DORT fixed source calculation gives a more closer result to the VENTURE calculation.

THe following conclusion can be drawn:

(1) The large discrepancy in k-eff between the diffusion and transport calculations appears to be due to the U-235 production cross section used in the transport calculation. A new cross section set will soon be released from Primm, and the transport calculations will be repeated with it.

(2) The k-calculation gives, in principle, the most reliable result, while the fixed source calculation is an approximation to it. However, the quality of the cross section set is very important, and must be carefully checked before performing the k-calculation.

(3) The relative difference in the results of the two transport calculations will not substantially be altered by the use of an improved cross section set. The difference of 0.8% in k-eff and about 2% in peak thermal flux should be noted; it

cannot be ignored in the discussion of many core characteristics parameters.

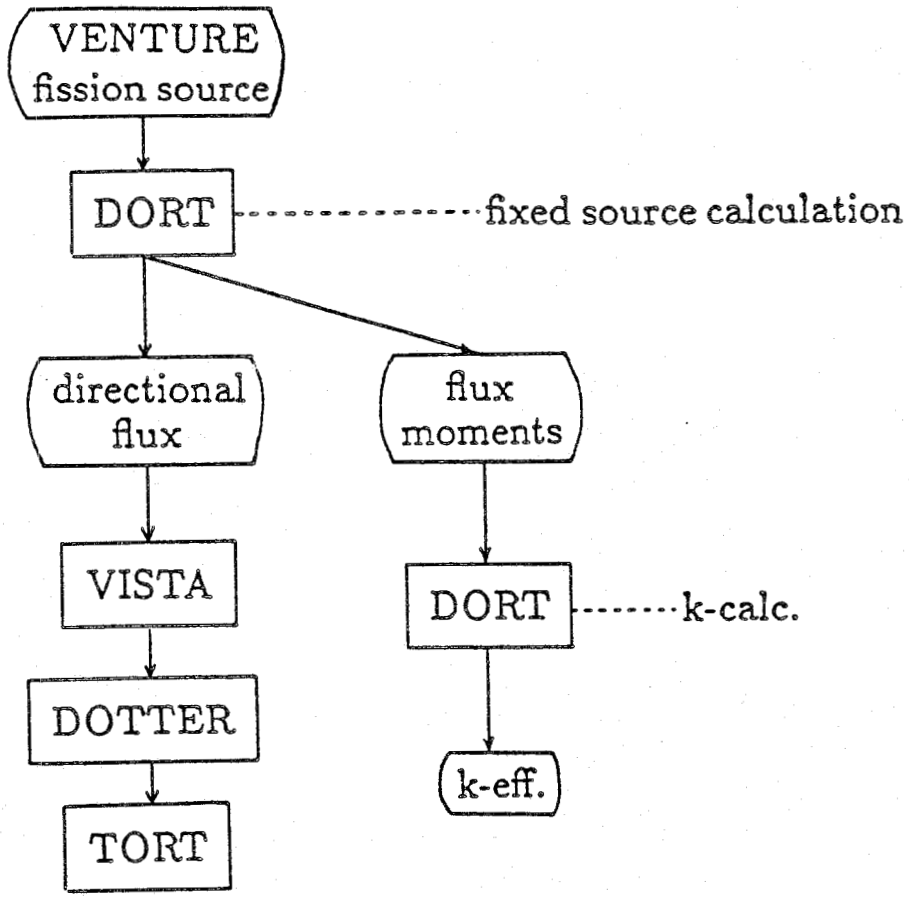

Fig. 1

Table I

Balance Table

(10^{19} neutrons/sec)

	Production	Absorption	Leakage	P/(A+L)
VENTURE	2.649	2.670	0.00122	0.9915
DORT-s	2.539(-4.2%)	2.656(-0.5%)	0.00198	0.9550
DORT-k	2.549(-3.8%)	2.660(-0.4%)	0.00202	

Radial Flux Profile

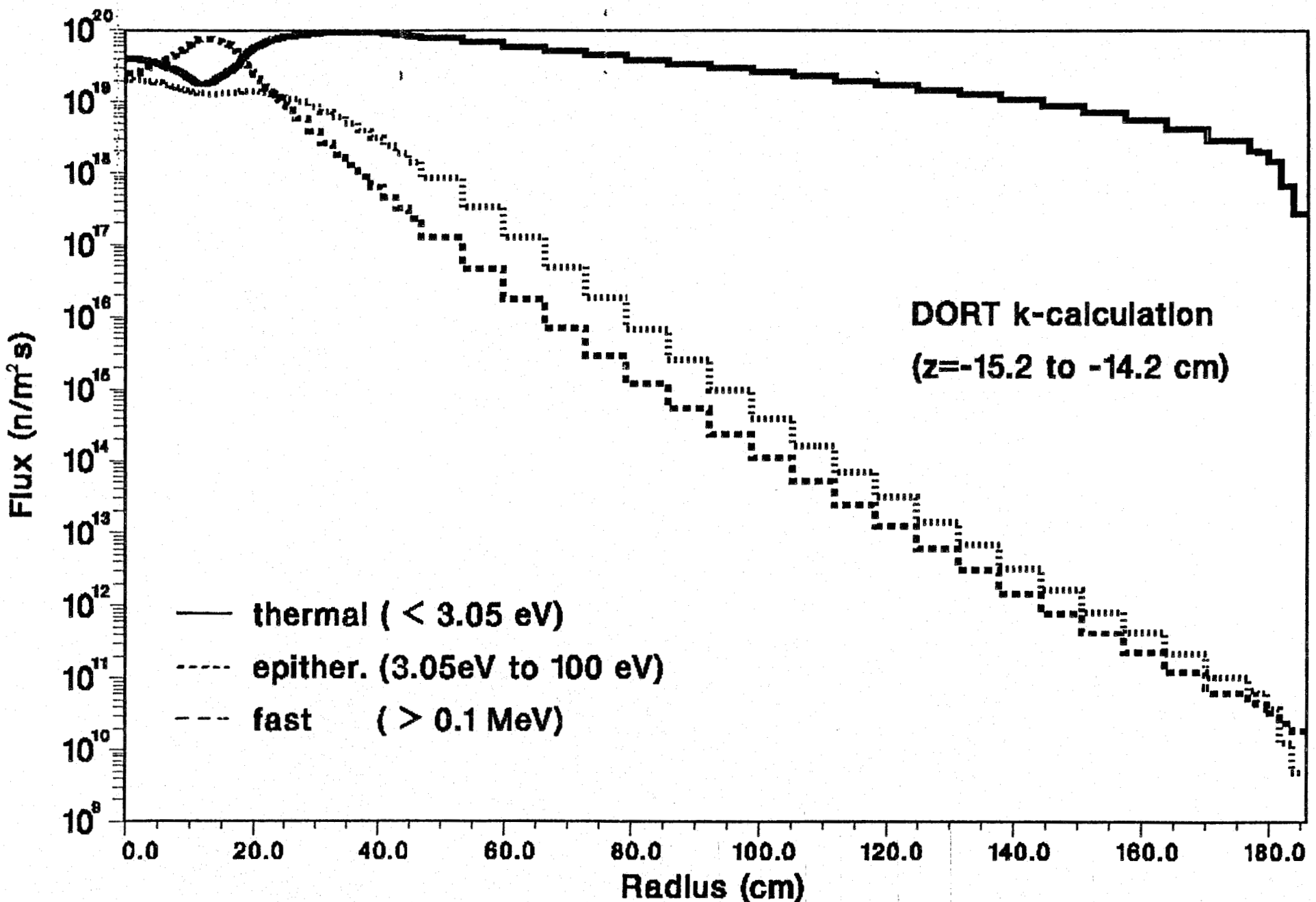

Fig. 2

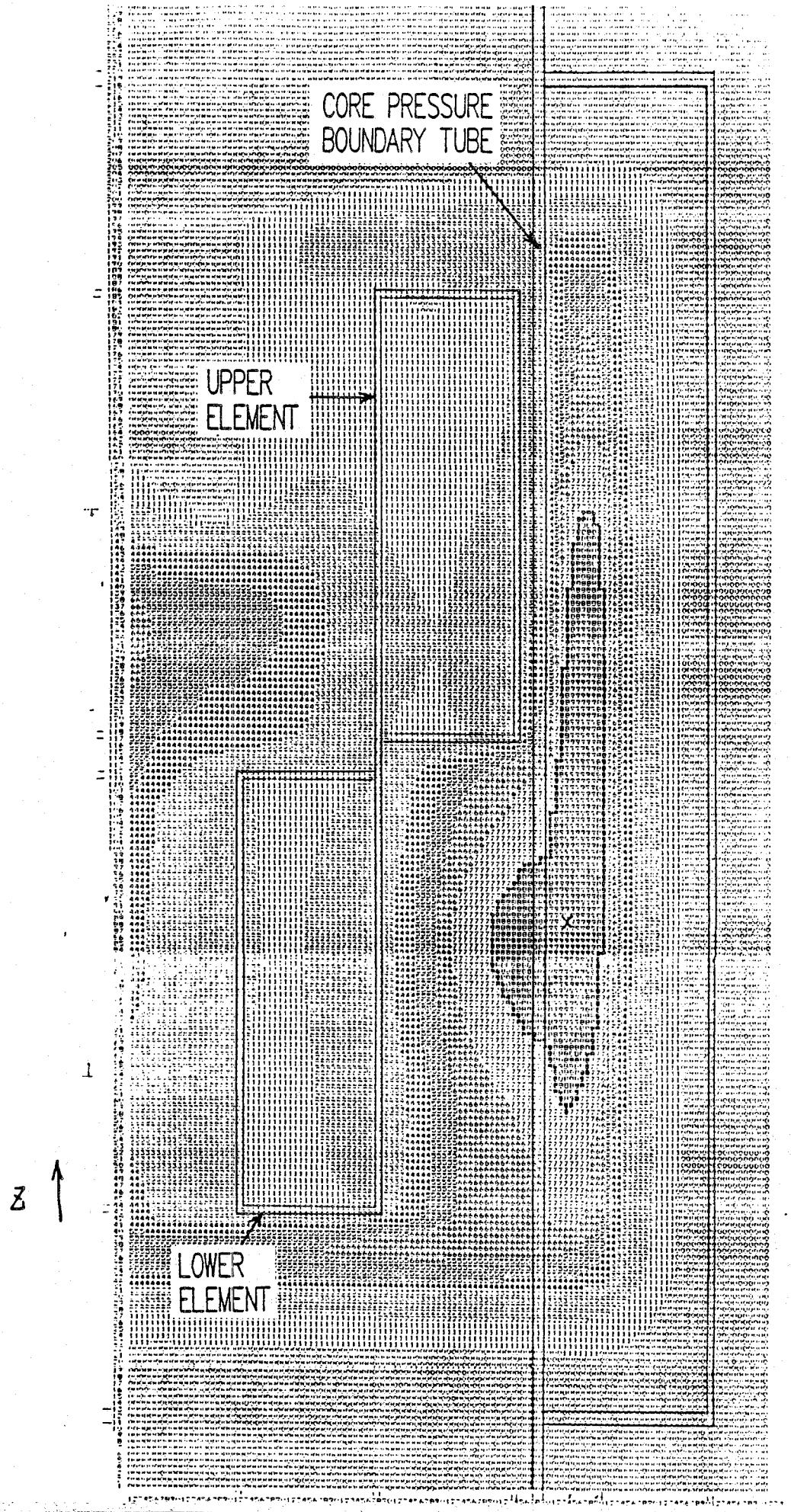

Fig. 3
thermal
flux
distribution
DORT-k

Region with thermal flux > 80 % peak value

DORT k-calc.

DORT fixed source calc.

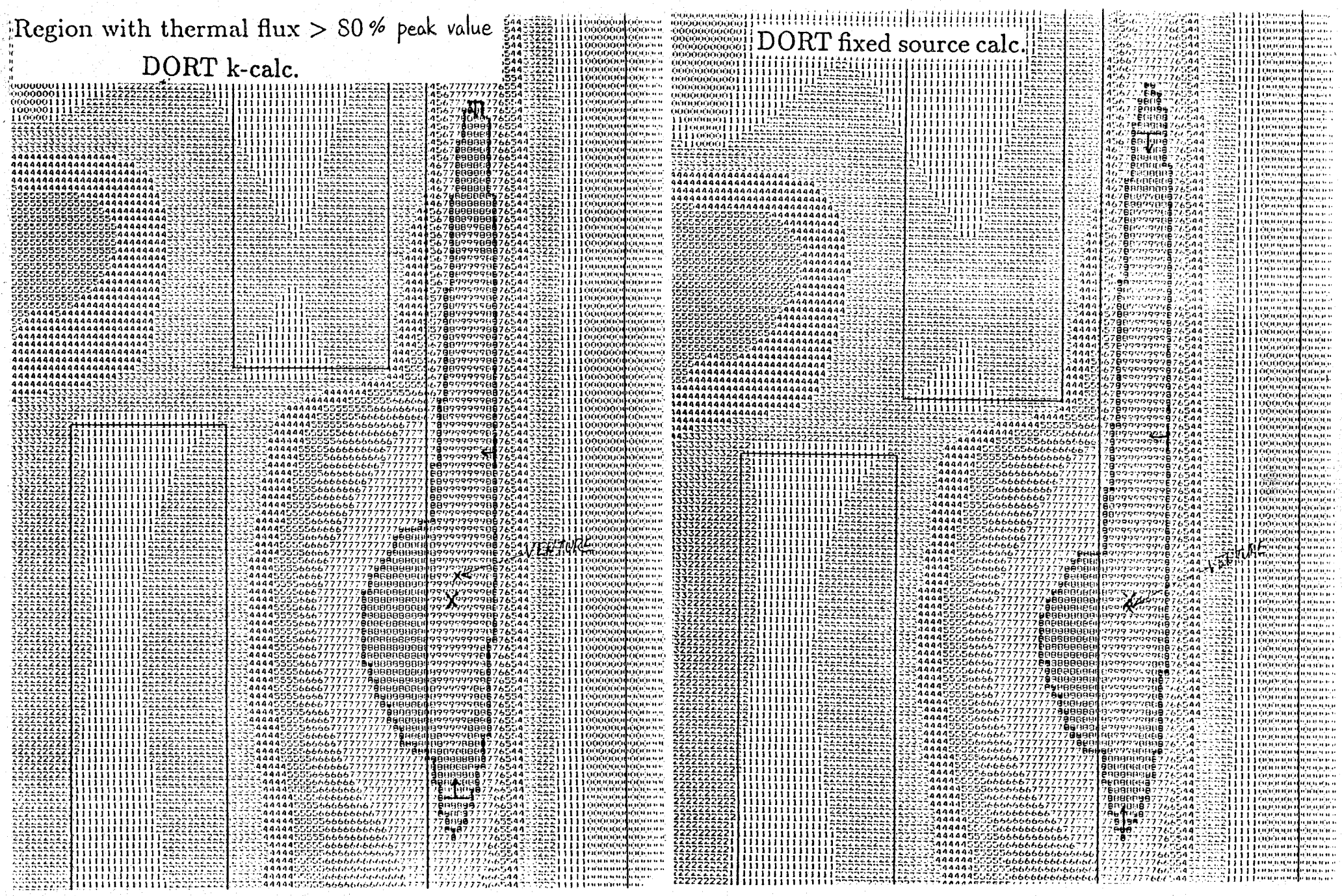

Fig. 4

ATTACHMENT 12

April and May 1989 Progress Report

HEATING RATE CALCULATIONS FOR THE ANS

Y. Y. Azmy

The computer codes HTR and H-CS are used to calculate heating rates, generate contour maps and coded plots, respectively, as described in previous reports. These two codes, together with sample input files for previous calculations, and files containing neutron and gamma kerma factors data have been successfully transferred to the E machine at Livermore. Necessary modifications were made to the codes to make them compatible with the operating system and the DISSPLA library version in use. Sample runs were performed to check the performance of the codes using scalar fluxes that have been generated at Livermore for the old ANS split core. The results are comparable to those obtained on the K-25 Cray. Concerning turn-around time, viewing the generated plots on-screen is as slow as the Livermore system, in general (~60 second wall clock time per plot). Hard copies, on the other hand, take about ten days (i.e., more than seven working days) to arrive here, as opposed to, at most, one day at K-25. However, Livermore has a very high quality plotting device that produces glossy prints for publication purposes.

ATTACHMENT 13

ANS Project Safety Activities - May 1989

The major activities of the month included transient and steady-state thermal-hydraulics analysis, severe accident analysis, and probabilistic risk assessment. There was no work in regulatory safety criteria and goals, WBS 1.2.3.1, because, as reported previously, it is planned for this task to remain inactive for the remainder of the fiscal year.

Transient thermal-hydraulic accident analysis, WBS 1.2.3.2, activities (report attached) included N. Chen's review of the RELAP5 model of the ANS under development at INEL, and A. Ruggles' comparison of the RELAP5 thermal-hydraulic correlations to other correlations in the literature.

The severe accident issues characterization task, WBS 1.2.3.5 (report attached), activities included modification of the fuel-coolant interaction (FCI, or "steam explosion") report to take into account technical review comments, and the initiation of a scoping study of core melting, relocation and fission product release.

The May report for the INEL RELAP task can be found in the monthly report of the INEL activities in support of the Advanced Neutron Source (near the beginning of the ANS monthly report). In the section on RELAP model development, C. D. Fletcher reports that the shutdown cooler loop model has been completed and is being checked out, and that a pressurizing pump system model is currently under development. Fletcher documented assumptions used in the development of the RELAP5 model of the main heat exchanger loop in a May 8, 1989 letter to R. M. Harrington (attached).

Activities in the PRA task, WBS 1.2.3.4 (report attached) continued the scoping study to determine the dominant accident sequences for the ANS.

R M Harrington

R. M. Harrington
FEDC, 574-1062 (FTS 624-1062)

MARTIN MARIETTA

Internal Correspondence

WBS 1.2.3.2

MARTIN MARIETTA ENERGY SYSTEMS, INC.

June 16, 1989

R. M. Harrington
J. A. Johnson

ANS Transient Thermal Analysis Task Monthly Progress Report for May 1989

RELAP5 Code Development and Validation (A. E. Ruggles)

The sensitivity of the Bergles and Rohsenow Correlation for the incipience of boiling to the single phase forced convection correlation chosen to predict the local wall temperature was examined in response to some concerns expressed by Don Fletcher at INEL. Figure 1 shows the heat flux at the incipience of boiling as predicted by the Bergles and Rohsenow correlation using either the Dittus-Boelter or Petukhov single phase forced convection correlations. The corresponding heat transfer coefficients are given in Figure 2. Uniform axial heat flux values have been used.

Don Fletcher also observed from hand calculations that the Gambill-Weatherhead correlation for the critical heat flux intersects the Saha-Zuber model for the onset of net vapor generation at high flow velocity. Figure 3 shows the Gambill-Weatherhead correlation (i.e., "Modified Gambill's Additive Method with Weatherhead's T_{sat}" per July 1988 Monthly) and compares it with other heat transfer limits of interest. Uniform axial heat flux values are assumed. Note that the Gambill-Weatherhead correlation is the one recommended to be implemented in the RELAP5 code for eventual use in ANS transient simulations.

RELAP5 Model Development and Review (N. C. J. Chen)

Portions of the RELAP Loop model have been assembled by INEL and are presently under review. A sketch of the model is presented in Figure 4. The core model (portion of Figure 4 labeled core) was discussed in previous monthly reports, both by INEL and myself. The model presently contains three active primary loops (only one shown in the figure) and one shutdown loop. The major components modelled in the primary coolant loop are the main heat exchangers, the circulation pump, and various piping components. The shutdown cooling loop is similarly modelled.

G. L. Yoder, 9204-1, MS-8045 (4-5282)

GLY:beh

Attachment

cc/att: D. W. Burton
N. C. J. Chen
D. G. Morris
A. E. Ruggles
C. D. West

FIGURE 1;

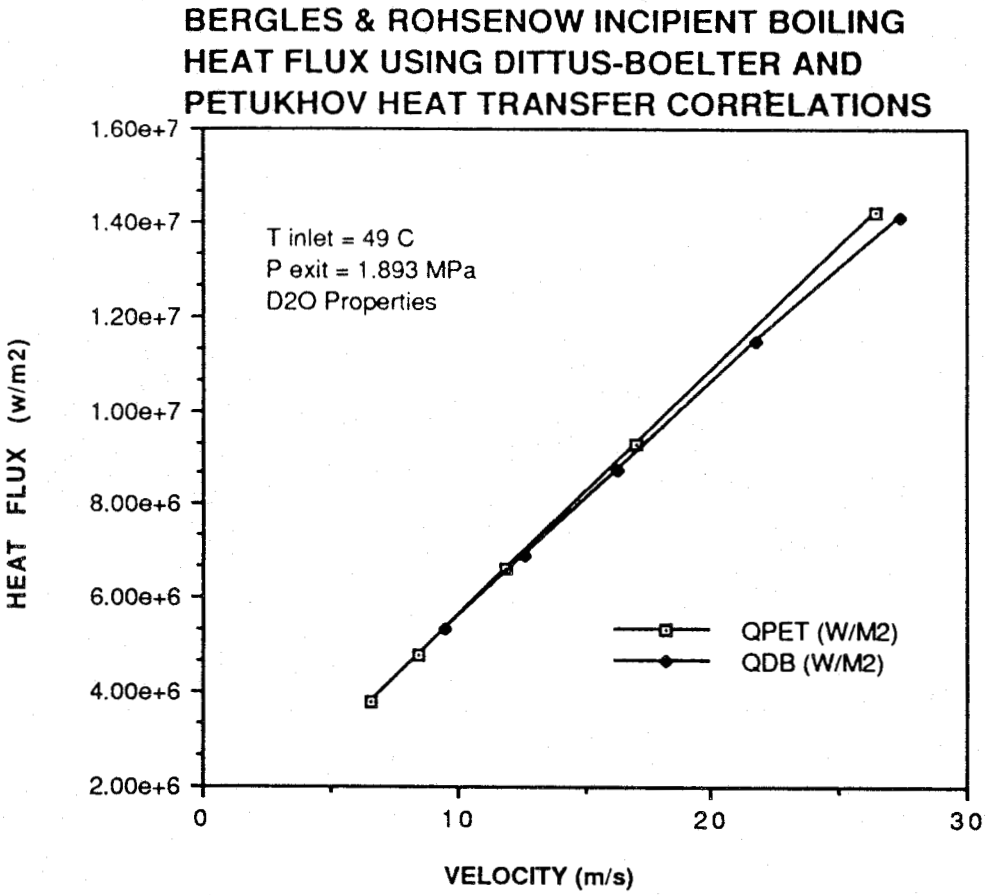

Figure 2: **Dittus-Boelter and Petukhov Single Phase Forced Convection Heat Transfer Coeficients**

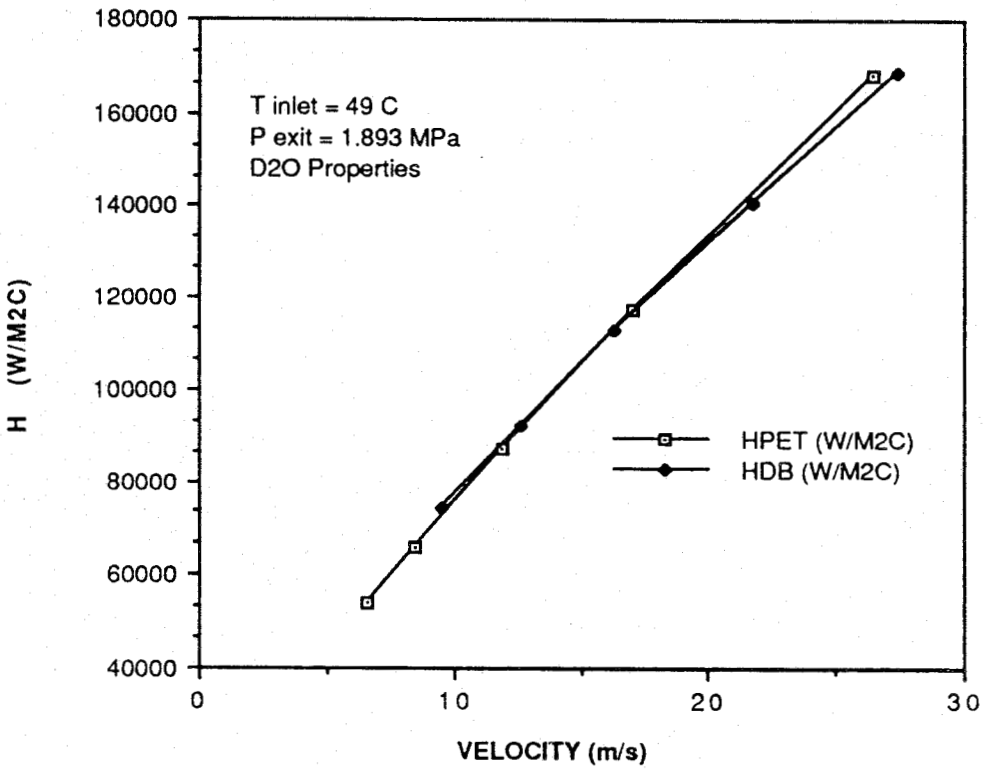

FIGURE 3;

COMPARISON OF HEAT TRANSFER LIMITS

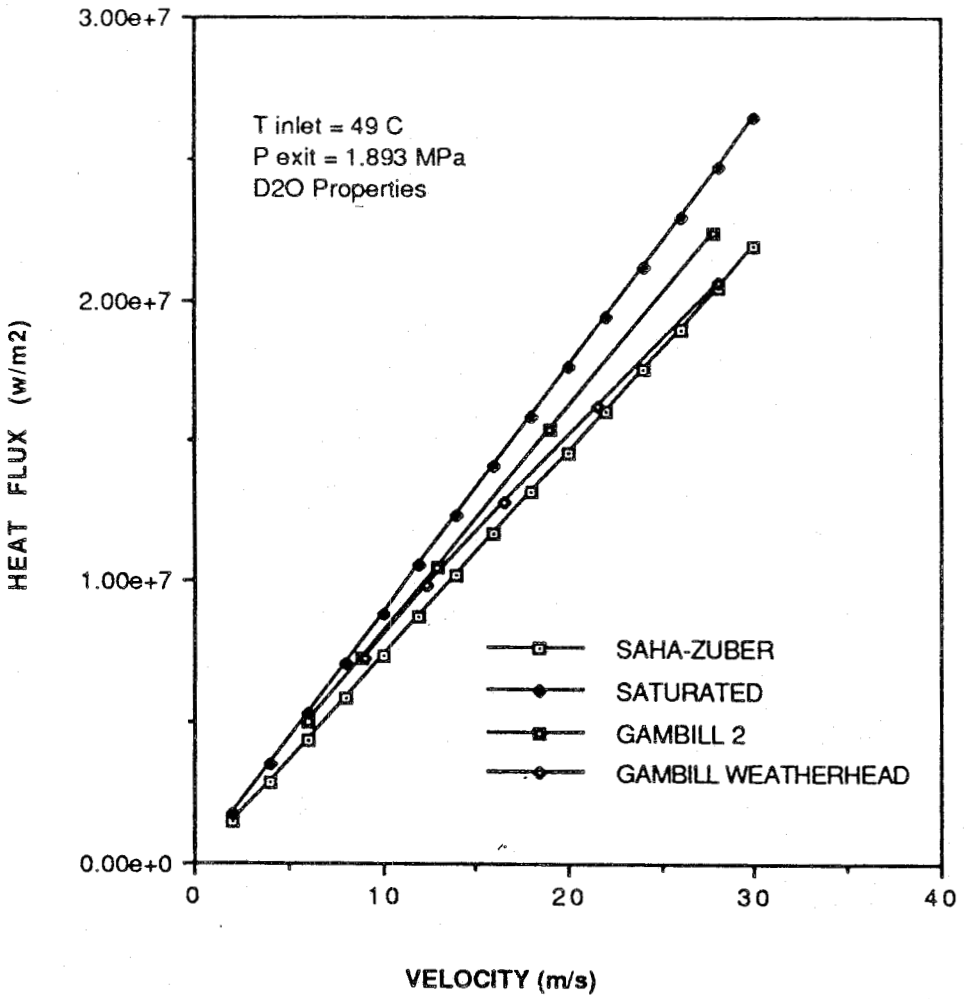

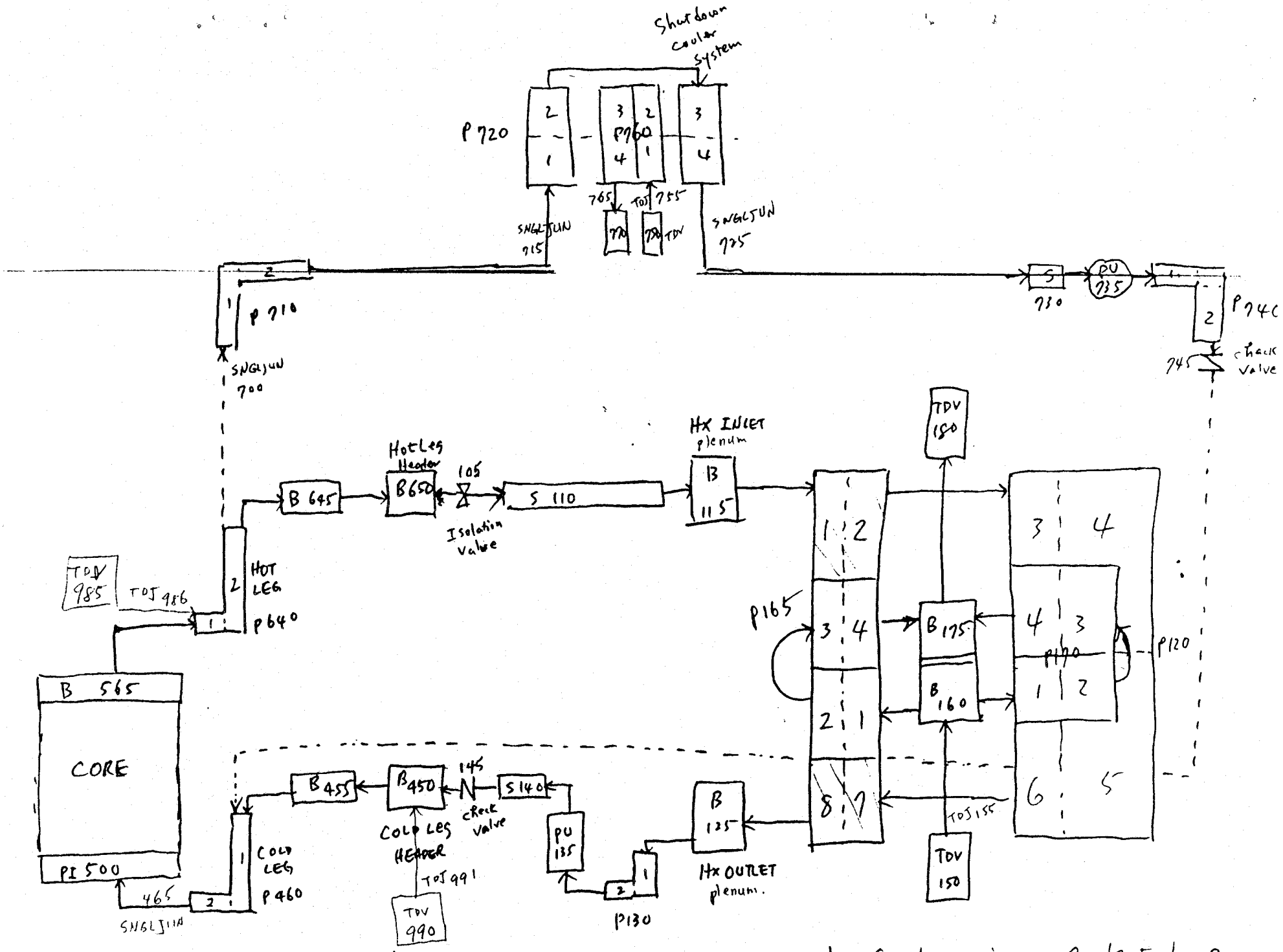

Figure 4: Schematic of the ANS RELAP5 model of the primary Coolant loop with shutdown cooler system

Idaho National Engineering Laboratory

WBS 1.6.2

May 8, 1989

R. M. Harrington
FEDC Building (MS 8218)
Advanced Neutron Source Project
Oak Ridge National Laboratory
P. O. Box 2009
Oak Ridge, TN 37831-8218

ASSUMPTIONS USED IN THE DEVELOPING THE RELAP5 MODEL OF THE ANS HEAT EXCHANGER LOOP - CDF-09-89

Dear Mr. Harrington:

The calculations needed to generate RELAP5 model input for the ANS heat exchanger loop have been completed. For your information, this letter documents the assumptions I used in developing this portion of the model. Your review of the following assumptions is requested:

1. The primary basis for the model is "Preliminary Description of the Advanced Neutron Source," F. J. Peretz, ORNL/ANS/INT-1 (Draft), June 1988, and its revision dated March 1989. The loop model is consistent with the conditions calculated by the core model for 350 MWt operation.

2. The cold and hot leg piping and headers are fabricated from 304L stainless steel and are uninsulated. In regions where the piping is immersed in the water pool, heat transfer from the pipe walls to the pool will be calculated assuming a constant 300K temperature boundary condition on the outer surface of the pipe. In regions where the piping is surrounded by air, an adiabatic boundary is assumed on the outer pipe wall.

3. The cold and hot leg distribution headers are assumed to be fabricated from 24" OD pipe and have a length of 10.5 feet. This dimension was estimated by assuming the 4-14" OD heat exchanger lines connected to each header are separated by 28" (centerline-to-centerline).

4. Pipe lengths and elevations were estimated from Peretz (see 1.) March 1989 revision, Figure 5.7.

5. The facility will include four identical heat exchanger loops; only three will be in use during normal operation. The model will include individual representations of the three operating loops. The fourth loop will not be included in the model. It was assumed the unused loop will be isolated from the primary coolant loop during operation.

6. The heat exchangers will be horizontal, but otherwise similar to those of HFIR (the HFIR modeling information was obtained from N.C.J. Chen). Each ANS heat exchanger is assumed to have 2260 tubes of 15.9 mm OD and 0.889 mm wall thickness. Average tube length is assumed to be 23.37 m.

7. The ANS primary coolant pump model was also based primarily on the HFIR pump. The ANS pump information used includes: coolant volume 0.6873 m^3, speed 185 rad/s, rated flow 814 kg/s, rated density 1098 kg/m^3, rated head 217.61 m, rated torque 8552 N-m, and moment of inertia 778 $kg\text{-}m^2$. The bearing friction is assumed to be 2% of rated torque. The single-phase pump homologous curves from the HFIR pump were used in Regions 1 and 2; B&W Bingham pump homologous curves were used in the other (non-standard) regions and fitted to meet the HFIR curves at the appropriate region boundaries. Two-phase pump multiplier and difference curves are based on Semiscale data.

8 The heat exchanger secondaries use light water as a working fluid. Flow loss was added such that the heat exchanger secondary differential pressure was 16 psid with a 90 psia outlet pressure (these values based on HFIR heat exchangers).

9. The two shutdown coolers will be lumped together in the model. The secondaries of the shutdown coolers will also use light water as a working fluid. The shutdown cooler pumps will be sized to deliver 18% of normal full core flow and remove 14% of full core power. Note no shutdown cooler flow will exist during normal operation. The shutdown cooler pump will be assumed to operate during normal operation, but no flow will be injected into the primary coolant system until the shutdown cooler pump head exceeds the main coolant pump head.

10. The flow losses due to the upper and lower flow screens have been included in the hot and cold leg piping regions of the model. At full flow, the upper screen introduces a 7.6 psid pressure drop and the lower screen introduces a 12.1 psid pressure drop.

Very truly yours,

C. D. Fletcher

C. D. Fletcher
Senior Engineering Specialist
Systems Engineering and Simulation

Enclosure:
As Stated

cc: C. Noble, DOE-ID
N. C. J. Chen, ORNL

ANS SEVERE ACCIDENT ANALYSIS REPORT

(MAY, 1989)

Rusi P. Taleyarkhan

Several areas in the ANS Severe Accident Safety Analysis Program were investigated during May, 1989. The results of these investigations and efforts are highlighted below.

Fuel-Coolant Interactions in ANS

The issue paper dealing with steam explosions relating to the ANS reactor design was completed and transmitted to the ANS Project Office for subsequent publication as an ORNL/TM report. Reviewer comments and suggestions have been incorporated in the completed report.

One of the key recommendations of the issue report on steam explosions was to obtain fundamental information on the propensity of molten U_3Si_2/Al mixtures to undergo steam explosion when brought in contact with water. In order to obtain such information (via small-scale tests) in conjunction with Savannah River Laboratory's (SRL) fuel-coolant experiments in progress at Sandia National Laboratory (SNL), communications were established with L. Nelson of SNL and M. L. Hyder of SRL. A formal invitation was extended by C. D. West and R. M. Harrington of the ANS Project Office to L. Nelson to visit Oak Ridge to conduct discussions and presentations on steam explosion experimentation and analysis.

A one-day meeting between ORNL and SNL staff was held at the Fusion Energy and Design Center. C. D. West provided an overview of the ANS program at ORNL. R. M. Harrington made a presentation on key features of the current ANS reactor design, and the safety analysis program in place. R. P. Taleyarkhan gave a presentation on the work performed during the past several months on the subject of steam explosion-related studies for the ANS reactor design. This scoping study report received a favorable review from M. Berman (Manager of the fuel-coolant interaction program at SNL). Thereafter, presentations were made by the SNL staff. M. Berman gave an overview of the work performed by SNL over the past decade on steam explosion issues for commercial LWRs under USNRC sponsorship. He also highlighted the quantitative and qualitative differences and similarities between steam explosions of various intensities and chemical explosions. D. Beck and L. Nelson presented various aspects of large-scale and small-scale steam explosion experiments performed at SNL. L. Nelson highlighted the virtues of conducting small-scale (i.e., with gram quantities of molten materials) experiments for obtaining valuable information in order to establish trends and to evaluate the propensity for various mixtures to undergo steam explosions with and without the use of external triggers. In particular, the SNL staff drew an interesting conclusion stating that, in spite of the thousands of steam explosion experiments conducted world-wide, it is still not possible to judge apriori whether or not a particular molten mixture would indeed undergo a steam explosion when brought in contact with water.

A discussion was subsequently held between C. D. West, R. M. Harrington, B. H. Montgomery, and R. P. Taleyarkhan of ORNL; and M. Berman, L. Nelson, and D. Beck of SNL regarding the possibility of conducting small-scale tests with U_3Si_2/Al fuel in conjunction with the current SRL experimental program. Several recommendations were made by the SNL staff and are being considered for feasibility. R. P. Taleyarkhan discussed with M. L. Hyder (of SRL) the possibility of adding U_3Si_2/Al material to the SRL test matrix. The initial response from SRL was favorable; however, details regarding fund transfer(s) and other accounting formalities still need to be resolved and are being looked into by the ANS Project Office. Separately, M. Berman provided several suggestions on how the ANS Project Office might proceed in order to tackle the steam explosion-related concern in the near future as well as in long-range planning. An interesting suggestion made by M. Berman dealt with designing an ANS reactor system which would be resistant to all conceivable loadings from steam explosions. In this scenario, it would be assumed that steam explosions would always occur when molten U_3Si_2/Al mixtures come in contact with water at various likely locations in the reactor system. The conversion ratio would be assumed to be the maximum possible value from thermodynamic considerations. Maximum possible loadings would then be evaluated and, in theory, design modifications (such as missile shields) could be introduced to counteract the evaluated loads. It is felt that such analysis and associated design work should await further progress in the probabilistic risk assessment, as well as in the development of front-end analytical tools (e.g., RELAP-5 model of the ANS).

The discussions between ORNL and SNL staff were positive, timely, and enlightening with regard to safety implications of steam explosions on various aspects of the ANS design.

Characterization of Core Melting, Relocation and Fission Product Release Issues for the ANS

During May, efforts were initiated to characterize severe accident issues in relation to core melting, relocation, and fission product release. Various aspects of these phenomena will be studied and documented as an issue paper. The format will be similar to that developed for the steam explosion issue paper with completion expected by July, 1989.

Scoping calculations were conducted to evaluate the effects of fuel heatup due to the thermite-like chemical reaction between U_3Si_2 and aluminum. Preliminary results indicate that the effect of this reaction would be dependent on the U_3Si_2 volume fraction, as well as the time span over which it's effects would be felt. Based upon information obtained from J. L. Snelgrove's presentation at the INEL safety meeting (March 1989), it was determined that for nominal volume fractions (i.e., 5%) in the ANS reference core design (i.e., 67-liter), even if all the U_3Si_2 were to react with aluminum the total energy released would be insufficient to cause all the

aluminum in the plates to melt. The experimenters at ANL used U_3Si_2 volume fractions of 32 to 45%. Scoping calculations show that under these conditions the exothermic reaction would release enough energy to completely melt all the aluminum in the core and superheat the aluminum by approximately 25-45°K. These calculations assumed the process to be adiabatic throughout the mixture. Preliminary evaluations for the ANS under decay heat conditions indicate that even with a 50% U_3Si_2 volume fraction, the exothermic energy released from the chemical reaction between fuel and aluminum would be insignificant in comparison with the energy release rate from the decay of radioactive nuclides in the fuel. This issue will be dealt with in greater detail during the course of evaluation of core melting and relocation. An interesting implication of this preliminary study involves the creation of molten U_3Si_2/Al mixtures with a desired amount of superheat for experimental testing purposes. For example, small-scale steam explosion experiments would need to create molten mixtures with a given amount of superheat. In such instances, where chemical reactions occur between mixture components, it is often difficult to control the melt superheat levels if the exothermic energy release rate is high. Based upon the preliminary evaluations discussed above, it seems that the maximum uncontrolled temperature rise would not exceed approximately 50°K. The temperature excursion may actually be significantly lower since the rate of exothermic energy release is quite slow, and occurs over a time span of several minutes as evidenced in the experiments conducted at ANL.

Reports, Papers, and Publications

The completed report on the ANS steam explosion issue paper has been transmitted to the ANS Project Office for publication as an ORNL/TM report.

A summary of the paper entitled "Analysis of Steam Explosions in Plate-Type Uranium-Aluminum Fuel Test Reactors" was prepared by R. P. Taleyarkhan for presentation at the technical session on Severe-Accident Analysis and Mitigation at the 1989 winter annual ANS/ENS conference. This paper is presently undergoing peer review.

Meetings and Trips

R. P. Taleyarkhan attended a meeting between C. D. West, R. M. Harrington, B. H. Montgomery of the ANS Project Office; and M. Berman, L. Nelson and D. Beck of SNL, to discuss the possibility of conducting small-scale experiments to obtain fundamental severe accident analysis-related information.

WBS 1.2.3.4

MONTHLY HIGHLIGHTS FOR MAY 1989

Probabilistic Risk Assessment for ANS

BNL Principal Investigator: R. Fullwood (FTS 666-2180)

ORNL Project Manager: M. Harrington (FTS 624 1062)

A first-order assessment of ANS internal risk is being performed by adapting initiator event sequences from the HFIR PRA with modifications according to the ANS preconceptual design. Large LOCA has been addressed previously and the following initiators (that dominated the HFIR risk) are being addressed: pressurizer, scram, instrument air, loose parts and reactivity transients. This work began as dominant scenario studies but based on ORNL comments has been switched to event tree analysis for the initiating events. This work is facilitated by the development of "event tables" in which 1 indicates success, 0 failure and - no never mind. While the event table is similar to an event tree, it allows more flexibility and permits the use of the power of the word processor. Upon completion, the matrix of the table is copied as an ASCII file and directly imported into the BETA code for evaluation and drawing the event tree.

The work to date has yet to discover a fuel damaging sequence with probability > 1.E-6/y, a fact that attests to the ruggedness of the ANS design.

ATTACHMENT 14

Internal Correspondence

MARTIN MARIETTA ENERGY SYSTEMS, INC.

June 9, 1989

J. A. Johnson

May Monthly Progress Report for ANS Project Quality Assurance Activities

WBS-1.2.5.1 Program Development

Discussions have continued with Project management relative to a Project Records Plan and a Document Management Procedure. These documents will establish how the Project will maintain records and control, track, and distribute project documents. Discussions have been held in the PRC on the inclusion of project staff direction previously distributed by memorandum into project administration and control procedures.

A tentative listing of activities, topics and/or procedure titles has been distributed to key project personnel for review, additions or deletions. A finalized listing should be ready for assignment of development priorities in June.

WBS-1.2.5.2 Program Monitoring

An audit was initiated of the HANS-1 capsule for fuels irradiation experimentation at HFIR. This is part of WBS 1.1.2., "Fuel Development." The audit is focused on the adequacy of the capsule fabrication records and the experiment design controls leading to fabrication. Initial results indicate the records support the capsule fabrication in accordance with design drawings.

Development of an audit checklist for verifying the input data and process utilized in the generation of the ANS Site Evaluation Report has continued. The audit of the Site Evaluation files is scheduled for completion within the next few months.

WBS-1.2.5.3 Project Support

A quality assurance orientation session on the requirements of ANSI/ASME NQA-1 was presented to the ANS R&D staff. This orientation will be presented to other project personnel in the future.

An NCR has been written to initiate an investigation into the failures of the cryostat windows and INVAR sleeve in a test system for development of the ANS cold sources. The NCR process will try to determine whether the failures were the result of component defects or installation errors and determine the actions needed to prevent recurrence.

Max L. Gildner

M. L. Gildner, 7964-E, MS-6391, ORNL (4-9133)

L. M. Jordan

L. M. Jordan, 9201-3, MS-8063, ORNL (6-3711)

MLG:dkc

cc: R. E. Fenstermaker
M. L. Gildner
L. M. Jordan
P. E. Melroy
C. D. West

ATTACHMENT 15

Internal Correspondence

MARTIN MARIETTA ENERGY SYSTEMS, INC.

June 15, 1989

J. A. Johnson

May Monthly Progress Report for Design Activities on the Advanced Neutron Source

General

A series of "key design decisions" have been recommended by the project director and staff, encompassing design issues in reactor systems, experiment systems, and balance of plant. A task team has been identified for initial efforts on each decision, and leaders have been agreed upon. Generally, these key design decisions are consistent with earlier priorities of the design team, and do not represent a diversion of effort. However, they do offer the opportunity for greater attention by project management on the issues facing the design teams, and offer a methodology for approval of the decisions being made early in the conceptual design. Specific "key decisions" are described under the appropriate WBS elements below.

Project funding for FY-90 is beginning to move through the Congressional budget process. Initial House markups again include direction to spend the amount requested, but do not increase the total funding for DOE Basic Energy Sciences programs (the situation of the past few years). Speculation is that Congress is behind on the budget process, and that next year will begin with a continuing resolution.

Engineering budgets generally appear on track for this point in the fiscal year, although some adjustments are needed by specific disciplines. These adjustments are now being identified and resolved.

Work on the transmittals is still underway, and the document backlog has not yet been distributed. Anyone wishing a copy of the project documents should contact the project office.

WBS 1.1.13, Facility Concepts

Input on materials selection issues continues. Recent attention has been focused on bringing the fuel plate stability studies done under the R&D tasks into the design effort. A further review of the performance of clad and unclad hafnium in absorbers at various power and research reactors is also being initiated.

WBS 1.2, Project Support

Extensive discussions have been held with DOE, Engineering, and ORNL management over the past few months on the method of contracting for an architect-engineer to participate in the second phase of the conceptual design, beginning at the end of FY-90. A key issue is whether Energy Systems will hold the contract for the A-E, or whether it will be a prime contract to DOE. Also under discussion is the mechanics of soliciting A-E firms. Under some scenarios, a statement of

work and initial advertisement in Commerce Business Daily will be required in the next two months; in others, the process would begin at the beginning of next fiscal year.

Additional staff is being used on a temporary basis to speed development of key procedures. This may be of particular value in resolving the document backlog, as well as initiating other key procedures for documentation and quality assurance.

WBS 1.3, Reactor Systems

The first two key design decisions under reactor systems cover the design of the removable core pressure boundary tube and the hardware for handling spent fuel, irradiation targets, aged core pressure boundary tubes, and spent control absorbers. These two systems are so closely related that they are designated RS-1a and RS-1b. Initial activity is being focused on the core pressure boundary tube design, especially the design of the connections and seals. An initial meeting has been held by this group, and definition of the basis and both functional and regulatory requirements is underway. The RS-1b task will be initiated once the CPBT task is proceeding effectively.

Task RS-2 deals with design of the reactor control hardware, including the inner control, shim and safety rods, the outer shutdown and safety rods, and the flux monitoring systems. It also includes development of the general control strategy, and requires a close interface to the R&D tasks for developing the neutronic characteristics of the control system. A kickoff meeting was held on June 15.

The last reactor systems task, RS-3, covers the design concepts for the reflector tank. This includes both the mechanical design of the tank and its penetrations (including the beam tube penetrations into the tank), and the methods of cooling the components inside the tank. Development of details for the design of the tank is considered a lower priority than the other reactor systems tasks. Some work in outlining the concepts will be required, however, to provide an effective interface to the other tasks.

General configuration development work continues as well. A series of CAD sketches have been used to overlay the potential positions for straight outer shutdown rods over the beam tube plan, and adjust the concepts to avoid interferences. Initial attempts to overlay sketches of irradiation facilities in the reflector tank are also underway.

Work is also continuing on modelling the transient thermal condition of the core pressure boundary tube, to determine temperatures and thermal expansion in the event of loss of flow along with a reactor scram. A NISAII finite element model is being developed for this purpose. Initial steady state runs have been checked with a simple TK Solver model to identify any errors in units, etc. Future efforts will include obtaining heating rates for the current reference core, and development of boundary conditions.

WBS 1.4, Experiment Systems

The single "key decision" task (ES-1) for the experiment systems team is allocation of experiment space in all areas of the facility, ranging from instruments in the guide hall to irradiation facilities in the reflector tank and inside the core pressure boundary tube. Since this is essentially a formalization of the general task of definition of the priorities and facilities to be included in the ANS, which was the main goal of the experiment systems team this year, the ES-1 task meetings

will be held as part of the regular bi-weekly team meetings.

Initial efforts on beam facilities will be directed on developing design concepts for the triple axis spectrometers and single crystal diffractometers. As design concepts for the individual instruments are developed, a full understanding of the use, variants, number, and space requirements for each instrument can be developed. This will feed into the ES-1 task for beam instruments.

Conceptual design work has begun on irradiation facilities in the reflector tank. Facilities identified at present include two materials irradiation positions adjacent to the core (outside the CPBT), three hydraulic rabbit tubes, three pneumatic rabbit tubes, and a number of isotopes production facilities. Preliminary layouts have been prepared for two materials irradiation guide tubes that will hold the capsule end of an experiment at the core midplane, with the tube extending up out of the reflector tank at a 15° angle to avoid interferences with the refueling hardware. These tubes will contain a concentric tubular liner that will control the flow of heavy water used to cool the experiment. The liner bore has been sized to be equivalent to an "RB*" position at the HFIR.

WBS 1.5 and WBS 1.6, Balance of Plant

The key decisions for the balance of plant again begins with two tasks so inter-related that they are designated BOP-1a and BOP-1b (although they were originally BOP 1 and BOP 2). BOP-1a addresses the sizing, layout and equipment selection for the primary circuit in terms of providing reliable normal operation. BOP-1b addresses decay heat removal, including transfer of decay heat from the core to various heat sinks under degraded conditions. The former task defines the system needed for effective operation of the reactor; the latter identifies the modes needed to safely dissipate decay heat under all conceivable situations. An iterative collaboration between the two tasks is expected in order to arrive at the final normal and emergency primary coolant systems.

A third task, now called BOP-2, covers reactor containment. This task will review the various containment concepts which could be considered for the ANS, and will define the components and operating parameters of the selected concept. A close interface between the decay heat removal task, and even more with the severe accident studies being conducted under the safety program, will be required in order to evaluate containment concepts and to provide input to the other tasks. The start of this task is being delayed slightly due to manpower constraints, but this is expected to last only a few weeks.

An initial survey of the ANS site has been completed. Stakes now mark the reactor centerline, and the orientation and perimeter of the reactor building. Plans for initial characterization efforts are now being developed, and contacts are being made with the appropriate environmental groups to obtain surveys for rare plants, etc.

F. J. Peretz

F. J. Peretz, FEDC (6-5516)

cc: R. O. Barnett
R. M. Beckers
H. C. Beeson
R. A. Brown
D. D. Cannon
R. M. Canon
R. O. Daugherty
L. J. Degenhardt
J. R. Dixon
C. P. Frew
R. W. Glass
C. L. Hahs
R. L. Johnson
G. F. Kalb
B. S. Maxon
C. S. Meadors
T. J. McManamy
R. Miller
H. R. Payne
W. H. Power
C. C. Queen
W. R. Reed
T. L. Ryan
J. P. Schubert
J. L. Snyder
P. B. Thompson
B. D. Warnick

MARTIN MARIETTA

Internal Correspondence

MARTIN MARIETTA ENERGY SYSTEMS, INC.

June 12, 1989

F. J. Peretz

May Monthly Report for Design Activities on the
Advanced Neutron Source Reactor

Component Cooling Calculations

Work is continuing on the ANS core pressure boundary tube (cpbt) transient thermal model. The model geometry has been completed, and an initial steady-state run has been made to check the geometry, units, and volumetric heating rates.

A TK Solver model was developed to calculate the gamma heating rate distribution in each finite element of the NISAII model. The model reads in the node coordinates and element data, then calculates the centroid of the element. It then interpolates a heating rate based on the radial and axial coordinates of the element centroid. The gamma heat distribution table was based on the neutronics calculation by Y. Azmy for the 40-L split core. The 40-L heating rate distributions will be used until the neutronic calculations are completed for the PS2 core.

The next step in the finite element model will be to apply realistic boundary conditions at the upper flange connection and at the lower seal. The steady-state temperature distribution will then be calculated and used in the stress run to determine the thermal expansion.

J R Dixon

J. R. Dixon, 1000, MS-6332, ORNL (4-8260)

JRD/blm

cc: R. W. Glass
T. W. Pickel
W. C. Stoddart
WO A-8019A-AA
File - JRD (NoRC)

WBS 1.4 EXPERIMENT SYSTEMS

R. Beckers, C. Hahs, T. J. McManamy

A. INSTRUMENTATION AND NEUTRON BEAM TRANSPORT

Progress on the ANS Experimental Systems during the month of May has included work on the scope, schedule, and criteria. Work breakdown structures have been generated for the five generic experiments. Manpower estimates and schedules have been prepared for the design of the Triple Axis Spectrometer and the Single Crystal Diffractometer. Utilization of experiment space has been recognized by the Program Director and Principle Engineer as a key technical decision, but the footprints of the experiments and their arrangement in the beam room and guide hall cannot be determined without completion of some preliminary calculations. The focus has been redirected to the Neutron Beam Transports. Beam Transport System Objectives for September 1989 have been determined and agreed upon by the Experimental Systems Team. This involves the identification of major components, the establishment of design criteria where available, the determination of the fitness of the "state of the art" for component design, and the recognition of areas in need of R&D and the status of any R&D in progress internationally. The purpose of this exercise is to extract the outstanding issues and to begin preliminary layouts where the known criteria and system interfaces can support the effort. It is intended that the team keep abreast of progress in the design of other systems to provide the necessary exchange of information where interfaces and space constraints are revelant.

B. IRRADIATION FACILITIES

Initial concepts prepared for the refueling cell and materials irradiation cells were presented to the project team on May 22, 1989. To prevent interference with operation of the polar carne in the beam room and to provide inherent protection from flooding of the refueling cell, a very tall cell configuration is required that will add another floor to the reactor building. Changes in criteria that would decrease the height of the refueling cell were discussed. These include: 1) use the cell only for handling reactor fuel cores, 2) provide shielding at the top of the refueling machine, and 3) relocate the hot cell outside the perimeter of the polar crane. The elimination of the hot cell for refueling was also discussed. In this conceptual multiple fuel storage cans in the storage pool would be accessed directly by the refueling machine.

Conceptual work has started to define the irradiation facilities in the reflector tank. Two materials irradiation positions adjoining the core, three hydraulic rabbit tubes, three pneumatic rabbit tubes and a number of isotope production positions at various thermal neutron flux levels will be required.

Preliminary layouts have been prepared for two materials irradiation guide tubes that will hold the capsule end of an experiment in a position adjoining the midpoint of the upper fuel core. These guide tubes are slanted 15° from vertical so that they avoid the support for the core pressure boundary tube. Each will be in a plane offset from a vertical midplane of the reactor. Each of the guide tubes will pass over one cold neutron source in its path to t he top of the reactor. Then each guide tube will pass through a nozzle in the neck

of the reflector tank (above the flat head). Each guide tube will contain a concentric tubular liner that will control the flow of D_20 used for cooling an experiment. The liner bore has been sized to be equivalent to an RB position at HFIR.

Internal Distribution

1. C. W. Alexander
2. R. G. Alsmiller
3. B. R. Appleton
4. Y. Y. Azmy
5. J. R. Buchanan
6. N. C. J. Chen
7. G. L. Copeland
8. F. C. Difilippo
9. J. R. Dixon
10. H. L. Dodds
11. F. F. Dyer
12. W. W. Engle
13. R. E. Fenstermaker
14. W. R. Gambill
15. R. K. Genung
16. M. L. Gildner
17. R. M. Harrington
18. J. B. Hayter
19. D. L. Henderson
20. D. T. Ingersoll
21. J. A. Johnson
22. L. M. Jordan
23. R. A. Lillie
24. A. L. Lotts
25. B. S. Maxon
26. R. Miller
27. B. H. Montgomery
28. R. M. Moon
29. F. R. Mynatt
30. R. K. Nanstad
31. L. C. Oakes
32. R. E. Pawel
33. F. J. Peretz
34. R. T. Primm, III
35. C. C. Queen
36. J. S. Rayside
37. H. Reutler
38. A. E. Ruggles
39. T. L. Ryan
40. D. L. Selby
41. H. B. Shapira
42. W. D. Shults
43. R. P. Taleyarkhan
44. P. B. Thompson
45. K. R. Thoms
46. D. B. Trauger
47. R. E. Uhrig
48. C. D. West
49. M. K. Wilkinson
50. G. T. Yahr
51. G. L. Yoder
52. A. Zucker
53. Laboratory Records (RC)

External Distribution

54. R. F. Domagala, RERTR Program, Argonne National Laboratory, 9700 South Cass Avenue, Argonne, IL 60439.
55. Jack Dorning, University of Virginia, Department of Nuclear Engineering and Engineering Physics, Charlottesville, VA 22901.
56. B. Chalmers Frazer, Materials Sciences Division, U.S. Department of Energy, Germantown, ER-132, Washington, D.C. 20545.
57. Ralph Fullwood, Brookhaven National Laboratory, Upton, NY 11973.
58. J. A. Lake, Manager, Nuclear Engineering and Reactor Design, Idaho National Engineering Laboratory, P. O. Box 1625, Idaho Falls, ID 83415.
59. John Marks, Research and Test Reactor Fuel Elements, Babcock and Wilcox Co., P. O. Box 785, Lynchburg, VA 24505.

60. John M. Ryskamp, Idaho National Engineering Laboratory, P. O. Box 1625, Idaho Falls, ID 83415.
61. J. L. Snelgrove, Coordinator, Engineering Applications, RERTR Program, Argonne National Laboratory, 9700 South Cass Avenue, Argonne, IL 60439.
62. Iran Thomas, Director, Materials Science Division, Office of Energy Research, U.S. Department of Energy, Germantown, ER-13, Washington, D.C. 20545.
63. R. P. Wadkins, Idaho National Engineering Laboratory, P. O. Box 1625, Idaho Falls, ID 84515.
64. D. K. Wilfert, Energy Programs, U.S. Department of Energy, Oak Ridge Operations, P. O. Box 2001, Oak Ridge, TN 37831.
65. R. J. Willard, U.S. Department of Energy, Oak Ridge Operations, P. O. Box 2001, Oak Ridge, TN 37831.